Effectiveness of Negative Air Ionization in Reducing Airborne Porcine Reproductive and Respiratory Syndrome Virus (PRRSV) and Aerosols

by

Amy La

A Thesis submitted to the Faculty of Graduate Studies of

the University of Manitoba

in partial fulfillment of the requirements of the degree of

MASTER OF SCIENCE

Department of Biosystems Engineering

Faculty of Engineering

University of Manitoba

Winnipeg

Copyright © 2014 by Amy La

ABSTRACT

Porcine reproductive and respiratory syndrome virus (PRRSV) causes disease in swine and economic losses for swine producers. An inexpensive and effective method for removing PRRSV from air is required to reduce aerosol transmission of PRRSV. A laboratory study was used to assess the performance of air ionization at removing bioaerosols contaminated with PRRSV. Aerosol properties were measured with an Aerosol Particle Size Spectrometer and air samples were collected with SKC biosamplers. PRRSV RNA was quantified with RNA extraction and quantitative reverse transcription polymerase chain reaction. Reduction in aerosol concentrations ranged from 61 – 93% by number count and 68 – 96% by mass. Initial particle size distribution and airflow rate affected the performance of EPI Air at reducing aerosol concentrations. Air ionization was effective at removing PRRSV from the air. The PRRSV RNA concentrations were reduced by 68 – 90% and the average PRRSV RNA after ionization ranged from 154 – 4594 VGCN m^{-3}.

ACKNOWLEDGEMENTS

I would like to thank my advisor, Dr. Qiang Zhang, for his mentorship and support during this project. I would also to thank my committee members Dr. David Levin and Dr. Kevin Coombs for their assistance during various components of this research.

Additional thanks goes to Thinesh Peranantham and Saranya Rajendran for their technical assistance during the laboratory analysis portion of this project as well as Calvin Ngan and Kelsey Smyth for their hard work at constructing the experimental chambers. I am also thankful for the help of Evelyn Fehr, Debby Watson, Dale Bourns, Robert Lavallee, and Matt McDonald.

I give many thanks to John Baumgartner, Matt Baumgartner, and Rick Bergmann for their help in installing the EPI air. I would also like to thank Manitoba Rural Adaptation Council (MRAC) and Manitoba Pork for their funding support on this project. I am grateful towards members of my lab for their support through challenging times.

Last but not least, I would like to thank God Almighty for giving me the strength and support to overcome my problems and for never giving me any obstacles that I could not overcome.

DEDICATION

With much love and appreciation, I would like to dedicate my thesis to my mom and dad, Le Phuong La and Minh Tan La, and my fiancé, Leno Jose Guzman Quinonez.

TABLE OF CONTENTS

ABSTRACT ..... **II**

ACKNOWLEDGEMENTS ..... **III**

DEDICATION ..... **IV**

LIST OF TABLES ..... **IX**

LIST OF FIGURES ..... **X**

CHAPTER 1. INTRODUCTION **1**

CHAPTER 2. OBJECTIVES **2**

CHAPTER 3. LITERATURE REVIEW **3**

3.1. Air Quality in Swine Production Facilities **3**

3.1.1. Size characterization of aerosols 4

3.1.2. Health consequences due to poor air quality 6

3.1.3. Methods of dust removal in swine production facilities 7

3.2. Porcine Reproductive and Respiratory Syndrome Virus **9**

3.2.1. Aerosol Transmission of PRRSV 10

3.2.2. Methods of protecting swine facilities against aerosol-transmitted pathogens 11

3.2.3. Air Sampling of PRRSV 13

3.2.4. RNA extraction and qRT-PCR of PRRSV 15

3.3. Air ionization **17**

3.3.1. Air ionization for aerosol reduction 17

3.3.2. Negative air ionization in animal facilities 19

3.3.3. Bactericidal action of air ionization 21

CHAPTER 4. METHODOLOGY 22

4.1. Overview of Methodology 22

4.2. Aerosol testing Chambers 22

4.2.1. Construction of chambers 23

4.2.2. Airflow control 25

4.2.3. Chamber calibration 27

4.2.4. Stabilization time 28

4.2.5. EPI installation and ion concentration measurement 30

4.2.6. Aerosol generation system 33

4.3. Biosampling 35

4.4. Virus detection and quantification 38

4.4.1. RNA extraction 38

4.4.2. Quantitative reverse transcription polymerase chain reaction 40

4.5. Aerosol sampling 44

4.6. Preliminary testing with water aerosols 45

4.7. PRRSV Experiment 46

4.7.1. Test procedures 46

4.7.2. Cleaning procedure 50

4.8. Data Analysis 51

4.8.1. Particle size analysis 51

4.8.2. Statistical Analysis 53

CHAPTER 5. RESULTS 56

5.1.1. Standard Curve for qRT-PCR 56

5.2. Chamber and Instrument Performance Tests 57

5.2.1. Airflow pattern in test chambers 57

5.2.2. Aerosol generation rates 59

5.2.3. Biosampler performance 59

5.2.4. Aerosol losses 61

5.3. Temperature and Relative Humidity 63

5.4. Ion concentrations 64

5.5. Effect of ionization on Particle Size Distribution 66

5.5.1. Number count vs. mass distribution 66

5.5.2. Bioaerosols before ionization 68

5.5.3. Bioaerosols after ionization 70

5.6. Aerosol concentration 77

5.6.1. Change in aerosol concentrations 77

5.6.2. Aerosol concentration before air ionization 79

5.6.3. Aerosol concentration after ionization 81

5.7. Aerosol-removal efficiencies for Different size distributions 84

5.8. Water aerosols and Bioaerosols Comparison 86

5.8.1. EPI effect on particle size distribution 86

5.8.2. Aerosol concentration difference 87

5.9. PRRSV RNA concentration in air 91

5.9.1. PRRSV concentration before ionization 92

5.9.2. EPI effect on PRRSV RNA concentration in air 94

CHAPTER 6. CONCLUSIONS 99

CHAPTER 7. RECOMMENDATIONS 101

APPENDIX A. LIMIT OF DETECTION CALCULATION FOR QRT-PCR 103

APPENDIX B. STATISTICAL ANALYSIS DETAILS 106

APPENDIX C. EQUILIBRIUM CALCULATION FOR WATER AND PBS AEROSOLS 113

REFERENCES 115

LIST OF TABLES

Table 1. Summary of damper settings, pressure differences, and voltages required to generate airflow rates of 34.0 and 135.9 $m^3 h^{-1}$ during experiments. 27

Table 2. Aerosol generation rates of Collison 6-jet nebulizer when supplied with 137.9 and 413.7 kPA of compressed air. 59

Table 3. Comparison of measured and calculated values of PRRSV concentration in air at steady-state before ionization..... 61

Table 4. Calculated and measured bioaerosol concentrations at steady-state before ionization. 62

Table 5. Aerosol concentration (standard deviation) of water aerosols in terms of number count and mass..... 90

Table 6. Comparison of the reduction of aerosol concentration for PBS (bioaerosols) and water aerosols..... 90

LIST OF FIGURES

Figure 1. Conceptual sketch of experimental chamber system used to conduct laboratory tests 23

Figure 2. Front view of the construction of the experimental chambers. 24

Figure 3. High Efficiency Particulate Air (HEPA) filter and installation for aerosol generation.25

Figure 4. HEPA filter, ductwork, IRIS damper, manometer, bypass damper, and high speed fan. 26

Figure 5. Estimated (a) stabilization time and (b) steady-state aerosol concentrations based on the aerosol generation rate and ventilation rate. 30

Figure 6. The EPI Air ionization system set-up inside experimental chambers. 31

Figure 7. Placement of ion counter 33

Figure 8. Aerosol generation system set-up. 34

Figure 9. Set-up of air sampling assembly for air sample collection with biosamplers. 36

Figure 10. Positions of biosamplers within experimental chambers. 37

Figure 11. Sequence of water aerosol tests. 45

Figure 12. Sequence of PRRSV test 49

Figure 13. Example of experimental data showing boundary between before and after ionization stages of experimental test 53

Figure 14. Standard (calibration) curve for quantification of concentration of PRRSV within an unknown sample 56

Figure 15. Smoke test at 34.0 m^3 h^{-1} in the source chamber after chamber modifications, images taken at four different times after smoke introduction. 58

Figure 16. Smoke test at 254.8 m^3 h^{-1} in the source chamber after chamber modifications, images taken at two different times after smoke introduction. 58

Figure 17. Bubblemeter set-up for biosampler calibration tests. 60

Figure 18. Condensation location prior to source chamber. 62

Figure 19. Temperature and relative humidity in trailer during tests 64

Figure 20. (a) Average voltage measured after activating negative air ionization and (b) average ion concentration measured during preliminary tests. (Treatment 1: 34.0 m^3 h^{-1},14.8 ml h^{-1}; Treatment 2: 34.0 m^3 h^{-1}, 33.0 ml h^{-1}; Treatment 3: 135.9 m^3 h^{-1}, 14.8 ml h^{-1}; Treatment 4: 135.9 m^3 h^{-1}, 33.0 ml h^{-1})..... 65

Figure 21. Particle size distributions (top: number count; bottom: mass) of the first replicate of an experiment before ionization with an airflow rate of 34.0 m^3 h^{-1} and an aerosol generation rate of 14.8 ml h^{-1}. 68

Figure 22. Summary of the #GMD and MGMD before ionization (Treatment 1: 34.0 m^3 h^{-1},14.8 ml h^{-1}; Treatment 2: 34.0 m^3 h^{-1}, 33.0 ml h^{-1}; Treatment 3: 135.9 m^3 h^{-1}, 14.8 ml h^{-1}; Treatment 4: 135.9 m^3 h^{-1}, 33.0 ml h^{-1})..... 69

Figure 23. Summary of the #GSD and MGSD before ionization (Treatment 1: 34.0 m^3 h^{-1},14.8 ml h^{-1}; Treatment 2: 34.0 m^3 h^{-1}, 33.0 ml h^{-1}; Treatment 3: 135.9 m^3 h^{-1}, 14.8 ml h^{-1}; Treatment 4: 135.9 m^3 h^{-1}, 33.0 ml h^{-1})..... 69

Figure 24. Summary of the #GMD and MGMD after ionization (Treatment 1: 34.0 m^3 h^{-1},14.8 ml h^{-1}; Treatment 2: 34.0 m^3 h^{-1}, 33.0 ml h^{-1}; Treatment 3: 135.9 m^3 h^{-1}, 14.8 ml h^{-1}; Treatment 4: 135.9 m^3 h^{-1}, 33.0 ml h^{-1})..... 71

Figure 25. Summary of the #GSD and MGSD after ionization (Treatment 1: 34.0 m^3 h^{-1},14.8 ml h^{-1}; Treatment 2: 34.0 m^3 h^{-1}, 33.0 ml h^{-1}; Treatment 3: 135.9 m^3 h^{-1}, 14.8 ml h^{-1}; Treatment 4: 135.9 m^3 h^{-1}, 33.0 ml h^{-1})..... 71

Figure 26. Reduction of #GMD and MGMD (Treatment 1: 34.0 m^3 h^{-1},14.8 ml h^{-1}; Treatment 2: 34.0 m^3 h^{-1}, 33.0 ml h^{-1}; Treatment 3: 135.9 m^3 h^{-1}, 14.8 ml h^{-1}; Treatment 4: 135.9 m^3 h^{-1}, 33.0 ml h^{-1}). 72

Figure 27. Percentage of aerosols greater than 0.5 μm after ionization during each treatment (Treatment 1: 34.0 m^3 h^{-1},14.8 ml h^{-1}; Treatment 2: 34.0 m^3 h^{-1}, 33.0 ml h^{-1}; Treatment 3: 135.9 m^3 h^{-1}, 14.8 ml h^{-1}; Treatment 4: 135.9 m^3 h^{-1}, 33.0 ml h^{-1})..... 75

Figure 28. Aerosol concentration at different aerosol sizes before and after ionization for (a) treatment 1: 34.0 m^3 h^{-1},14.8 ml h^{-1}; (b) treatment 2: 34.0 m^3 h^{-1}, 33.0 ml h^{-1}; (c) treatment 3: 135.9 m^3 h^{-1}, 14.8 ml h^{-1}; (d) treatment 4: 135.9 m^3 h^{-1}, 33.0 ml h^{-1}. 77

Figure 29. Examples of aerosol concentration of bioaerosols during PRRSV experiments during treatments 2 and 4 by (a) number count and (b) mass. 79

Figure 30. Aerosol concentration of bioaerosols before ionization by (a) number count and (b) mass (Treatment 1: 34.0 m^3 h^{-1},14.8 ml h^{-1}; Treatment 2: 34.0 m^3 h^{-1}, 33.0 ml h^{-1}; Treatment 3: 135.9 m^3 h^{-1}, 14.8 ml h^{-1}; Treatment 4: 135.9 m^3 h^{-1}, 33.0 ml h^{-1})..... 80

Figure 31. Aerosol concentration of bioaerosols after ionization by (a) number count and (b) mass (Treatment 1: 34.0 m^3 h^{-1},14.8 ml h^{-1}; Treatment 2: 34.0 m^3 h^{-1}, 33.0 ml h^{-1}; Treatment 3: 135.9 m^3 h^{-1}, 14.8 ml h^{-1}; Treatment 4: 135.9 m^3 h^{-1}, 33.0 ml h^{-1})..... 81

Figure 32. Reduction in aerosol concentration of bioaerosols due to ionization in terms of (a) number count and (b) mass (Treatment 1: 34.0 m^3 h^{-1},14.8 ml h^{-1}; Treatment 2: 34.0 m^3 h^{-1}, 33.0 ml h^{-1}; Treatment 3: 135.9 m^3 h^{-1}, 14.8 ml h^{-1}; Treatment 4: 135.9 m^3 h^{-1}, 33.0 ml h^{-1}). 82

Figure 33. Removal efficiency of the EPI system for aerosols by mass for treatments with (a) an airflow rate of 34 m^3 h^{-1} and (b) an airflow rate of 135.9 m^3 h^{-1}. 86

Figure 34. Aerosol concentration during treatment 2 tests for (a) water aerosols and (b) bioaerosols. 88

Figure 35. PRRSV RNA concentration in the air in the source and recipient chambers before ionization (Treatment 1: 34.0 m^3 h^{-1},14.8 ml h^{-1}; Treatment 2: 34.0 m^3 h^{-1}, 33.0 ml h^{-1}; Treatment 3: 135.9 m^3 h^{-1}, 14.8 ml h^{-1}; Treatment 4: 135.9 m^3 h^{-1}, 33.0 ml h^{-1})..... 93

Figure 36. PRRSV concentration in air within source and recipient experimental chambers after ionization (Treatment 1: 34.0 m^3 h^{-1},14.8 ml h^{-1}; Treatment 2: 34.0 m^3 h^{-1}, 33.0 ml h^{-1}; Treatment 3: 135.9 m^3 h^{-1}, 14.8 ml h^{-1}; Treatment 4: 135.9 m^3 h^{-1}, 33.0 ml h^{-1})..... 95

Figure 37. (a) Reduction of PRRSV concentration within source chamber air due to ionization and (b) Percentage of PRRSV RNA concentration remaining in source chamber after ionization (Treatment 1: 34.0 m^3 h^{-1},14.8 ml h^{-1}; Treatment 2: 34.0 m^3 h^{-1}, 33.0 ml h^{-1}; Treatment 3: 135.9 m^3 h^{-1}, 14.8 ml h^{-1}; Treatment 4: 135.9 m^3 h^{-1}, 33.0 ml h^{-1})..... 95

Figure 38. PRRSV collected from wall swabs in source chamber (Treatment 1: 34.0 m^3 h^{-1},14.8 ml h^{-1}; Treatment 2: 34.0 m^3 h^{-1}, 33.0 ml h^{-1}; Treatment 3: 135.9 m^3 h^{-1}, 14.8 ml h^{-1}; Treatment 4: 135.9 m^3 h^{-1}, 33.0 ml h^{-1})..... 97

CHAPTER 1. INTRODUCTION

Porcine reproductive and respiratory syndrome virus (PRRSV) causes a disease that highly affects the swine industry globally. PRRS disease causes mortality and other complications in infected pigs, ultimately leading to profit losses for swine producers. PRRSV is difficult to vaccinate against due to ineffective vaccines and/or risky vaccines, and also because of the existence of multiple isolates of PRRSV, which causes swine herds to remain susceptible to the disease despite previous infection and/or vaccination.

The swine industry has developed biosecurity protocols to limit the transmission of PRRSV. Despite these attempts, a pertinent issue with PRRSV is its ability to transmit from infected facilities to uninfected facilities via aerosol transmission. Aerosol transmission occurs when PRRSV-naïve swine are infected by aerosols carrying infectious PRRSV. In the few studies where air sampling methods were used to quantify airborne PRRSV concentrations, the methods varied from study to study, causing it to be difficult to compare results. A need for a method that could unify air sampling measurements is required to understand important parameters of aerosol transmission, such as the variation of shedding rate of PRRSV over an infection period. Established biosecurity protocols cannot effectively protect swine facilities against PRRSV infections caused by aerosol transmission. Therefore, the swine industry is in need of methods for protecting swine production facilities from aerosol transmission. Currently, mechanical filters are utilized in some critical swine facilities, such as breeding barns. However, existing swine production facilities require extensive modification to install mechanical filters and this task is expensive and difficult. Inexpensive means of protecting swine production facilities from PRRSV are urgently needed by the swine industry.

Air ionization is an old and established technology that improves air quality within a room. Installing air ionization systems within animal production facilities requires little labour and is relatively inexpensive compared to mechanical filtration systems. In animal production facilities, air ionization is typically utilized to reduce aerosols (dust). Since airborne viruses such as PRRSV are mostly attached to aerosols, removing aerosols from air should lead to reduction of viruses in the air, thus preventing airborne transmission of diseases. In other words, the air ionization technology is a potential alternative for protecting swine facilities against aerosol transmission of PRRSV. To date few studies been conducted to assess the effectiveness of air ionization in removing PRRSV from the air. The purpose of this research was to understand how negative air ionization reduces airborne PRRSV.

CHAPTER 2. OBJECTIVES

The objectives of this study were to conduct laboratory experiments to:

1. determine the characteristics of a negative air ionization in system in terms of reducing concentrations of aerosols containing PRRSV and changing the aerosol particle size distribution;
2. assess the effectiveness of the air ionization system in removing PRRSV from the air; and
3. determine the effect of airflow (ventilation) rate on the effectiveness of the air ionization system in removing aerosols and PRRSV.

In the process of meeting these objectives, a secondary objective was to develop an air sampling method that could be used in future studies to facilitate the comparison of airborne PRRSV concentrations in different studies.

CHAPTER 3. LITERATURE REVIEW

3.1. Air Quality in Swine Production Facilities

Air quality is defined as the "characterization of the air content compared to its normal composition under clean conditions" (Lemay and Chénard 2001); an increase in airborne contaminants within swine production facilities, such as particulate matter (dust particles), gases, and bioaerosols results in a decrease in the air quality (Lemay and Chénard 2001). Bioaerosols are aerosols (such as dust particles) that contain biologically active microorganisms such as bacteria, endotoxins, fungi (Lemay and Chénard 2001), and in some cases, viruses. For example, Donham et al. (1986) found bacteria and fungi within particulate matter that had gravitationally settled within five swine buildings. In another study, the concentrations of total aerosols and bioaerosols detected in a swine production facility were seven and twelve times greater than that found in the ambient air, respectively (Agranovski et al. 2004).

Aarnink et al. (1999) reported that dust composition in a swine facility was more than 10% feed, more than 10% skin and 1-3% feces and crystalline dust (Zhao et al. 2014). Donham et al. (1986) determined that dust particles in swine production facilities were primarily from feed and that these particles were larger and would deposit in the nose and pharynx. The authors also found that fecal matter was the primary dust source at smaller particulate matter size ranges. A recent study (Cambra-López et al. 2011) found that feed was a negligible source of airborne particulate matter, and that manure and skin were the most prevalent sources of coarse and fine particulate matter in swine production facilities. Zhao et al. (2014) compiled a literature review detailing possible sources of microorganisms within animal production facilities including: fecal matter, mucous of the respiratory tract, feed, litter, animal skin, farm workers, farm visitors, and

ambient air; these microorganisms may become airborne from settled dust that may re-enter the air through animal activity.

Animal production facilities produce many gaseous contaminants, including ammonia, hydrogen sulfide, methane, and carbon monoxide (Hartung and Phillips 1994). Hydrogen sulfide, which can cause both swine worker death (Lemay and Chénard 2001) and animal death, comes from anaerobic bacterial decomposition of specific amino acids within animal waste, while ammonia comes from "bacterial and enzymatic decomposition" of nitrogen within urine and other waste (Hartung and Phillips 1994).

3.1.1. Size characterization of aerosols

The behavior of aerosols in the air is dictated by their sizes, which are often described by the aerodynamic diameter. The aerodynamic diameter of a specific particle is the diameter of a hypothetical spherical particle with a density of 1 g/cm^3 that has the same settling velocity as the particle (Cambra-López et al. 2010). Particulate matter that has an aerodynamic diameter of 10 μm and less and 2.5 μm and less are classified as the particulate matter 10 (PM_{10}) and particulate matter 2.5 ($PM_{2.5}$), respectively, and their concentrations are quantified in terms of their mass or number count in m^3 of air (Zhao et al. 2014). Inhalable dust was defined as less than 100 μm in size, thoracic dust was defined as less than 10 μm in size, and respirable dust was defined as less than 4 μm or 5 μm in size (Zhao et al. 2014). Respirable airborne dust particles can enter the lower respiratory tract, including the lungs, and can become a greater health hazard if there are other contaminants present on the dust, such as absorbed microorganisms or gas molecules (Lemay and Chénard 2001).

Particle size distributions can provide a detailed characterization of particulate matter within a swine production facility. The particles are organized based on their aerodynamic diameters to provide the composition of the particles in terms of its fractional or cumulative frequency distribution (Cambra-López et al. 2010). The particle size distribution can be described by the number count or mass of particles across aerodynamic diameters. The number count distribution curve can differ from that of the mass distribution; for example, the mass particle size distribution may show that a small particle size has the same aerosol concentration as a large particle size, while the number count particle size distribution would show that the small particle size has a greater aerosol concentration than the larger aerosol concentration. In this example, there were a large number of small aerosols whose added mass was equivalent to a small amount of large aerosols. When the particle sizes are graphed on a logarithmic scale, the particle size distribution resembles a normal distribution curve (Cambra-López et al. 2010) and the characteristics of the particle size distribution are described by two important parameters – the geometric mean or median diameter (GMD) and the geometric standard deviation (GSD). Previous studies have utilized resistive-pulse particle analyzers (Heber et al. 1988a, 1988b), optical counters (Bundy and Hazen 1975; Bundy 1984; Agranovski et al, 2004; Gustafson 1999), and cascade impactors (Donham et al. 1986; Siggers et al. 2011) to measure particle size distributions of aerosols. Cascade impactors were also used to determine the size ranges of bioaerosols containing microorganisms such as bacteria and fungi (Siggers et al. 2011; Sowiak et al. 2012). Agranovski et al. (2004) measured an average median diameter of 2.23 μm by number count in a swine barn. An average geometric mean diameter of 17.9 μm and a geometric standard deviation of 2.2 μm (Predicala et al. 2001) as well as an average mass median diameter of 31.55 μm and a geometric standard deviation of 1.86 μm were measured in mechanically-

ventilated swine buildings. An average geometric mean diameter was 18.1 μm with a geometric standard deviation of 2.1 μm in a naturally-ventilated swine building (Predicala et al. 2001).

3.1.2. Health consequences due to poor air quality

Contaminated air within swine production facilities can evoke respiratory disorder symptoms in swine workers. A survey of swine veterinarians showed that increased exposure to swine barns was linked to symptoms such as increased phlegm production, airway obstruction, abnormal pulmonary function, and non-prescribed inhaler use (Andersen et al. 2004). A study of Quebec swine workers showed that chronic bronchitis was more common and airflow obstruction was more evident within the swine workers than non-swine workers; the amount of time spent within a swine facility daily, but not the number of years, also affected the occurrence of chronic bronchitis and airflow obstruction (Cormier et al. 1991). To reduce exposure to airborne contaminants, effective dust masks such as the N95 respirators are commonly utilized in swine facilities. Dosman et al. (2000) found that males not previously associated with swine barns that were exposed to swine barn air without N95 particulate respirators had significantly higher severity of some symptoms – coughing, chest tightness, and phlegm but not headache, shortness of breath, and nasal irritation – than those that wore N95 particulate respirators. Human exposure limits of 2.4 mg m^{-3} for total dust and 0.23 mg m^{-3} for respirable dust (Donham 1991) were previously recommended. These exposure limits are less than the recommended limits of the Occupational Health and Safety Act of Ontario (OSHA), which specified a time-weighted average exposure limit (TWAEV) of 10 mg m^{-3} and 3 mg m^{-3} for inhalable and respirable particulates. High concentrations of respirable bioaerosols were detected in a study of Polish swine facilities (Sowiak et al. 2012). The authors discussed that the high levels of bioaerosols

were considered a health hazard for swine workers due to their ability to penetrate the trachea, bronchi, and alveoli. Another survey of swine practitioners indicated that 13% of the swine practitioners developed zoonotic infections from working in swine production facilities, which was significantly correlated to the number of years they were employed as a swine practitioner (Hafer et al. 1996).

Donham (1991) performed a swine-health study on Swedish swine facilities that found significant correlation between ammonia and the occurrence of arthritis and abscesses as well as lesions due to porcine stress syndrome. The authors also found significant correlation between the airborne bacterial concentration and pneumonia, arthritis, and abscess occurrence in swine. Concentrations of respirable dust greater than 0.8 mg m^{-3} were associated with pneumonia, pleuritis, death loss, and arthritis, while concentrations of total dust above 3.5 mg m^{-3} were associated with death loss in swine. The study recommended exposure limits of 3.7 mg m^{-3} and 0.23 mg m^{-3} for total and respirable dust, respectively, for swine health. Additionally, previous studies have shown that harmful respiratory diseases of swine are transmittable via aerosol transmission including Porcine Reproductive and Respiratory Syndrome Virus (PRRSV), *Mycoplasma hyopneumoniae* (Dee et al. 2010), *Bordetella bronchiseptica* (Brockmeier and Lager 2002), *Actinobacillus pleuropneumoniae* (Torremorell et al. 1997), and Foot-and-Mouth Disease (FMD) (Mikkelsen et al. 2003).

3.1.3. Methods of dust removal in swine production facilities

Ventilation is an effective way of improving air quality in swine facilities. Studies have compared mechanical ventilation and natural ventilation and found that naturally ventilated

rooms had higher levels of respirable dust (Phillips et al. 1989), and total mass concentration of dust (Heber et al. 1988b), while ammonia levels in naturally ventilated rooms were lower than that in mechanically ventilated rooms (Phillips et al. 1989). However, Predicala et al. (2001) did not find any differences in air quality between a naturally ventilated building and a mechanically ventilated building.

Spraying water was shown to reduce total dust by 29%, but have no effect on respirable dust (Takai and Pederson 2000). Andres and Banhazi (2013) measured dust reduction by spraying canola oil in a swine building and found that the spraying oil was significantly effective at reducing inhalable dust in both the weaner and grower rooms but respirable dust was reduced in the weaner room only. Siggers et al. (2011) compared the reductions of airborne dust, endotoxin, bacterial, and fungi at different size ranges when a sprinkler system was utilized to sprinkle canola oil in a swine barn. The reduction in total dust was 86%, while the removal efficiency was greatest for the size range of 3.3 – 4.7 μm at 91.2% and decreased to 66% at a size range of 0.4-0.7 μm (Siggers et al. 2011). The oil sprinkling also caused a reduction of 82.5% in total endotoxin concentration as well as 16%, 32.2%, and 52% reduction in total bacteria, enteric bacteria, and fungi.

Guarino et al. (2007) tested the performance of soybean oil and two commercial oil-based feed additives for dust reduction. All of the treatments significantly reduced the inhalable and respirable dust concentrations but spraying 240 g of soybean oil to 8 kg of feed resulted in the highest reduction of dust at 90% and was more successful at reducing respirable dust concentrations. Rule et al. (2005) atomized a proprietary solution containing corn oil, adipic acid, ethyl alcohol, eucalyptus, and water into a swine finisher barn and measured its effect on dust, bioaerosols, and ammonia. The authors determined that the effectiveness of dust removal

increased as the time of application and size of dust increased; reduction of 40% occurred at 1 micron but increased to 90% at 10 μm. The authors also found that there was a 90% reduction in total viable bacteria after treatment.

Takai and Pedersen (2000) studied the use of combining techniques for reducing dust. Adding 4% of animal fat to feed and spraying with a rapeseed oil-water mixture caused significant reductions of 55% to 75% on total and respirable dust, respectively, when spraying was performed without taking into consideration the amount of animal activity (Takai and Pedersen 2000). When animal activity was taken into account, spraying with oil-water mixture and adding 4% animal feed caused a reduction of 79% and 76% on total dust and a reduction of 88% and 76% on respirable dust at spraying rates of 3.1 g day^{-1} pig^{-1} and 3.3 g day^{-1} pig^{-1}, respectively.

3.2. Porcine Reproductive and Respiratory Syndrome Virus

The Porcine Reproductive and Respiratory Syndrome Virus (PRRSV) is a pathogenic single-stranded, enveloped RNA virus that is 50-65 nm in diameter (Cho et al. 2006). The PRRSV is categorized into the order Nidovirales, the family Arteriviridae, and the genus *Arterivirus* (Egli et al. 2001). The North American strain of the virus, VR-2332, and the European strain, Lelystad virus, caused similar diseases in swine when they emerged in the late 1980 and early 1990, respectively (Egli et al. 2001). VR-2332 and Lelystad virus share 58-78% amino acid identities in their open reading frames (ORF) and are closely related to EAV (equine arteritis virus) and LDV (lactate dehydrogenase-elevating virus) (Murtaugh et al. 1995). Currently, many field isolates of PRRSV exist that have varying levels of virulence. The variety

of PRRSV isolates means that it is possible for a farm to become re-infected with PRRSV despite a previous infection with PRRSV. Porcine reproductive and respiratory syndrome virus can cause respiratory disease leading to respiratory failure, and mortality of younger pigs (Egli et al. 2001) as well as decreased herd performance in terms of farrowing rates, weaned piglets, growth rates, and growth efficiency (Hermann et al. 2007). The United States loses an annual profit of $664 million according to a 2013 study (Holtkamp et al. 2013) and Canada has profit losses of $100 million annually (VIDO-InterVAC 2014). PRRSV can transmit from pig to pig via direct and indirect routes, including fomites, transport vehicles, vectors, and aerosols (Cho and Dee 2006).

Commercial vaccines include killed-virus PRRSV vaccines as well as modified-live PRRSV vaccines. Modified-live PRRSV vaccines are considered more effective than killed-virus PRRSV vaccines but neither type of vaccine is able to eliminate infection or transmission of the PRRSV virus (Hu and Zhang 2002). Some field isolates were also the result of modified live vaccines reverting back to virulent strains of PRRSV (Opriessnig et al. 2002). Experimental vaccines are in development (Hu and Zhang 2002), but currently vaccination does not provide a foolproof prevention method for PRRSV.

3.2.1. Aerosol Transmission of PRRSV

Aerosol transmission is an important mode of transmission for the PRRSV. While biosecurity protocols were developed to prevent transmission of PRRSV, these protocols are unable to prevent the transmission of PRRSV via indirect methods, such as aerosol transmission (Desrosiers 2011). Previous studies that sought to experimentally confirm the occurrence of

aerosol transmission of PRRSV had a mix of positive and negative results. Several studies attempted to experimentally validate the airborne transmission of PRRSV by exhausting air potentially contaminated with PRRSV from an infected building into trailers filled with naive recipient swine (Otake et al. 2002; Trincado et al. 2004; Fano et al. 2005). Aerosol transmission did not occur in these studies, possibly because the PRRSV isolate, MN-30100, used to infect the swine, is a low pathogenic strain (Cho et al. 2006). Other studies demonstrated aerosol transmission of PRRSV from an experimental unit containing pigs infected with different strains of PRRSV – such as European PRRSV (Kristensen et al. 2004), VR-2332 (Torremorrell et al. 1997), NADC-22 (Brockmeier and Lager 2002) and MN-184 (Cho et al. 2007) – to a second experimental unit containing PRRSV-naïve pigs. Aerosol transmission did not occur for some isolates, such as MN-1b (Torremorrell et al. 1997) and MN-30100 (Cho et al. 2007). Pitkin et al. (2009) and Dee et al. (2010) demonstrated that PRRSV was aerosol transmitted from an infected swine building to a neighboring PRRSV-naive swine building that was not protected with mechanical filters. Long distance airborne transport of PRRSv was documented in two studies in which PRRSV was captured in air samples collected downwind of infected pig barns at distances of 4.7 km (Dee et al. 2009a) and 9.1 km (Otake et al. 2010).

3.2.2. Methods of protecting swine facilities against aerosol-transmitted pathogens

Mechanical filters, such as HEPA (high efficiency particulate air) filters, have been shown to be quite effective in reducing aerosol transmission of PRRSV between experimental chambers (Dee et al. 2005a, 2006a, 2006b). However, mechanical filters of the same rating did not all necessarily perform equally (Dee et al. 2009b). A two-stage filtration system was installed in a swine building located downwind from an infected swine building and effectively

protected PRRSV-naïve swine housed in the building from PRRSV (Pitkin et al. 2009; Dee et al. 2010, 2011). The same building also effectively protected swine from PRRSV when the filtration system was replaced with filters of a different rating (Dee et al. 2010, 2011). Similarly, when the filtration system was subsequently replaced with mechanical fiberglass filters that were given an electrostatic charge, the filtration system effectively protected swine (Dee et al. 2011). A 12-month study of air filtration systems in swine facilities within a swine-dense region showed that the herds within the filtered facilities were not infected with PRRSV during the span of the study, while the herds from the unfiltered facilities became infected with new PRRSV isolates (Spronk et al. 2010). A similar 40-month study showed that filtered facilities had significantly lower new PRRSV infections within breeding herds compared to non-filtered facilities. Installation of air filtration systems within formerly non-filtered facilities significantly reduced the quantity of new PRRSV infections (Dee et al. 2012)

The expensive cost of implementing HEPA filtration systems in commercial swine facilities caused researchers to seek out equally effective but more economical technologies to mitigate PRRSV (Dee et al. 2005, 2006a, 2006b, 2009b). A study evaluating the performance of antimicrobial filters showed that it was possible for PRRSV to pass through the filters but their infectiousness was lost in the process (Dee et al. 2009b). Additionally, the study showed that a disinfectant evaporative-cooling (EVAP) system was a potential alternative to mechanical filters as the disinfectant provided a virucidal effect against PRRSV RNA (Dee et al. 2009b). In a production model study, an antimicrobial filter with a mixture of virucidal and bactericidal compounds was installed in a swine building located downwind of the infected swine building and was found to effectively protect the naïve facility from PRRSV (Dee et al. 2010, 2011).

3.2.3. Air Sampling of PRRSV

Sampling PRRSV in the air is a critical step in studying aerosol transmission of PRRSV. Various techniques have been used to collect air samples for detecting and quantifying PRRSV in the air, such as a liquid cyclonic collector (Dee et al. 2005b, 2009a, 2009b, 2010; Cho et al. 2007; Hermann and Zimmerman 2008; Pitkin et al. 2009; Otake et al. 2010; Alonso et al. 2012), various glass impingers (Torremorell et al. 1997; Otake et al. 2002; Trincado et al. 2004; Fano et al. 2005; Hermann et al. 2006, 2007, 2008, 2009; Hermann and Zimmerman 2008; Cutler et al. 2011), and collection bags (Cho et al. 2006). Hermann et al. (2006) speculated that the detection of airborne viruses was dependent on the concentration of airborne virus in the air, the air sampler's ability to capture airborne virus, and the ability of diagnostic assays at detecting the virus. Cho et al. (2006) used a conical breathing mask, breathing valve, and collection bag to collect air samples from swine infected with either PRRSV isolate MN-184, MN-30100, or coinfected with *Mycoplasma hyopneumoniae*. While the PRRSV isolate did not statistically affect the airborne concentration of PRRSV in exhaled air during a shedding event, swine infected with PRRSV isolate MN-184 shed the PRRSV more frequently. Frequency of shedding would affect the chances of detecting PRRSV in air samples, as air sampling must coincide with a shedding event for detection to occur. In a different study, Hermann and Zimmerman (2008) collected air samples from individual swine that were infected with PRRSV isolates VR-2332 or VR-2385 using a conical mask connected to a AGI-30 glass impinger. All air samples were negative for PRRSV despite oral swabs testing positive for PRRSV RNA; the authors concluded that it was possible that PRRSV RNA was not present in the exhaled air but it was also possible that the sample collection time, analytical sensitivity of the sampling system and diagnostic testing, and the isolate pathogenicity contributed to the inability to detect PRRSV in air samples.

It must be noted that qRT-PCR was used as a diagnostic assay to measure PRRSV concentration in air samples in both of these studies.

From a review of previous studies, Hermann et al. (2006) stated that impingers were "more effective than filters, bubblers, or impactors at collecting airborne viruses". Impingers draw converged air through a liquid medium to collect airborne contaminants, which can be analyzed with techniques such as qRT-PCR for virus particles (Hermann et al. 2006; Hermann and Zimmerman 2008). Impinger design, sampling time, composition of collection medium, and preservation of virus infectivity using added compounds are some factors that affect the efficiency of impingers at collecting airborne viruses (Hermann et al. 2006). Hermann et al. (2006) tested the effect of various additives on MARC -145 cell lines and the infectivity of PRRSV, including: antifoam solutions, which are used to decrease foaming that can occur during impingement; protectants, which can decrease virus inactivation; sorbents, such as activated carbon, which may allow for enhancement of the viral infectivity; and ethylene glycol to determine if it can allow for air sampling at sub-zero temperatures. The additives that performed best were added to the collection mediums of various tested impingers, including the SKC biosampler, the AGI-30 glass impinger, and the AGI-4 impingers, which were tested at different sampling periods. The diagnostic assay used in this study was qRT-PCR. Overall, the study found that PBS with ethylene glycol resulted in the highest quantity of PRRSV, indicating that ethylene glycol could be used for sub-zero air sample measurements. Since Antifoam A Emulsion was shown to have no detrimental effects on the MARC-145 cells lines or the $TCID_{50}$ titers, it was utilized within the nebulizer to minimize foaming during aerosolization of the virus (Hermann and Zimmerman 2008; Hermann et al. 2007, 2009; Cutler et al. 2011). Hermann et al. (2006) also found that the SKC biosampler and AGI-30 collected more virus than the AGI-4.

The SKC biosampler collected more viruses at sampling times of 15 and 20 minutes than the AGI-30 impinger, although the two impingers operating at the same sampling airflow rate.

The performance of four air samplers – the AGI-30 impinger, the AGI-4 impinger, the SKC Biosampler, and the Midwest MicroTek liquid cyclonic collector – was assessed to determine their analytical sensitivity (i.e., the amount of aerosolized PRRSV required for detection of the virus during qRT-PCR; Hermann and Zimmerman 2008). The authors found that there was not a statistically significant difference between the analytical sensitivity of the air samplers. The air samplers had analytical sensitivities of $1 \times 10^{1.1}$ $TCID_{50}$ – $1 \times 10^{1.2}$ $TCID_{50}$, which is equivalent to 13-16 median tissue culture infectious doses ($TCID_{50}$).

3.2.4. RNA extraction and qRT-PCR of PRRSV

Quantitative Reverse Transcription Polymerase Chain Reaction (qRT-PCR) is commonly used to detect and quantify PRRSV in samples (e.g., liquid medium from impingers) collected with air samplers. RNA extraction is an important precursor to qRT-PCR as it is needed to "obtain nucleic acid templates of sufficient purity and appropriate quantity" (Guarino et al. 1997). Guarino et al. (1997) previously evaluated the performance of four RNA extraction kits (TRIzol, Ultraspec-3RNA, QIAamp viral RNA mini kit, and QIAamp tissue kits) on extracting PRRSV isolate VR2332 diluted in Eagle's Minimum Essential Medium (EMEM) or swine serum. TRIzol was previously used to extract PRRSV viral RNA from serum (Yoon et al. 1999; Egli et al. 2000), swine organs (Egli et al. 2000), and cell cultures (Gilbert et al. 1997). The Qiagen QIAamp Viral RNA mini kit was successfully used to extract PRRSV viral RNA from oral fluids (Prickett et al. 2008), cell culture supernatants (Murtaugh et al. 2002; Jacobs et al. 2010), serum

(Murtaugh et al. 2002; Wasilk et al. 2004), dust samples (Kaufford et al. 2010), and air samples (Hermann et al. 2006, 2007). Guarino et al. (1997) extracted PRRSV RNA using the four kits and performed RT-PCR and Agarose Gel Electrophoresis with Ethidium Bromide dye on the extracted RNA samples. The results of the study showed that the Qiagen QIAamp viral RNA mini kit was the most sensitive and allowed for detection of PRRSV at an approximate concentration of 10 $TCID_{50}$ per 100 µl. TRIzol and the QIAamp tissue kit allowed detection of PRRSV at concentrations of 100 $TCID_{50}$ per 100 µl.

In the past, researchers designed their own primers and/or probes for reverse transcription polymerase chain reaction (RT-PCR) on samples to detect PRRSV (Christopher-Hennings et al. 1995; Gilbert et al. 1997). Nowadays, there are commercial kits available that contain all the necessary reagents to perform quantitative reverse transcription polymerase chain reaction successfully. Examples of these reagent kits are the VetMax North American and European PRRSV Reagents, the VetAlert PRRSV North American and European Reagents, AcuPig PRRSV real-time PCR reagents. Because of the diversity of PRRSV isolates with varying genetic makeup, it is important for these kits to have primers and probes that can detect the diversity of PRRSV isolates in a sample, including North American and European isolates. Harmon et al. (2012) compared qRT-PCR performance of the VetMax and VetAlert reagents on serum, lung tissue, oral fluid, as well as other samples. The study found that both kits had some instances of false-negative results. Gerber et al. (2013) compared the VetMax, VetAlert, and AcuPig reagents on boar serum, semen, blood swabs, and oral fluids of boars infected with one of six PRRSV isolates. The VetMax reagents had a significantly greater detection rate of PRRSV within positive samples (67.2%) than the VetAlert (61.7%) and AcuPig (62.5%) reagents.

3.3. Air ionization

Air ionization is a technology that involves the generation of air ions to remove volatile organic compounds, particulate matter, and microbials from the air (Daniel 2002). While the mechanism seems deceivingly simple, air ionization involves a complicated set of chemical reactions that create and utilize reactive oxygen species and reactive charged species that can improve overall air quality (Daniel 2002). Devices that produce air ions have a cornucopia of names, including but not limited to ion emitters (Lee et al. 2004; Grinshpun et al. 2005), ion generators (Mayya et al 2004; Sawant et al. 2012), air ionizers (Daniel 2002; Wu et al. 2006; Sawant et al. 2012; Grabarczyk 2001), corona ionizers (Grabarczyk 2001) and ionic air purifiers (Lee et al. 2004; Grinshpun et al. 2005). Devices are also categorized based on whether it produces one (unipolar) or two (bipolar) types of ions, which can be negative or positive; bipolar air ionizers are supplied with alternating current (AC), while unipolar devices are supplied with direct current (DC) that produce positive or negative ions based on the voltage supplied (Daniel 2002). Corona ionizers or corona-discharge ionizers use corona discharge to create air ions (Fletcher et al. 2008; Mayya et al. 2004); a corona discharge occurs when an electrode or conductor has a potential gradient over a critical value that allows it to ionize surrounding gas or fluid, resulting in an electrical discharge (Gunston 2009).

3.3.1. Air ionization for aerosol reduction

Several studies compared the natural decay of aerosol concentration to the decay due to air ionization and found air ionization led to faster reduction in aerosol concentration (Wu et al. 2006; Sawant et al. 2012; Grinshpun et al. 2005; Rosentrater et al. 2004; Lee et al. 2004). Grabarczyk (2001) found that a portable ionizer was not effective at reducing aerosol

concentrations in an unventilated room due to the limited space that contained its electrostatic fields and ion streams; comparatively, a whole-room "ion shower" air ionizer was able to reduce aerosol concentrations in the unventilated room within one hour to what was equivalent to 3 and 3.5 air changes per hour for 0.4-2.5 micron and 0.3-0.4 micron aerosols, respectively. Lee et al. (2004) tested three ionic air purifiers, two that produced negative ions and one that produced positive ions, and found that each was able to remove aerosols from the air. The ionic air purifier with highest ion emission rate was the most effective and removed 97% of 0.1 μm smoke aerosols and 95% of 1 μm smoke aerosols within 30 minutes from the air of an unventilated test chamber. Grinshpun et al. (2005) tested five ionic air purifiers within a wooden unventilated test chamber with a mixing fan. The authors found that amongst the three stationary purifiers, the one that had the highest ion production rate was able to remove 100% of the aerosols within the measured aerosol size range of 0.3 – 3 μm within 10-12 minutes. Additionally, aerosol concentration was better reduced with higher ion production and greater rate of air mixing (33 CFM vs. 900 CFM) for two wearable ionic purifiers (Grinshpun et al. 2005). The study also found that the aerosol properties – in this case, polydisperse NaCl particles, monodisperse polystyrene latex (PSL), and cells of *Pseudomonas fluorscens* – had little effect on the air cleaning efficiency of the purifiers. Sawant et al. (2012) tested a specially-designed ion generator with optimized performance in an unventilated glass container and found that the natural decay of aerosol concentration as well as the decay of aerosol concentrations due to negative air ionization differed depending on the type of particulate matter, which in this case included fog, dhoop candle smoke, and vehicle smoke. The wall material within test chambers was also found to affect the efficiency of negative air ions at reducing aerosol concentrations as

air ionization provided different levels of performance with the use of stainless steel, wood, PVC, wallpaper, and cement paint as wall materials (Wu et al. 2006).

3.3.2. Negative air ionization in animal facilities

Studies of air ionization within animal production facilities have typically focused on negative ion generation in ventilated animal production facilities where aerosols were continuously being produced by animals. It has been shown that negative air ionization in poultry production facilities resulted in significant reduction of airborne dust concentrations in broiler breeder houses (Mitchell et al. 2004; Richardson et al. 2003a, 2003b) and hatching cabinets (Mitchell and Waltman 2003) as well as both naturally and artificially generated dust in a caged layer room (Mitchell et al. 2000). Negative air ionization was also shown to be effective in reducing PM_{10} concentrations in poultry production houses (Mitchell and Baumgartner 2007; Cambra-López et al. 2009) as well as $PM_{2.5}$ concentrations (Cambra-López et al. 2009). Results from Nicolai and Hofer (2007) indicated that there was a reduction in total spatial particulates, $PM_{10,}$ and $PM_{2.5}$ in a swine production facility due to the utilization of negative air ionization. Dust particles at sizes of 0.05 μm, 2.5 μm, and 10 μm were significantly reduced using negative air ionization in a swine nursery barn (Rademacher et al. 2012). Tanaka and Zhang (1996) found that negative air ionization decreased dust concentrations within a swine grower/finisher barn and the reduction efficiency was affected by dust accumulation on walls and ventilation rate.

Field studies of negative air ionization have indicated that it significantly reduced total airborne bacteria (Richardson et al. 2003a), total airborne gram negative bacteria (Mitchell et al. 2004; Richardson et al. 2003a, 2003b), ammonia (Mitchell et al. 2004), and gram-negative

bacteria on egg belts and egg shells (Richardson et al. 2003a) in broiler breeding houses. Negative air ionization also significantly reduced airborne salmonella and enterobacteriaceae compared to the untreated control (Mitchell and Waltman 2003). However, the ionization was less effective in reducing airborne salmonella compared to the hydrogen peroxide treatment nor did it reduce *E. coli*, *Staphylococcus* species, or fungi compared to the formaldehyde treatment. Contrary to other studies, Cambra-López et al. (2009) reported that ionization did not reduce airborne microorganisms, ammonia, or odour. These different observations might have been due to using different measuring procedures than other studies; for example, the odour attached to dust was not taken into account as dust filtering was performed before quantifying odour (Cambra-López et al. 2009).

Removal of airborne dust using negative air ionization leads to the removal of airborne bacteria. Richardson et al. (2003a, 2003b) reported that the reduction of airborne dust due to the negative air ionization treatment corresponded to the subsequent reduction in airborne gram-negative bacteria. Additional corroboration was seen in a study by Richardson et al. (2003b) in which a broiler breeder room with ionization treatment had a statistically significant increase in *Salmonella*-positive samples collected from swabbing the walls, slats, litter, and equipment compared to a control room. This indicated that the ionization system removed airborne dust contaminated with *Salmonella* from the air and attached the contaminated dust to surfaces. Overall, the removal of airborne dust could possibly correspond to a health benefit for animals living in facilities due to the reduction in airborne transmission of pathogens (Richardson et al. 2003b).

3.3.3. Bactericidal action of air ionization

Kerr et al. (2007) utilized air ionization in an intensive care unit and found that there were fewer infections but more isolates of *Acinetobacter* species when the air ionizer was activated compared to when the ionizer was deactivated. Fletcher et al. (2007) performed a study in which microorganisms (*Staphylococcus aureus, Mycobacterium paragortuitum, Pseudomonas aeruginosa, Acinetobacter baumanii, Burkholderia cenocepacia, Bacillus subtilis, and Serratia marcescens*) were exposed to positive and negative corona discharge. The authors also performed additional experiments by placing a mica sheet and a grounded wire mesh in between the electrodes and the agar plates to differentiate between the bactericidal effect of the electric field and ozone, respectively. The study indicated that negative and positive air ions were not the predominant reason for bacterial cell death during air ionization but rather the oxidative action from ozone produced during air ionization as well as electroporation, from exposure to electric fields, to a lesser degree. *Mycobacterium parafortuitum* was an exception to this conclusion as only the electric field affected its survivability. Timoshkin et al. (2012) also used a grounded wire mesh to test for the effect of ozone on survivability of *E. coli* and *S. aureus* when exposed to corona discharge treatment. Longer exposure times to negative corona discharge corresponded with higher levels of produced ozone and also a greater reduction in surviving bacteria, with *S. aureus* having a greater sensitivity to ozone exposure than *E. coli*. For both studies, it was possible that other neutral reactive species in addition to ozone were able to contact the agar plates and cause bactericidal action (Timoshkin et al. 2012) but additional studies are required as confirmation.

CHAPTER 4. METHODOLOGY

4.1. Overview of Methodology

A series of laboratory tests were devised to assess the performance of negative air ionization at improving air quality via the removal of PRRSV-contaminated bioaerosols. Two enclosed experimental chambers were constructed for conducting these laboratory tests. Ventilation rate in the experimental chambers was controlled and PRRSV was aerosolized into the experimental chambers at predetermined aerosol generation rates. A negative air ionization system was installed in each chamber. Measurements in experiments included the aerosol particle size distribution and concentration, concentration of PRRSV RNA in the air, and concentration of PRRSV RNA on chamber walls. A particle analyzer was used to measure the aerosol properties, and biosamplers were used to collect samples which were then analyzed by the quantitative reverse transcription polymerase chain reaction to quantify the PRRSV RNA in the samples. The aerosol properties and the PRRSV RNA concentrations were compared before and after the air ionization was activated to assess the performance of the air ionization system.

4.2. Aerosol testing Chambers

A conceptual sketch of the chamber system used to conduct experiments is displayed in Figure 1. The chamber system consisted of two experimental chambers, the negative air ionization system, a system for generating and controlling ventilation rate, and an aerosol generation system. Each of the systems in discussed in further detail in the following sections.

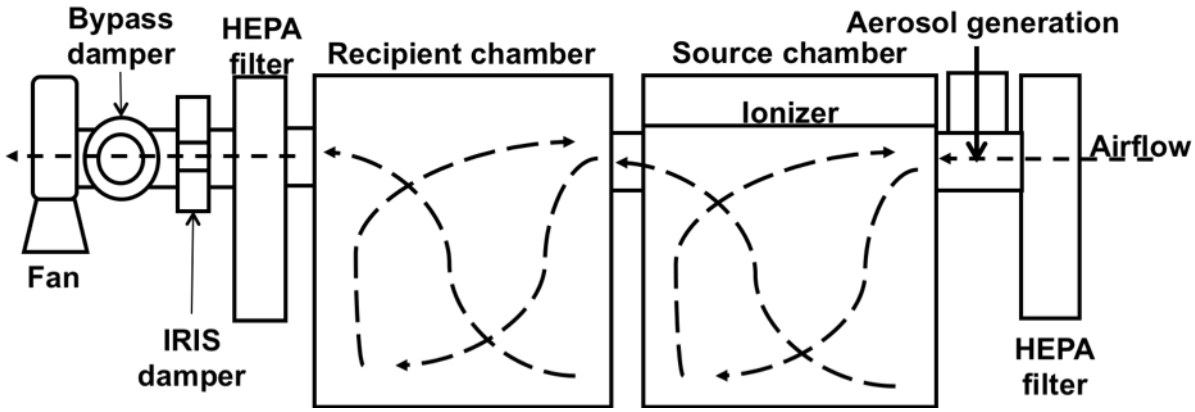

Figure 1. Conceptual sketch of experimental chamber system used to conduct laboratory tests

4.2.1. Construction of chambers

Two chambers were framed with wood and lined with stainless steel (as the interior surfaces) (Figure 2). The internal dimensions for each chamber were 130, 99, and 107 cm in length, width, and depth, respectively. The edges of the chamber, where two stainless steel sheets met, were sealed with Bondo® putty and then covered with aluminum foil tape. Removable doors (61.1, 61.1, and 3.2 cm in length, width, and depth, respectively) as well as airtight door frames were installed at the front of both chambers; the door frames ensured that air leakage did not occur at the door-chamber junction when the doors were closed. Galvanized steel baffles were installed to the inlets of both chambers to direct the airflow downwards in the chambers to facilitate the mixing of air inside the chambers. A galvanized steel duct with a diameter of 12.7 cm was used to connect the two chambers. The chamber that generated aerosols was identified as the source chamber, while the chamber that aerosols flowed into after exiting the source chamber was identified as the recipient chamber.

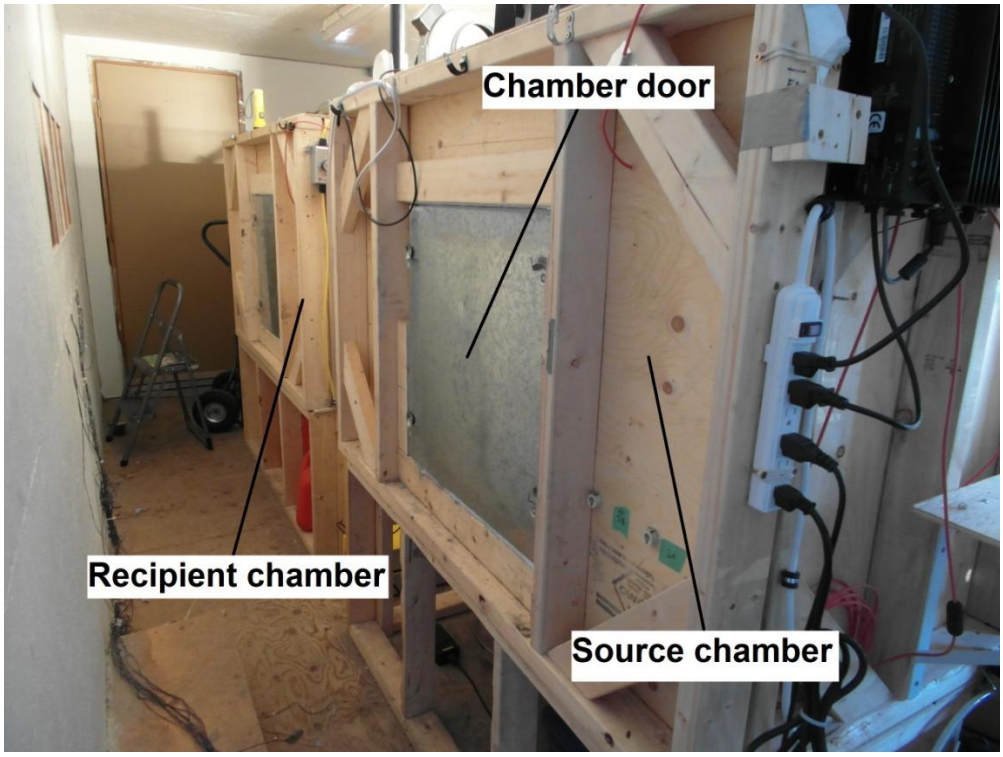

Figure 2. Front view of the construction of the experimental chambers.

A prefilter and a HEPA filter (model no. 01XS-24Z12Z12, Camfil Farr, Canada) with a removal efficiency of 99.97% at 0.3 μm were installed prior to the source chamber to remove contaminants from incoming air. Similarly, two filters were installed at the outlet of the recipient chamber to remove viral contaminants from the air before releasing it. The purpose of the prefilter was to increase the lifespan of the HEPA filter. A 12.7 cm diameter tee wye fitting was installed between the filters and the source chamber and positioned such that the angled branch extended to the right of the filters; the branch was used as a means to introduce virus carrying aerosols generated by a nebulizer (Figure 3).

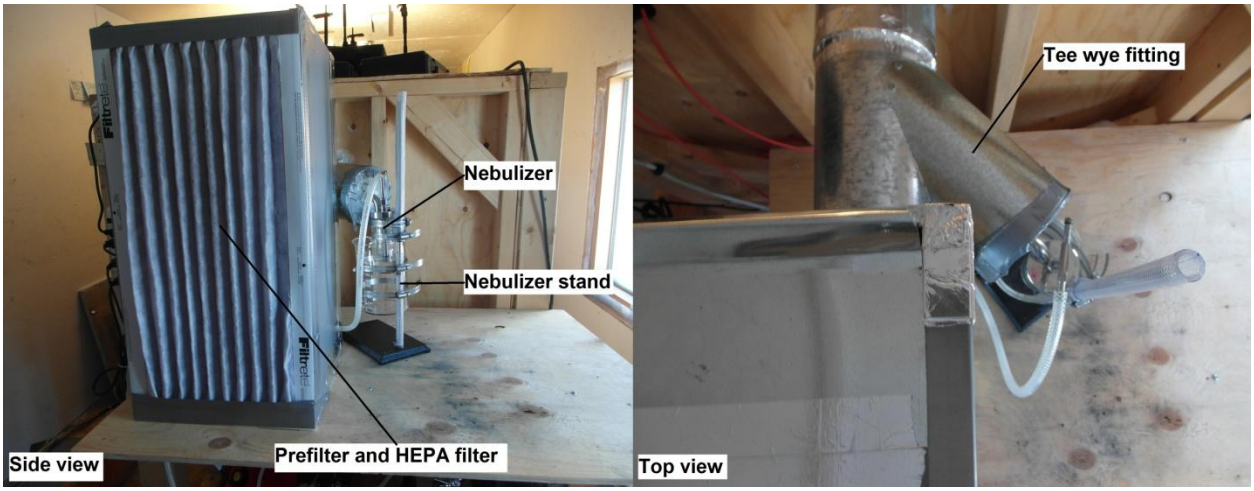

Figure 3. High Efficiency Particulate Air (HEPA) filter and installation for aerosol generation.

4.2.2. Airflow control

A high speed fan (VortexVTX800, Atmosphere, Terrebonne, Quebec) was installed in the downstream to simulate negative pressure ventilation in swine barns. In between the fan and the recipient chamber were a series of ducts and fittings as well as two dampers for controlling airflow within the system. The ventilation rate within the system was controlled with a 12.7 cm diameter IRIS damper (IRIS-S-05, Continental Fan Manufacturing Inc., Mississauga, Ontario), an air diffuser (diameter of 15.24 cm), and a rotary potentiometer. The IRIS damper was installed in the exhaust duct to control cross-sectional area of air flow. The pressure difference across the IRIS damper due to the change in cross-sectional area and the k-factor of the IRIS damper shutter position were used to calculate the ventilation rate in the system (Continental Fan, 2013):

$$q = k\sqrt{\Delta p} \quad (1)$$

$$\Delta p = \left(\frac{q}{k}\right)^2 \quad (2)$$

where

q = airflow (cfm)

k = constant of proportionality

Δp = pressure difference across the IRIS damper.

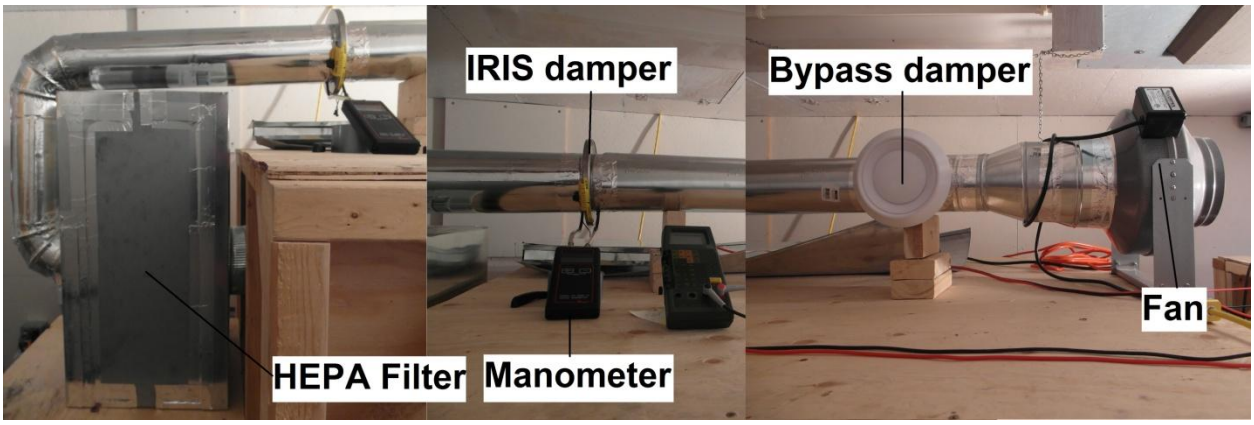

Figure 4. HEPA filter, ductwork, IRIS damper, manometer, bypass damper, and high speed fan.

The pressure difference across the IRIS damper was measured with a digital manometer (475-00-FM, Dwyer, Michigan City, Ind.). The air diffuser (alternative name: bypass damper) served as bypass for air to enter the system. When the bypass damper was open, the fan would pull air through both the chamber system (i.e., the first set of filters, the experimental chambers, the second set of filters, the ductwork, and the IRIS damper) and the bypass entrance, causing the ventilation through the system to decrease. Therefore, the bypass allowed for the fan to generate a significantly decreased ventilation rate while operating at the same voltage and IRIS damper setting. Lastly, the rotary potentiometer was used to adjust the fan voltage until the pressure difference across the IRIS damper reached the value required to generate a specific ventilation rate. Table 1 shows the pressure difference across the IRIS damper, the damper settings, and fan voltages to generate ventilation rates of 34.0 and 135.9 $m^3 h^{-1}$ during experiments, which were

the recommended ventilations rates per head of sow and litter in cold and mild weather, respectively (Midwest Plan Service, 1983).

Table 1. Summary of damper settings, pressure differences, and voltages required to generate airflow rates of 34.0 and 135.9 $m^3 h^{-1}$ during experiments.

Settings	**34.0 $m^3 h^{-1}$**	**135.9 $m^3 h^{-1}$**
Damper Position	5	2
K	117	294
Pressure Difference (in H_2O)	0.0292	0.0740
Voltage (V)	100	90
Bypass Damper	Open	Closed

4.2.3. Chamber calibration

A series of smoke tests and airflow calibration tests were performed to monitor airflow in the chambers at specific air flow rates as well as to determine specific settings of the dampers and fan that would generate desired airflow rates. It was important to establish that the airflow within the experimental chambers had an airflow pattern that demonstrated the mixing of air within the chambers. Aerosols that were generated into the experimental chambers, such as the PRRS virus, were carried by the flowing air and required mixing to be uniformly distributed within the chambers. In order to observe the airflow pattern, a smoke test was performed using Regin coloured smoke cartridges of various colours.

The chambers were completely sealed during operation. To observe flow patterns, a temporary plexiglass door was installed in lieu of the permanent aluminum door in order to provide a transparent area to video record the airflow pattern inside the chambers. During a smoke test, the fan was set to operate at approximately 34.0 $m^3 h^{-1}$ and 254.8 $m^3 h^{-1}$. The smoke cartridges were lit and placed in the angled branch of the five-inch Tee wye. The smoke

movement within the chambers was recorded with a video camera. The video was uploaded onto a computer and analyzed.

4.2.4. Stabilization time

A steady-state condition occurred when the aerosol concentration within the chambers reached a level that did not increase or decrease with time while aerosols were generated at a constant rate. It was critical in this laboratory study that a steady-state aerosol concentration was established in the test chambers when aerosol and PRRSV samplings were performed. Thus, calculations were performed to determine the time required to reach a steady-state concentration of aerosols in the chambers. First, the theoretical concentration of aerosols at steady-state was calculated with the following formula:

$$C_{ss} = \rho \times \frac{A}{V} \tag{3}$$

where

C_{SS} = concentration of aerosols at steady- state (mg m^{-3})

A= aerosol generation rate of nebulizer (ml s^{-1})

V= ventilation rate (m^3 s^{-1}).

ρ= density of water (1000 mg ml^{-1})

Then, the aerosol concentrations in the source and recipient chamber at specific times were calculated incrementally, assuming that the aerosol concentration at time step n = 0 was 0 mg m^{-3}.

$$C_{1a_n} = \frac{X_{1a,n-1} + X_{1a,n} - X_{2a,n}}{V_C} \quad (4)$$

$$C_{2a_n} = \frac{X_{2a,n-1} + X_{2a,n} - X_o}{V_C} \quad (5)$$

$$X_{1a,n-1} = C_{1a,n-1} \times V_C \quad (6)$$

$$X_{2a,n-1} = C_{2a,n-1} \times V_C \quad (7)$$

$$X_{1a,n} = A \times \rho \times (n - (n-1)) \quad (8)$$

$$V_O = V \times (n - (n-1)) \quad (9)$$

$$X_{2a,n} = \frac{X_{1a,n-1} + X_{1a,n}}{V_C} \times V_O \quad (10)$$

$$X_O = \frac{X_{2a,n-1} + X_{2a,n}}{V_C} \times V_O \quad (11)$$

where

n= time since aerosolization was initiated (s)

$C_{1a,n}$ = aerosol concentration in the source chamber at time n (mg m^{-3})

$C_{2a,n}$ = aerosol concentration in the recipient chamber at time n (mg m^{-3})

$C_{1a,n-1}$ = aerosol concentration in the source chamber at time n-1 (mg m^{-3})

$C_{2a,n-1}$ = aerosol concentration in the recipient chamber at time n-1 (mg m^{-3})

$X_{1,n}$ = mass of aerosols entering the source chamber between time n-1 and n (mg)

$X_{2a,n}$ = mass of aerosols entering the recipient chamber between time n -1 and n (mg)

$X_{1a,n-1}$ = mass of aerosols in the source chamber at time n -1(mg)

$X_{2a,n-1}$ = mass of aerosols in the recipient chamber at time n-1 (mg)

X_O = mass of aerosols leaving the recipient chamber between time n-1 and n (mg)

V_C = volume of the source chamber (m^3)

V_O = volume of air exiting the source chamber or recipient chamber in one second (m^3)

The stabilization times required were plotted against the ventilation rate for two aerosol generation rates of 14.8 and 33.0 ml h^{-1} (Figure 5a and b). The chambers were assumed to have reached the steady-state when the difference in concentration between the two chambers was

within 1%. The determined times to reach the steady-state were used to decide when to take aerosol samples in the experiments.

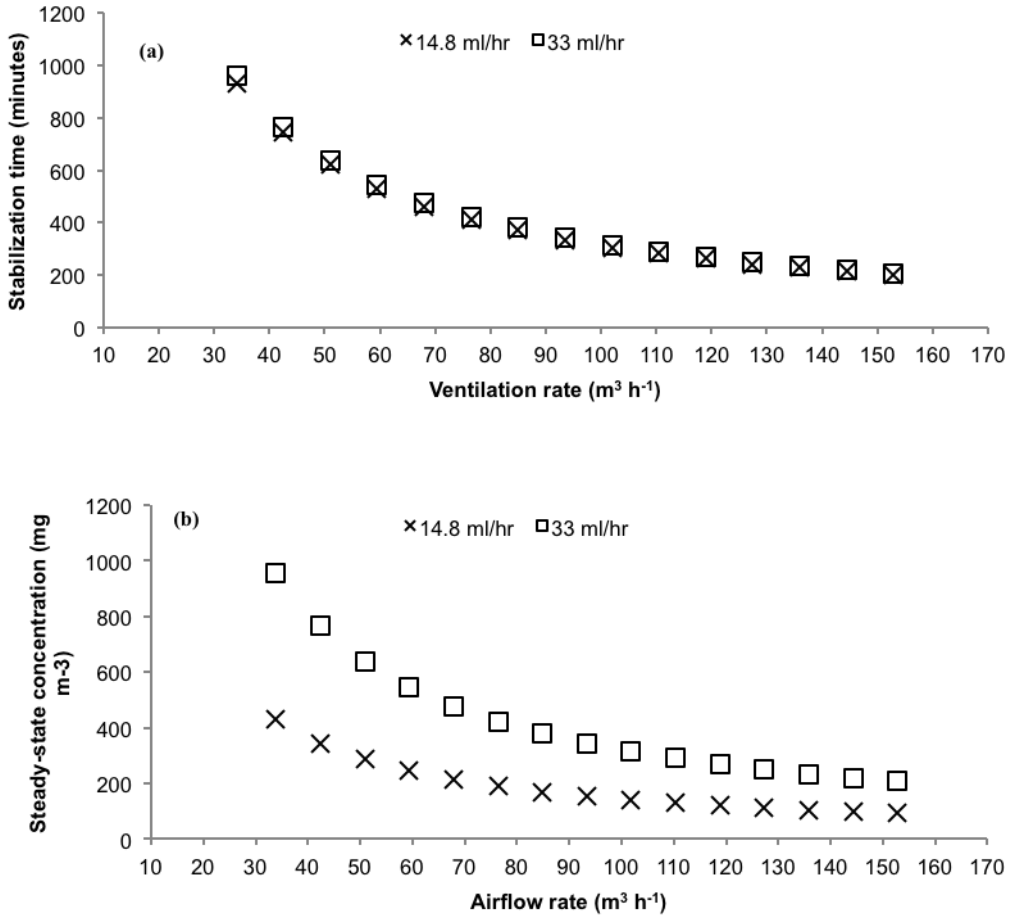

Figure 5. Estimated (a) stabilization time and (b) steady-state aerosol concentrations based on the aerosol generation rate and ventilation rate.

4.2.5. EPI installation and ion concentration measurement

A commercial air ionization system, EPI Air (Baumgartner Environics Inc., Olivia, Minn.) was used in this study. EPI stands for Electrostatic Particle Ionization, which is a type of "ion shower" corona ionizer that creates electrostatic fields and ion streams within an entire room (Garbarczyk et al. 2001). The EPI Air system utilizes dark corona discharge to generate negative

air ions with low heat generation and negligible ozone (M. Baumgartner, General Manager at BEI Inc., Olivia, MN). An EPI Air system was installed by representatives of BEI. The EPI system has several key components, including corona lines, corona points, insulators, high voltage wire, and a power supply (Figure 6). Two sets of corona lines spanned the length of each experimental chamber, parallel to the direction of airflow. Corona points were attached with zipties to the corona line, whose ends were attached to insulators using cable ties. The insulators were connected to suction cups that suctioned to the wall and suspended the corona lines inside the chambers. High voltage wires connected the two corona lines to a power supply that provided high voltage and low current electricity to the corona points, which emitted negative ions into the air when energized by high voltage (EPI Air 2013). Another wire connected the chamber wall to the ground on the power supply.

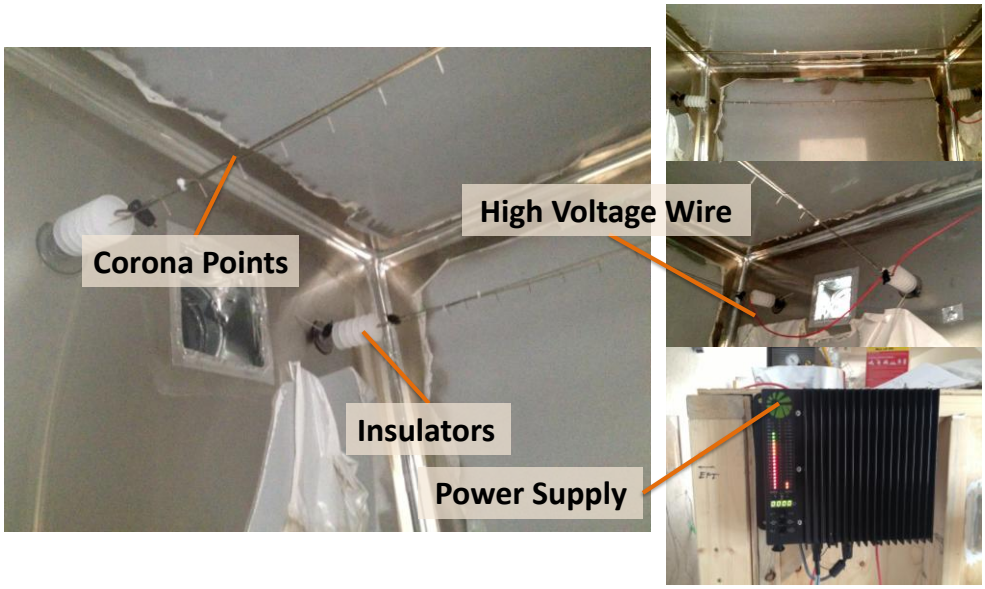

Figure 6. The EPI Air ionization system set-up inside experimental chambers.

During experiments, the electrical field inside the chambers was measured with a Charge Plate Monitor (Model 288b, Monroe Electronics, Nyndonville, NY), which was commonly used to assess the performance of ionization systems. The plate assembly was placed inside the source chamber during experiments, while the main device was placed outside of the source chamber. The charge plate monitor was connected to a laptop computer and controlled with software that allowed real-time measurement of the electric field inside the source chamber. The measurement mode chosen was balance mode which "grounded the plate and then allowed it to float to any voltage in response to air ion imbalances" (MEI 2008).

An ion counter (AIC 200 million model, AlphaLab Inc., Salt Lake City, Utah) was used to measure the ion concentrations at four locations within the source chamber, whilst the ventilation rate was 34.0 or 135.9 $m^3 h^{-1}$. The ion counter was placed in four different locations in the source chamber (Figure 7). The fourth location (D) was located 30 cm off the floor of the second location (B). Due to the space constraints within the source chamber (not enough space to accommodate all biosamplers and ion measurement instrument) ion concentrations at specific air flow rates were measured in a separate set of pre-tests rather than during aerosolization experiments.

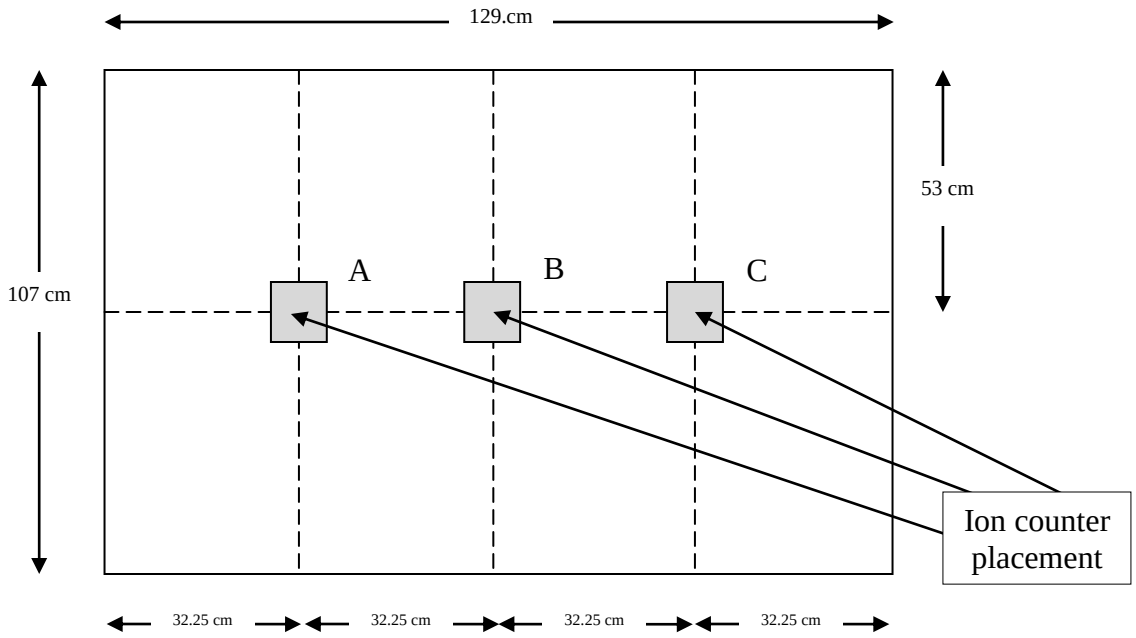

Figure 7. Placement of ion counter

4.2.6. Aerosol generation system

An aerosol generation system was designed to incorporate the generation of both liquid and solid aerosols. Compressed air was used to drive the system. Both streams had pressure regulators and valves that allowed for the control of the pressure of the compressed air supplied to each stream to achieve the desired generation rates (Figure 8). In this thesis research, only liquid aerosols were used.

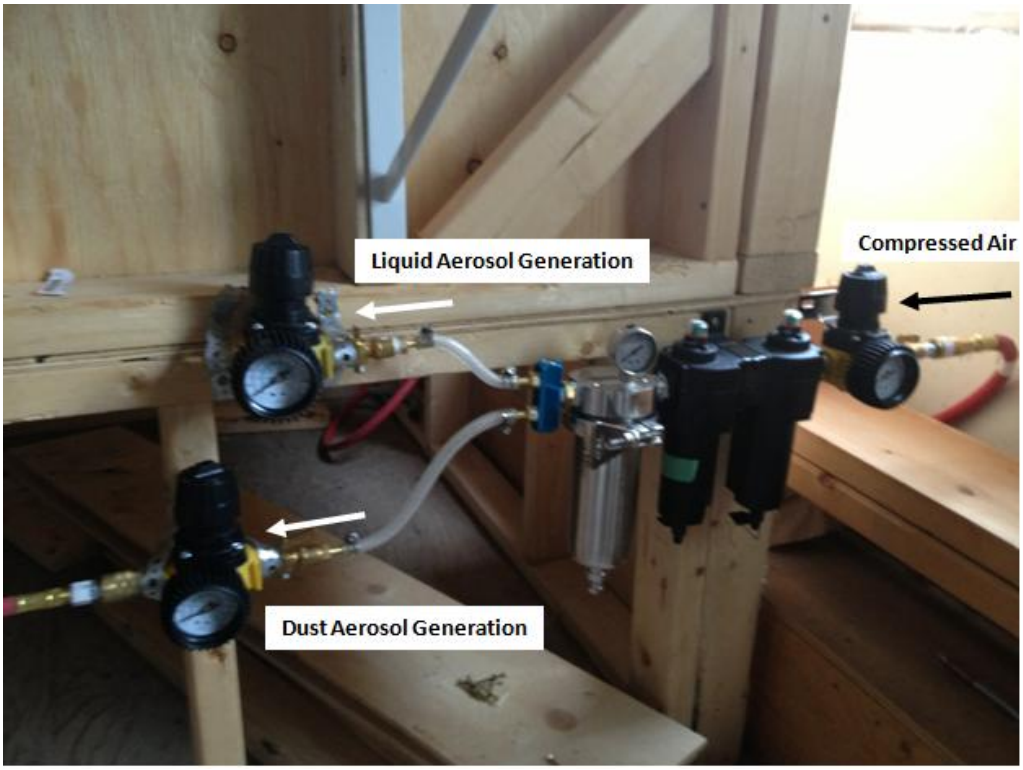

Figure 8. Aerosol generation system set-up.

A 6-jet Collison Nebulizer (CN25, BGI Inc., Waltham, MA) was used to generate liquid aerosols when supplied with a clean source of compressed air. The 6-jet Collison Nebulizer produced aerosols at rates of 14.8 ml h^{-1} and 33.0 ml h^{-1} when supplied with compressed air at pressures of 137.9 and 413.7 kPa, respectively, as determined using a series of preliminary tests. Collison nebulizers were used by other researchers to aerosolize PRRSV (Hermann et al. 2006, 2007, 2009; Hermann and Zimmerman 2008). The liquid used to generate liquid aerosols was Phosphate Buffered Saline (PBS) containing PRRSV. The strain of PRRSV used in this study was a modified live vaccine produced by Boehringer-Ingelheim (St. Joseph, MO) typically used to vaccinate swine for PRRSV; it is a strain that other researchers have used in their research for

PRRSV in chamber studies (Dee et al. 2006a, 2006b). The vaccine virus was grown in MARC-145 cells and quantified in terms of the amount of plaque forming units (PFU).

4.3. Biosampling

PRRSV in the air was collected using the SKC biosamplers (model no. 225-9594, SKC Inc. Eighty Four, PA). The SKC biosamplers were previously used by other researchers to collect air samples of PRRSV (Hermann et al. 2006, 2007, 2009; Hermann and Zimmerman 2008). Biosamplers were first calibrated using a bubble airflow meter to determine the sampling rate of each biosampler, which was found to be 12.857 L min^{-1}. Contaminants within the air were collected and concentrated within 20 ml of PBS that was stored within the biosampler.

Two biosamplers were installed in each chamber (Figure 10) and they were placed inside 400-ml beakers that were filled with ice during experiments to reduce loss in PRRSV infectivity. The biosamplers were secured onto their designated stands with zipties and pointed perpendicular to the airflow towards the centerline of the experimental chambers. The biosampler located in the front of the chamber collected air samples prior to ionization, while the biosampler located at the back of the chamber collected air samples after the EPI system was activated. The locations of the biosamplers in the source chamber were labeled Source-Before (SB) and Source-After (SA), while the locations of biosamplers in the recipient chamber were Recipient-Before (RB) and Recipient-After (RA). Each of the four biosamplers was connected to 0.635 cm ID Tygon tubing that connected to the hose barbs of the valved wall fittings that locked (sealed) when disengaged to prevent air leakage.

The air sample collection system was set up to allow for a single VAC-U-GO pump (model no. 228-9605, SKC Inc. Eighty Four, PA) to collect air samples using the four biosamplers during the span of each experiment (Figure 9). A series of brass adaptors and tubing were installed to connect the biosamplers to the pump through a liquid trap. The purpose of the liquid trap was to capture liquids that might escape the biosamplers and prevent the liquids from entering the pump and causing damage. Two valved panel mount wall fittings (PLCD1600412, Colder Products Company, St. Paul, Minn.) were installed onto each chamber to allow for air sampling of biosamplers at specific times of each test. When the sampling fitting (PLCD4200412, Colder Products Company, St. Paul, Minn.) was inserted into a wall fitting, the biosampler associated with that fitting began to collect air samples. The exhaust of the pump was also connected back to the recipient chamber to compensate airflow and prevent introduction of stray virus into the environment.

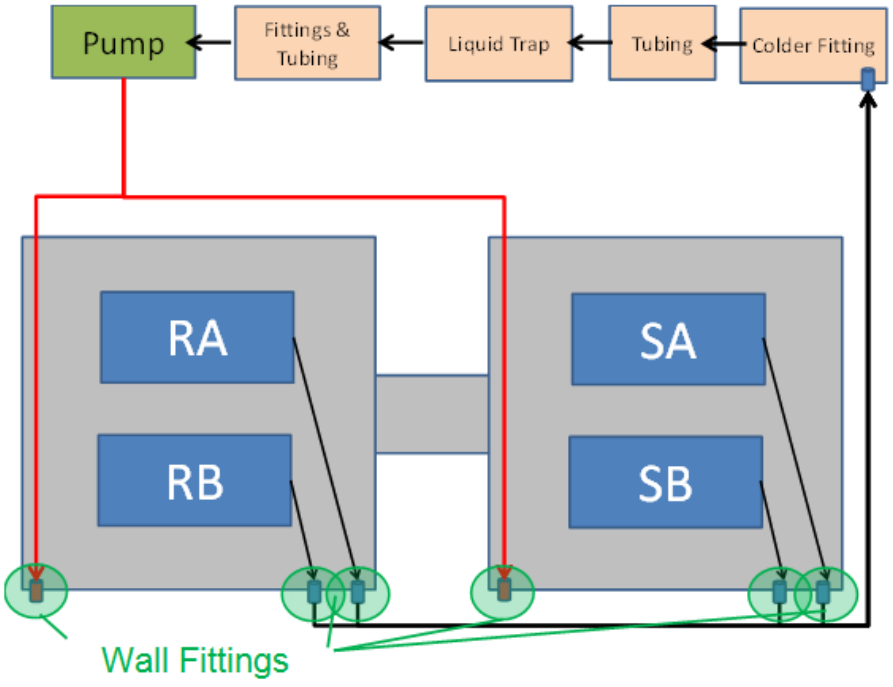

Figure 9. Set-up of air sampling assembly for air sample collection with biosamplers.

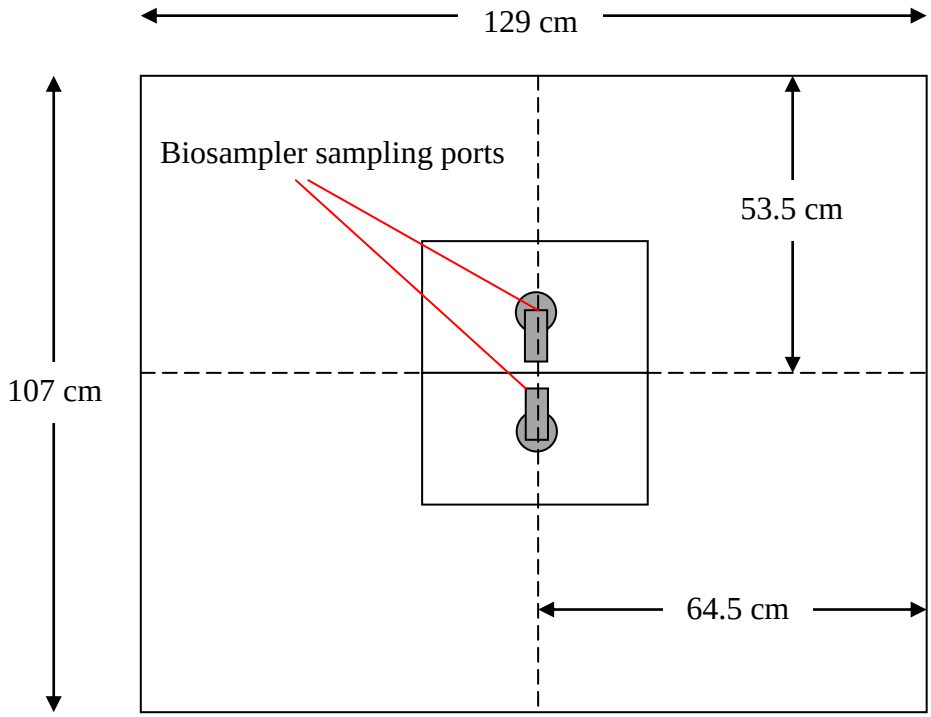

Figure 10. Positions of biosamplers within experimental chambers.

A preliminary test was performed to determine if the biosamplers were able to collect PRRSV within air samples collected from the experimental chambers. For this test, 3.5 x 10^8 PFU ml^{-1} of the grown vaccine strain of PRRSV was diluted into 35 ml of PBS solution, providing a stock solution with a concentration of 1.0 x 10^7 PFU ml^{-1}. A ventilation rate 34.0 m^3 h^{-1} and compressed air pressure of 137.9 kPa were selected to provide the "worst-case scenario" for virus concentration in the air. Locations of each biosampler were randomized within the experimental chambers. The test showed that PRRSV was collected in each biosampler, regardless of location. The concentration of PRRSV RNA collected ranged from 1.05×10^7 to 1.65×10^7 Viral Genome Copy number per m^3 (VGCN m^{-3}).

A second preliminary test was performed to run a full-scale experiment with a higher concentration of PRRSV to ensure that a difference in PRRSV in air samples before and after ionization could be detected. A high titer of virus (3.5×10^8 PFU ml^{-1}) was diluted to a volume of 40 ml of PBS (8.75×10^6 PFU ml^{-1}) and used as the aerosolizing medium. An airflow rate of 34.0 m^3 h^{-1} and an aerosol generation rate of 33.0 ml h^{-1} (treatment 2) were used. The timeline of this test is the same what occurred during the main experimental tests. The biosamplers captured 5.83×10^5 VGCN m^{-3} – 2.34×10^7 VGCN m^{-3}. Additionally, the precision of the qRT-PCR was good; results of the qRT-PCR had standard errors ranging from 0.39 – 0.45 VGCN ml^{-1}. The preliminary test also showed that the EPI was working as it was able to reduce the aerosol concentration by 91% and 96%, respectively.

4.4. Virus detection and quantification

4.4.1. RNA extraction

A preliminary step to quantifying the original amount of viral RNA using quantitative reverse transcriptase polymerase chain reaction (qRT-PCR) was to extract the RNA from both the MARC-145 cells that they were grown in as well as from their biological structure. A popular kit that is used in various studies to isolate PRRSV RNA is the Qiagen QIAamp Viral RNA mini kit (52906, Qiagen, Netherlands). The steps involved in extracting viral RNA included (Qiagen 2012): (i) the lysis of a sample in a lysis buffer to denature and inactivate RNases and to ensure the isolation of viral RNA; (ii) adjustment of the buffer (through the addition of ethanol) to facilitate the binding of viral RNA to the spin column membranes; (iii) binding of nucleic acids to the spin column membrane; (iv) removal of contaminants from the

membrane using wash buffers; (v) using an elution buffer to remove the isolated viral RNA from the membrane and into a solution that can be analyzed with various test methods such as qRT-PCR.

A total of 72 samples, including air samples and pooled wall swab samples, were collected during the span of 12 experimental tests. Three replications of RNA extraction were performed per sample. RNA extraction was separated into 12 sessions of 6 samples, providing a total of 18 RNA extractions per session. The order that samples were analyzed was randomized. In preparation of an RNA extraction session, a solution consisting of Buffer AVL, Carrier RNA-Buffer AVE solution, and Xeno RNA (4405548, Applied Biosystems, Foster City, CA) was compiled with volumes of 11.2 ml, 112 µl, and 8 µl of each item, respectively. The RNA extraction was then performed as specified by the manufacturer (Qiagen 2012). The solution previously described was added at volumes of 560 µl into eighteen 2-ml tubes, labelled with their corresponding sample name. Air samples or wall swab samples were added at volumes of 140 µl to the 2-ml tubes. The tubes were vortexed for 15 seconds and incubated at room temperature for 10 minutes. The tubes were then centrifuged at 6000 x g for 1 minute. Ethanol (100%) was added to each of the tubes at volumes of 560 µl. Tubes were vortexed for 15 seconds again and centrifuged at 6000 x g for 1 minute. Half of the solution within each tube (630 µl) was transferred to a spin column and centrifuged at 6000 x g for 1 minute. The 2-ml tubes containing the spin columns' filtrate were disposed of and switched for new 2-ml tubes. The remaining solution was transferred to the spin column and centrifuged again. The 2-ml tubes containing the spin column filtrate were disposed of and replaced with new 2-ml tubes. Buffer AW1 was added to each spin column at a volume of 500 µl. The spin columns were centrifuged at 6000 x g for 1 minute and the 2-ml filtrate-containing tubes were replaced. Buffer AW2 was added to each spin

column at a volume of 500 µl and the spin columns were centrifuged at 20000 x g for 3 minutes. After replacing the 2-ml tubes, the spin columns were centrifuged again at 20000 x g for 1 minute. The spin columns were moved into clean 2-ml centrifuge tubes with caps and 40 µl of Buffer AVE was added to each spin column, which was then centrifuged at 6000 x g for 1 minute. An additional 40 µl of Buffer AVE was added to each spin column and the spin columns centrifuged again. The spin columns were disposed. A small volume (10 µl) of extracted RNA from each centrifugal tube was moved into a corresponding 0.625 ml tube for further analysis and the remainder was stored in a -80 degree freezer. A nanodrop spectrophotometer was then used to measure the quality of the extracted RNA within each extracted sample.

4.4.2. Quantitative reverse transcription polymerase chain reaction

Quantitative reverse transcriptase polymerase chain reaction (qRT-PCR) allows for the quantification of the initial viral genome copy number within a sample. Viral RNA is firstly reverse transcribed into cDNA with enzymes called reverse transcriptase (Life Technologies 2012). The next step involves 40 cycles in which the PCR machine is set to cycle through three thermal profiles to instigate different reactions: (i) denaturation, in which high temperatures are used to separate double-stranded cDNA into single strands; (ii) annealing, in which primers and probes are able to attach to complementary sequences on the single strands of DNA; (iii) extension, in which DNA polymerase extends the lengths of the primers to copy the single strand of cDNA that had a complementary sequence to the primer (Life Technologies 2012). In qRT-PCR, probes play an important role in the quantification of initial sample concentration. TaqMan probes contain two dyes (the reporter dye and the quencher dye; Life Technologies 2012); the

quencher dye, when in close proximity to the reporter dye, induces an event called Fluorescence Resonance Energy Transfer (FRET) in which the reporter's energy is transferred to the quencher dye rather than emitted (Life Technologies 2012). During the third step of qRT-PCR, when the DNA polymerase extends, it cleaves off the probe and releases the reporter dye, separating it from the quencher dye and allowing the reporter dye to emit fluorescence. The fluorescence that the reporter dye releases when cleaved is measured with the PCR machine and is used to measure the amplification of nucleic acid in the sample (Life Technologies 2012).

The VetMAX NA and EU PRRSV Reagents (4468465, Applied Biosystems, Foster City, CA) were used to perform one-step qRT-PCR, in which reverse transcription and real-time PCR are performed in the same tube (Life Technologies 2012). RNA extraction of the 72 samples collected during examples in triplicate produced 216 samples with extracted RNA. Each of these extracted samples was processed in triplicate with qRT-PCR to determine the initial viral genome copy number present in each sample. Samples were divided into nine groups to allow for nine sessions of qRT-PCR. Each session consisted of a total of 78 samples including: 3 replicates of 24 extracted samples; 3 positive controls, which was a mix of North American and European PRRSV (4405548, Applied Biosystems, Foster City, CA), mixed according to the manufacturer instructions; and 3 negative controls, which was simply nuclease-free water. A master mix of reagents was mixed according to the manufacturer's instructions at volumes sufficient for 78 reactions. The master mix was pipetted at a volume of 18 µl into 78 PCR tubes. Samples were added into each corresponding tube at a volume of 7 µl to obtain a final volume of 25 ul per tube. The PCR machine that was used was a CFX Connect Real-Time System (BIO-RAD, Hercules, CA). The thermal profile (the temperature within the machine at different times during the qRT-PCR analysis) allows for the activation of different enzymes and events. The

thermal profile was set according to that used to analyse PRRSV in other studies (Hermann et al. 2006, 2007) and is as follows: (i) 50 ˚C for 30 minutes (Reverse Transcription), (ii) 95˚C for 15 minutes (Enzyme Activation), and (iii) 40 cycles of 94˚C for 15 seconds (Denaturation) and 60˚C for 60 seconds (Combined Annealing and Extension).

Quantification of the concentration of PRRSV in a sample required the development of a standard curve that described the cycle threshold that corresponded with known initial concentrations of PRRSV. The cycle threshold value is the cycle in which a concentration of PRRSV reaches a certain level of fluorescence and amplification called the threshold. Samples with greater initial concentrations of PRRSV would amplify faster and therefore have a smaller cycle threshold. For this study, PRRSV at a concentration of 1×10^7 PFU ml^{-1} was serial diluted six times to provide concentrations of 1×10^6 PFU ml^{-1}, 1×10^5 PFU ml^{-1}, 1×10^4 PFU ml^{-1}, 1×10^3 PFU ml^{-1}, 1×10^2 PFU ml^{-1}, and 1×10^1 PFU ml^{-1}. RNA extraction was performed in triplicate per concentration to provide a total of 21 extracted samples; however, the third sample of the 1×10^1 PFU ml^{-1} sample was lost, revising the total to 20 extracted samples. Further analysis using qRT-PCR was performed in triplicate for the samples, providing a total of nine replicates at each dilution level with the exception of the 1×10^1 PFU ml^{-1} dilution level. Three positive and negative controls were also included in the qRT-PCR analysis. The cycle thresholds of each dilution level of PRRSV were determined using the PCR software's regression method. The cycle threshold of each sample was plotted according to the initial known concentration of PRRSV to construct a standard curve for quantification of the concentration of PRRSV in samples with unknown concentrations.

The viral genome copy number concentration (VGCN ml^{-1}) of each sample was determined using the cycle threshold of each sample and the standard curve. For air samples, the

total viral genome copy number collected during air sampling was estimated using the volume of PBS measured during the sample collection:

$$A_{P,Sample} = C_{P,Sample} \times V_{PBS} \quad (12)$$

$$C_{P,Air} = \frac{A_{P,Sample}}{q \times t} \quad (13)$$

where

$A_{P,Sample}$ = Amount of genome copies of PRRSV collected within one air sample (VGCN)

$C_{P,Sample}$ = Concentration of genome copies of PRRSV collected within one air sample, as determined using qRT-PCR results and standard curve (VGCN ml^{-1})

$C_{P,\text{ Air}}$ = Concentration of genomic copies of PRRSV per unit volume of air (VGCN m^{-3})

V_{PBS} = Volume of PBS measured from biosampler for specific sample (ml)

q = sampling rate of biosamplers, 12.857 L min^{-1}.

t = sample collection period for biosamplers, 5 min.

For wall swab collection, the following formula was used to calculate the amount of PRRSV RNA collected from walls:

$$A_{P,Wall} = C_{P,Wall} \times V_{PBS,wall} \quad (14)$$

where,

$A_{P,Wall}$ =The amount of PRRSV RNA collected from wall swabs (VGCN),

$V_{PBS,wall}$ = Volume of PBS collected from tube used to store wall swabs (ml),

$C_{P,Wall}$ = Concentration of PRRSV RNA found in wall swab liquid, quantified using qRT-PCR and standard curve (VGCN ml^{-1})

4.5. Aerosol sampling

Aerosol concentration and particle size distribution before and after ionization treatment were the focus of this study. Concentration and size distribution were monitored with an Aerosol Particle Size Spectrometer (APSS; LAP 322, Topas GmbH, Germany). The device focuses a laser diode in one direction at a stream of aerodynamically focused aerosols to generate scattered light signals (Topas GmbH, 2013). An Avalanche photoelectric cell is used to convert the light signals into electrical pulses; the relationship between pulse height and optical geometric mean diameter is used to calculate the particle size distribution of the aerosol stream (Topas GmbH 2013). The aerosol particle size spectrometer has a total flow rate of 3 L min^{-1} and measured particles sizes ranging from 0.2 to 40 μm. The device also has sophisticated software called PASWIN that is used to run the device as well as analyze the measurements (Topas GmbH 2013). The PASWIN software is able to perform many calculations for different types of distributions, including determining the aerosol concentration per size range in terms of number count, volume, and mass.

The APSS was connected to a laptop computer during experiments to perform measurements in real-time and set to continuously count particles for intervals of 10 s for size ranges of 0.234 to 40 μm. The APSS was physically placed outside of the experimental chambers and Tygon tubing (0.635 cm ID) was used to collect air from inside of the source chamber during experiments through a sampling fitting (PLCD4200412, Colder Products Company, St. Paul, Minn.) installed on the chamber wall. The exhaust of the APSS was returned to the source chamber.

4.6. Preliminary testing with water aerosols

Prior to performing tests using the PRRSV in the experimental chambers, water was utilized as the aerosolizing agent to understand the performance of EPI. Utilizing water aerosols did not require stringent cleaning of the chambers and equipment nor the use of biosamplers, thus allowing for repeated tests in a short period of time. Additionally, it allowed for the users to familiarize themselves with the equipment during an experiment prior to using the sensitive PRRSV material.

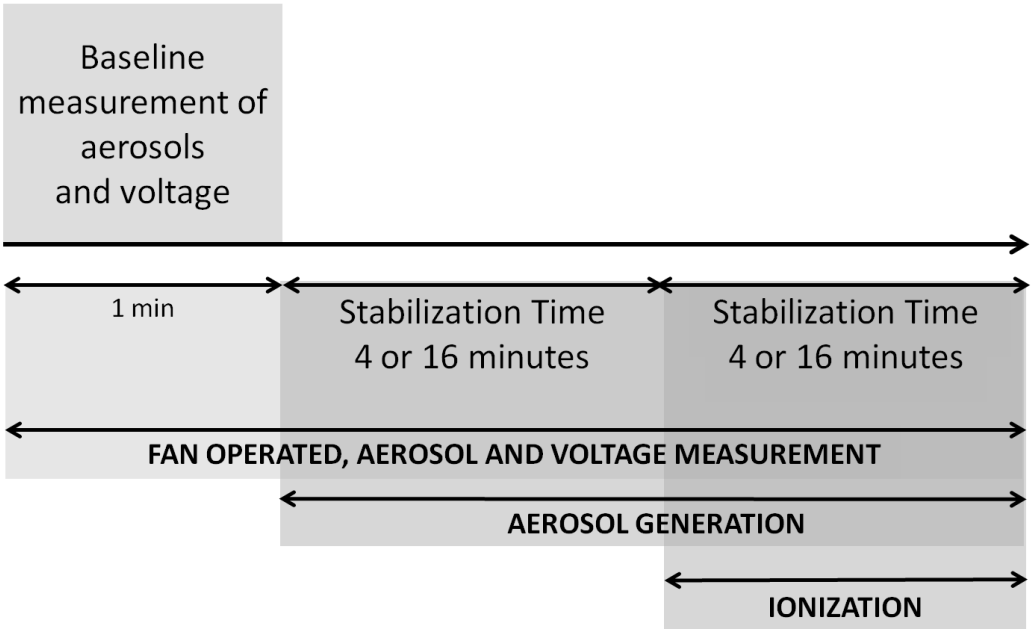

Figure 11. Sequence of water aerosol tests.

Twelve tests were performed with the same parameters as those chosen for the PRRSV experiments. Two airflow rates of 34.0 $m^3 h^{-1}$and 135.9 $m^3 h^{-1}$ and two aerosol generation rates of 14.8 ml h^{-1} and 33.0 ml h^{-1} were used in combination, with three replicates for each treatment. The order of the tests was randomized.

The timeline of each test is shown in Figure 11. Baseline measurements were performed using the APSS and charge plate monitor for a minute prior to beginning aerosol generation. The charge plate monitored the electric field in the chamber and the APSS continually measured particle properties. The EPI Air was then initiated and the particle properties and electric field were continually measured during a second stabilization period. It should be noted that the stabilization time was based on the time to reach the steady-state conditions (Figure 5).

4.7. PRRSV Experiment

4.7.1. Test procedures

Two airflow rates of 34.0 $m^3 h^{-1}$ and 135.9 $m^3 h^{-1}$ and two aerosol generation rates of 14.8 ml h^{-1} and 33.0 ml h^{-1} were used during PRRSV chamber experiments to determine the effect of airflow and aerosol production on the performance of the EPI system. The four treatments were as follows: (1) a ventilation rate of 34.0 $m^3 h^{-1}$ and an aerosol generation rate of 14.8 ml h^{-1}, (2) a ventilation rate of 34.0 $m^3 h^{-1}$ and an aerosol generation rate of 33.0 ml h^{-1}, (3) a ventilation rate of 135.9 $m^3 h^{-1}$ and an aerosol generation rate of 14.8 ml h^{-1} and (4) a ventilation rate of 135.9 $m^3 h^{-1}$ and an aerosol generation rate of 33.0 ml h^{-1}. The treatments were tested in triplicate and the order of chamber tests was randomized.

During each test, a series of sample collection and measurements were performed including: 1) two air samples per chamber, before and after ionization, using biosamplers; 2) one wall swab sample per chamber for measuring virus concentrations in aerosols that accumulated on the walls due to ionization, pooled from swabbing six circles with diameters of 12.1 cm in each chamber; 3) particle size distribution in terms of number count and mass concentration

measurements during the span of each test using the particle size spectrometer; and iv) voltage (ion concentration) readings using the charge plate monitor during the span of the tests.

The experiments occurred during the months of February and March in 2014. The facility containing the experimental chambers was heated with an electrical heater to maintain the room temperature at 25 ˚C. A humidifier was operated the day before a test to raise the humidity in the facility to 60%. Due to the extremely cold temperatures, it was very difficult to raise the humidity substantially.

Prior to tests, preliminary preparations were performed within a Biosecurity cabinet of a level two laboratory to ensure PRRSV samples were not contaminated. A 40-ml solution consisting of 39 ml of PBS and 1 ml of PRRSV (with an initial concentration of 1×10^7 PFU ml^{-1}) was added to the nebulizer. PBS (20 ml) was also added to the four biosamplers and to two 50-ml centrifuge tubes, which were used to store wall swab samples. Six Whatman paper (WHT1005042, Fisher Scientific, Ottawa, Ontario) were stored inside two used pipet boxes that were wiped with 70% ethanol for collecting wall swab samples. A third 50-ml centrifuge tube was filled with 30 ml of PBS to be used for wetting the Whatman paper in the swabbing process.

Prior to commencing a chamber test, the IRIS damper, white damper, and fan voltage were adjusted to generate the required airflow rate. The nebulizer was placed inside a beaker filled with ice and secured to a laboratory stand. The tip of the nebulizer was inserted into a hole of an aluminum cap used to close off the end of the tee wee fitting. The temperature and relative humidity in the room was measured with a handheld Hygrometer Humidity and Temperature Meter (Model RH85, Omega, Stamford, Connecticut) at the beginning of each test. Pressure regulators were adjusted to generate the proper compressed air pressure to achieve the required

aerosol generation rate. The particle size spectrometer and the charge plate monitor measurements were initiated to measure the aerosols and voltage inside the chamber. Measurements occurred for one minute prior to aerosolization and continued after aerosolization (Figure 12). To initiate virus aerosolization into the source chamber, compressed air was supplied to the nebulizer. A stabilization period of 16 minutes and 4 minutes for 34.0 $m^3 h^{-1}$ and 135.9 $m^3 h^{-1}$, respectively, was required for the aerosols to achieve a steady-state concentration. After completion of the stabilization period, air sampling was initiated. The sampling pump was connected to the wall fitting associated with the first biosampler in the recipient chamber for five minutes and then connected to the wall fitting associated with the first biosampler in the source chamber for another five minutes.

The EPI system was activated after completing the first set of measurements, and another stabilization period occurred to allow the aerosols to achieve steady state concentration with ionization (Figure 12). For the second stage of air sampling, the pump was connected to the wall fittings associated with the second biosamplers in the recipient and source chambers for five minutes each. At the end of the test, the supply of the compressed air to the nebulizer was terminated to stop aerosolization and the fan and ionizer were operated for an additional five minutes to clear residual aerosols from the air.

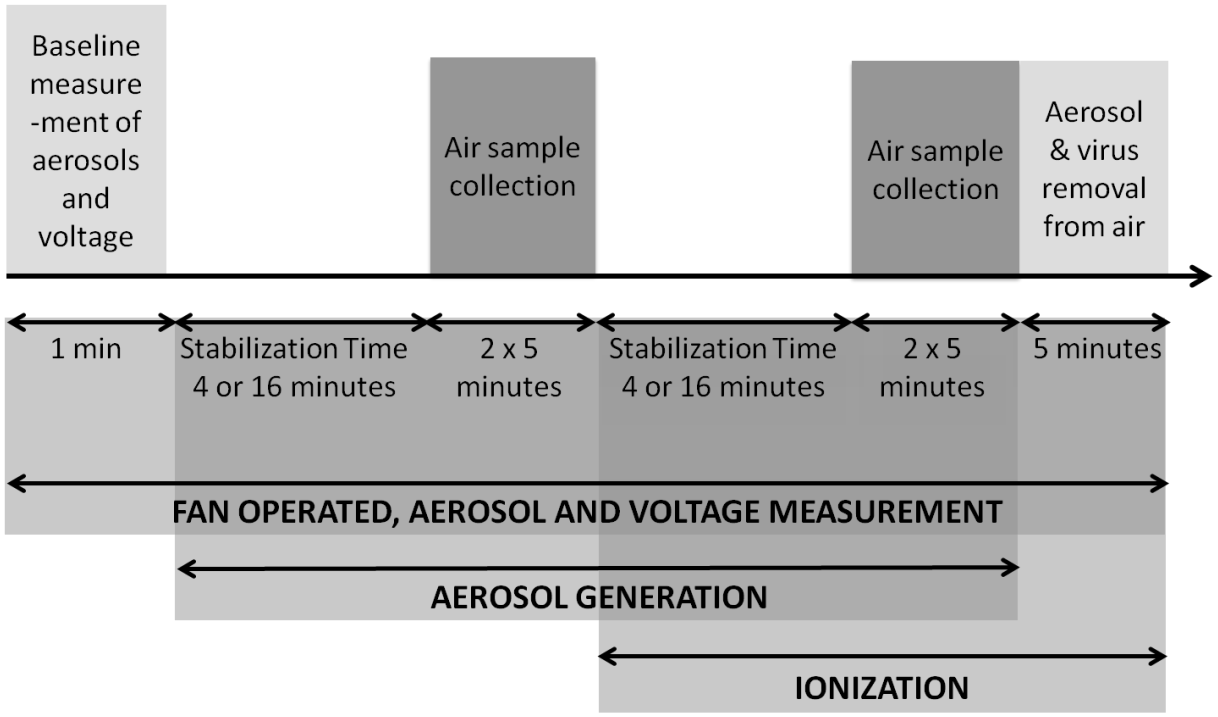

Figure 12. Sequence of PRRSV test

Immediately after opening the chambers doors, wall swabs were collected using 42.5 mm circular Whatman filter dipped in PBS. Six circular areas in each chamber were swabbed with one Whatman paper per circular area. Filter papers belonging to the same chamber were pooled and then stored in 20 ml PBS in 50-ml conical tubes for transport to the laboratory.

Upon arrival to the laboratory, the volumes of biosampler air samples were measured and transferred to 50-ml conical tubes. Wall swab samples were vortexed for 10 seconds and the PBS was extracted into fresh conical tubes for storage. For each sample, three 1.5 ml aliquots were stored and were later processed with RNA extraction and qrt-PCR. The remaining volumes of each sample were kept in the 50-ml conical tubes for Plaque Assay analysis. Samples are frozen at -80˚C prior to analysis.

4.7.2. Cleaning procedure

At the end of each test, a cleaning procedure was performed to remove residual PRRSV from the experimental chambers and equipment. Material that was transportable (e.g., tubing, fittings, biosamplers, and glassware) were placed inside of a box specifically designated for transporting contaminated materials to another facility for disinfection. All other materials that were not transportable (e.g., experimental chambers, charge plate monitor, and biosampler stands) were disinfected on-site.

Autoclavable materials – such as tygon tubing, glassware, biosamplers, and the nebulizer –were sterilized with an autoclave (Model # 533LS, Getinge, Sweden). Non-autoclavable material was placed inside of a large 4-L beaker filled with Virkon detergent (Virkon, DuPont Disinfectants, United Kingdom), which is often used to disinfect swine facilities, diluted to a concentration of 0.5% for 30 minutes. The material was then rinsed and set aside to dry for the next test. The charge plate monitor components that were placed inside the experimental chamber were wiped with a 70% solution of isopropanol.

Items that were too large for other modes of disinfection were placed inside the experimental chambers as they were disinfected. As a preliminary step, all surfaces within the experimental chambers were sprayed with a 0.5% solution of Virkon detergent using a spray bottle. A fogger (Sani-Tizer, Curtis Dyna-Fog Ltd., Westfield, IN) filled with 0.5% solution of Virkon detergent was then placed inside one of the experimental chambers facing the left wall. The chamber doors were closed and the fogger was operated for seven minutes. The fogger was then rotated to face the right wall and operated again for another seven minutes. The procedure

was repeated for the second chamber. After a contact time of 30 minutes, chamber doors were removed and excess Virkon detergent was removed and the chambers were rinsed with water. Excess water was removed from the chambers and residual water was allowed to evaporate. Biosampler stands were hand-dried.

4.8. Data Analysis

4.8.1. Particle size analysis

Data that were collected during the experiments were analyzed to determine the effect of ionization on the geometric mean diameters, geometric standard deviations, and total aerosol concentrations. The geometric mean diameter and average standard deviation were calculated in the PASWIN program with the following formulas (Topas GmbH 2013):

$$d_g = \frac{1}{n}\sum_{ll}^{ul}(\log(d_i)\times f_i) \tag{15}$$

$$s_g = \sqrt{\frac{1}{n}\sum_{ll}^{ul}\left(\log\left(\frac{d_i \times f_i}{d_g}\right)\right)^2} \tag{16}$$

where

d_g= geometric mean diameter (μm)

s_g = geometric standard deviation (μm)

n= number of size classes

ul = the upper limit of the size range that the particle sizer was measuring (μm)

ll = the lower limit of the size range that the particle sizer was measuring (μm)

f_i = fraction of mass with an aerodynamic diameter d_i.

The PASWIN software calculated the mass concentration of aerosols during each test based on the number count of aerosols. The volume concentration was calculated from the aerodynamic diameter of aerosols and converted to the mass concentration using the user-inputted density of the aerosols (ρ=1000 kg m^{-3} for water).

During a test, the aerosols were continuously generated and allowed to reach steady state concentration prior to activating the EPI system, and the aerosol concentration would decrease suddenly after the activation. A point on the concentration-time graph was identified as the boundary between the before ionization and after ionization, based on when the reduction in aerosol concentration was first discernible. This point was considered the start of the second stabilization period, which occurred due to the commencement of ionization (Figure 13). A total of six measurements (approximately 60 second of continuous measurement) prior to the completion of the stabilization periods were used to find the average geometric mean diameter, average geometric standard deviation, and the average concentration of aerosols before ionization and after ionization. Changes in geometric mean diameter, geometric standard deviation, and aerosol concentration due to ionization were calculated as follows:

$$R_d = \frac{d_{g,i} - d_{g,f}}{d_{g,i}} \times 100\% \quad (17)$$

$$\Delta_s = \left| \frac{s_{g,i} - s_{g,f}}{s_{g,i}} \right| \times 100\% \quad (18)$$

$$R_C = \frac{C_i - C_f}{C_i} \times 100\% \quad (19)$$

where

R_d = reduction in geometric mean diameter due to ionization treatment (%)

$d_{g,i}$ = the average geometric mean diameter of aerosols before negative air ionization (μm)

$d_{g,f}$ = the average geometric mean diameter of aerosols after negative air ionization (μm)

Δ_s = change in geometric standard deviation due to ionization treatment (%)

$d_{s,i}$ = the average geometric standard deviation of aerosols before negative air ionization (μm)

$d_{s,f}$ = the average geometric standard deviation of aerosols after negative air ionization (μm)

R_C = reduction of aerosol concentration due to ionization treatment (%)

C_i = the average total concentration of aerosols before negative air ionization (mg m^{-3})

C_f = the average total concentration of aerosols after negative air ionization (mg m^{-3})

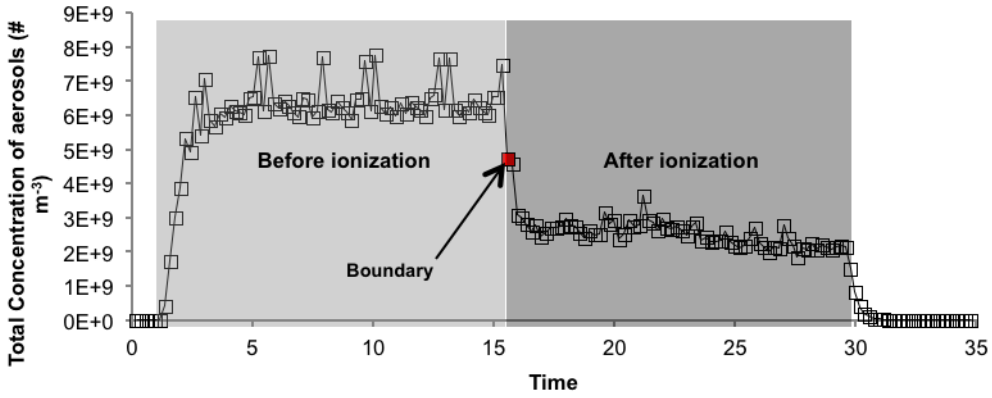

Figure 13. Example of experimental data showing boundary between before and after ionization stages of experimental test

4.8.2. Statistical Analysis

Statistical analysis was performed using the Proc Mixed method in SAS 9.3 (SAS Institute Inc., Cary, NC). The level of significance was 5% or P=0.05. Datasets that did not have a normal distribution were transformed, if possible, to obtain a normal distribution before statistical analysis. Transformation was accomplished by performing a function on all the values in the dataset. For example, percentages were often divided by 100, square-rooted, and then the inverse sines of the values were determined to change the dataset to a normal distribution. If a transformation was used to turn the dataset to a normal distribution, the transformation is indicated in Appendix B with other details of the statistical analyses.

The order of treatments was randomized during testing in order to achieve a Completed Randomized Factorial Design for geometric mean diameter, geometric standard deviation, and aerosol concentration for the source chamber. Wall swabs taken from the source chamber were also statistically analyzed as a Complete Randomized Factorial Design. The Factorial design facilitated the assessment of the airflow rate effect, aerosol generation rate effect, and the interaction effect between airflow rate and aerosol generation rate on aerosol concentration and distribution measurements before ionization and after ionization. These measurements were statistically analyzed with the Restricted Maximum Likelihood (REML) estimation method. The Satterthwaite method, which assumes heterogeneous variance amongst treatments, was used to improve the reliability of statistical analysis in cases where a chi-square test indicated it improved the results of the statistical analysis.

Air sampling measurements from the two chambers before ionization were considered replicates, with the difference being the location the measurements occurred. Therefore, PRRSV RNA concentration in the air before ionization was statistically analyzed as a Randomized Complete Block Factorial design, using the chamber location as a random factor and the airflow rate and aerosol generation rate as fixed factors. The estimation method utilized was the Type 3 method, which is the preferred method to use when datasets contained unbalanced data. Unbalanced data occurs when there is not an equal amount of replicates per treatment, which was the case for the PRRSV concentrations because the PRRSV results from one experiment were neglected due to a mix-up with biosampler placement. PRRSV RNA concentration after ionization and the reduction of PRRSV RNA concentration in the source and recipient chambers were statistically analyzed separately as Complete Randomized Designs with the Type 3 estimation method.

Aerosol concentrations and airborne PRRSV RNA concentration were additionally analyzed using the Scheffé's comparison test (SAS Institute Inc., Cary, NC) to determine if there were statistically significant differences between the measurements that had two different treatments. Specific details of the procedures and statistical results are shown in Appendix B.

CHAPTER 5. RESULTS

5.1.1. Standard Curve for qRT-PCR

The standard curve was developed to determine the concentrations of PRRSV RNA contained in air samples (Figure 14). The equation relating the cycle threshold to the log(Concentration) is useful for evaluating the quality of the standard curve. Firstly, qRT-PCR reactions with efficiency of 100% (i.e. when each RNA template doubles after each cycle) provide a standard curve with a slope of -3.32 (Life Technologies 2012; Taylor et al. 2010). Efficiency between 90% and 110% is considered a good reaction and the slope range corresponding to these efficiencies is -3.58 to -3.10 (Life Technologies 2012; Taylor et al. 2010). The measured slope was -3.16, which falls within the recommended guidelines. Furthermore, an R^2 value of 0.983 was obtained, which is also greater than the recommended qRT-PCR R^2 value of 0.98 (Taylor et al. 2010).

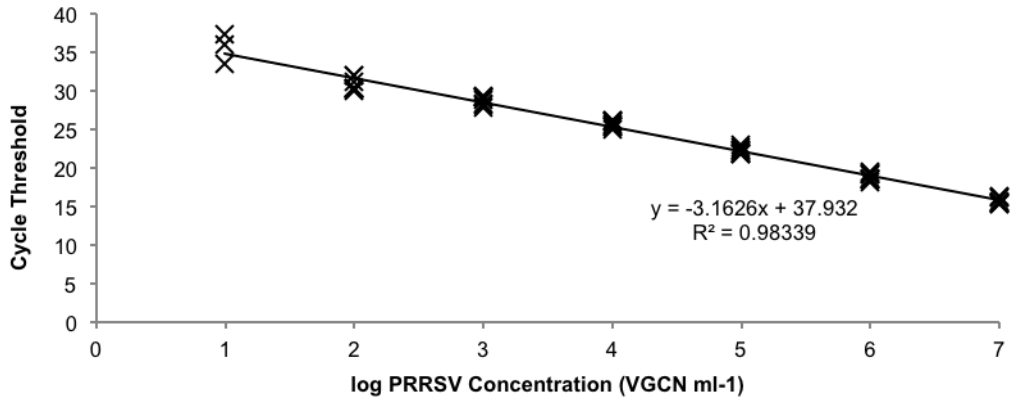

Figure 14. Standard (calibration) curve for quantification of concentration of PRRSV within an unknown sample

The standard curve was developed using dilutions expressed in plaque forming units (PFU) of PRRSV (i.e., infectious PRRSV). It should be noted that for animal viruses it is known that particle-to-PFU ratios are greater than 1 because many inactive dead viruses are produced along with the infectious virus. This means that the viral genome copy number in the samples used to develop the standard curve were actually greater than the known PFU by some factor. In developing the standard curve, it was assumed that the particle-to-PFU ratio was 1:1 but the dilutions of particle count (VGCN) were likely not identical to dilutions in PFU. In the following sections, it was assumed that the particle-to-PFU ratio was 1:1 as the PRRSV RNA concentration in unknown samples was calculated from standard curve equation relating cycle threshold to VGCN.

The particle-to-PFU ratio was estimated by calculating the limit of detection from the lowest concentration used during development of the standard curve (1×10^1 PFU ml^{-1}). The limit of detection was 0.123 PFU (4.9 PFU ml^{-1}), as detailed in Appendix A. It was assumed that there was 1 VGCN present at this dilution level, providing a particle-to-PFU ratio of 1:0.123 or 8.1:1. However, it is possible that there was more than 1 VGCN within this dilution ratio, so it is possible the ratio is different.

5.2. Chamber and Instrument Performance Tests

5.2.1. Airflow pattern in test chambers

Smoke tests showed that air entering the chambers was directed downwards due to the installation of baffles at the inlet of both chambers (Figure 15 and Figure 16). The downward movement of the airflow minimized potential short-circuits and encouraged the air mixing inside

of the chambers. Evidence of this is shown in both Figure 15 and Figure 16. Overall, the video capture of the smoke tests in both chambers showed that adequate mixing to air occurred at 34.0 $m^3 h^{-1}$ and 254.8 $m^3 h^{-1}$, although air was mixed more slowly at the airflow rate of 34.0 $m^3 h^{-1}$ than at 254.8 $m^3 h^{-1}$.

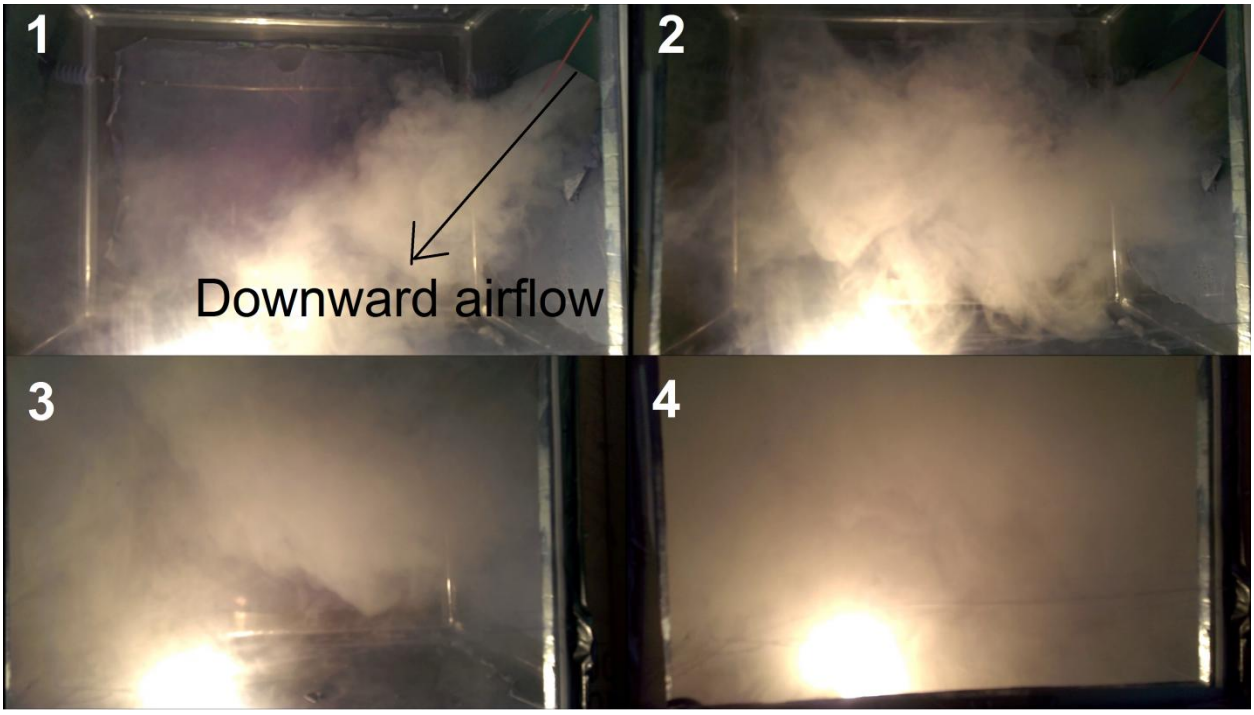

Figure 15. Smoke test at 34.0 $m^3 h^{-1}$ in the source chamber after chamber modifications, images taken at four different times after smoke introduction.

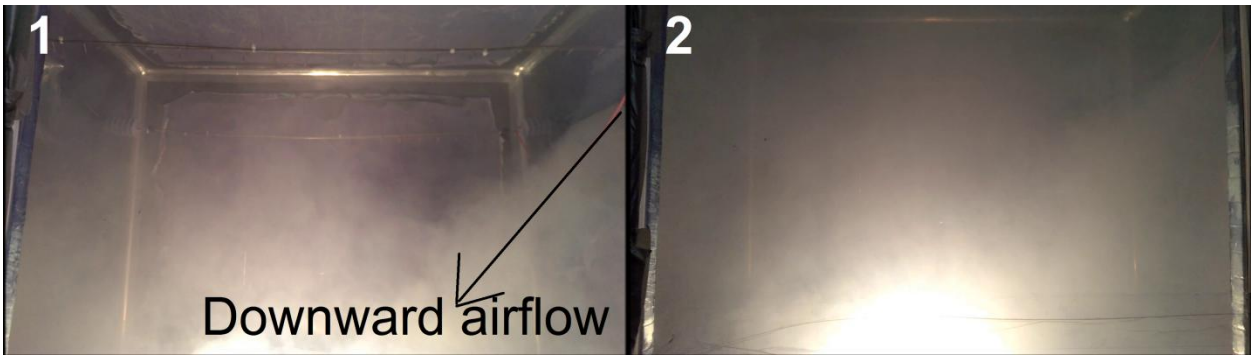

Figure 16. Smoke test at 254.8 $m^3 h^{-1}$ in the source chamber after chamber modifications, images taken at two different times after smoke introduction.

5.2.2. Aerosol generation rates

The aerosol generation rates of the nebulizer when operated with compressed air at air pressures of 137.9 and 413.7 kPa were determined by mass balance. Approximately 50 ml of water was added to the nebulizer per trial. Each trial lasted 30 minutes. The initial weight of the Collison Nebulizer with water was recorded per trial and final weight was recorded at the end of the trial. The aerosol generation rate was determined from the weight change and the duration of test. There were a total of six trials – three replicates at 137.9 and 413.7 kPa. The order of trials was randomized. The results of the test are shown in Table 2. It was observed that the measured aerosol generation rates were 64% and 53% higher than the corresponding rates suggested by the manufactures of the nebulizer for operating pressures of 137.9 and 413.7 kPa, respectively.

Table 2. Aerosol generation rates of Collison 6-jet nebulizer when supplied with 137.9 and 413.7 kPA of compressed air.

Compressed air pressure (kPa)	Manufacturer's aerosol generation rate (ml h^{-1}) (BGI Inc. 2014)	Average measured aerosol generation rate (ml h^{-1})	Standard Deviation (ml h^{-1})
137.9	9	14.8	0.2
413.7	21.5	33.0	0.9

5.2.3. Biosampler performance

The manufacturers of the SKC biosamplers recommended using a flow meter to calibrate and measure the sampling rate of the biosamplers. Consequentially, a calibration test was

designed to measure the sampling rate of each biosampler. Firstly, to reduce the effect of biosampler location on the results, the location of each biosampler during its airflow measurement was randomized using Microsoft Excel. The air sampling collection system was connected as described in the main methodology and 20 ml water was added into each biosampler. A bubble airflow meter was connected to the sampling apparatus of the biosampler (Figure 17). The VAC-U-GO pump was turned off at the end of each test and back on at the beginning of the next test. The bubblemeter measurements over the five minute period were averaged to give one average value per test, providing a total of twelve average five-minute flow rates for the biosamplers.



Figure 17. Bubblemeter set-up for biosampler calibration tests.

The calibration results showed that the biosamplers did not differ significantly ($P<0.05$) in terms of their average five-minute flow rate. The average sampling flow rate for all of the

biosamplers was 12.857 L min^{-1}, which is slightly greater than the manufacturer's average of 12.5 L/min.

The biosamplers collected less PRRSV RNA than the calculated steady-state concentration of aerosols (Table 3). The difference between the calculated values and the measured values ranged from 0.7 – 1.5 logarithmic (base 10) units. This meant that some viruses aerosolized by the nebulizer did not enter the test chambers. This was attributed to the losses of aerosols along the airflow path, as discussed in the next section (5.2.4).

Table 3. Comparison of measured and calculated values of PRRSV concentration in air at steady-state before ionization

	Concentration PRRSV RNA in air (VGCN m^{-3})				
	Calculated	**Actual (Source chamber)**		**Actual (Recipient chamber)**	
Treatment	**Avg.**	**Avg.**	**Std. dev.**	**Avg.**	**Std. dev.**
1	107723	3647	3008	6143	3530
2	239975	27045	11574	13403	6555
3	26304	3307	820	1479	285
4	58596	12212	8078	7319	6687

5.2.4. Aerosol losses

It was observed that measured aerosol concentrations were much lower than the values calculated by equation (3) (Table 4). This meant some aerosols were "lost" between the nebulizer and the test chambers. There were several reasons for the difference between the calculated and measured values. Firstly, the calculated concentration assumed all aerosols generated by the nebulizer were brought to the chambers by the flowing air, but in reality some large size aerosols might not be entrained or carried along with the moving airflow. Secondly, the air stream carrying aerosols from the nebulizer "shot" to the wall of the main airflow duct

(Figure 18), causing aerosols to be attached on the duct wall. In other words, some aerosols might have condensed on this portion of the duct wall, causing them to not enter the source chamber.

Table 4. Calculated and measured bioaerosol concentrations at steady-state before ionization

Treatment	Calculated (mg m^{-3})	Measured (mg m^{-3})
1	430	0.62
2	958	1.47
3	105	0.34
4	235	0.47

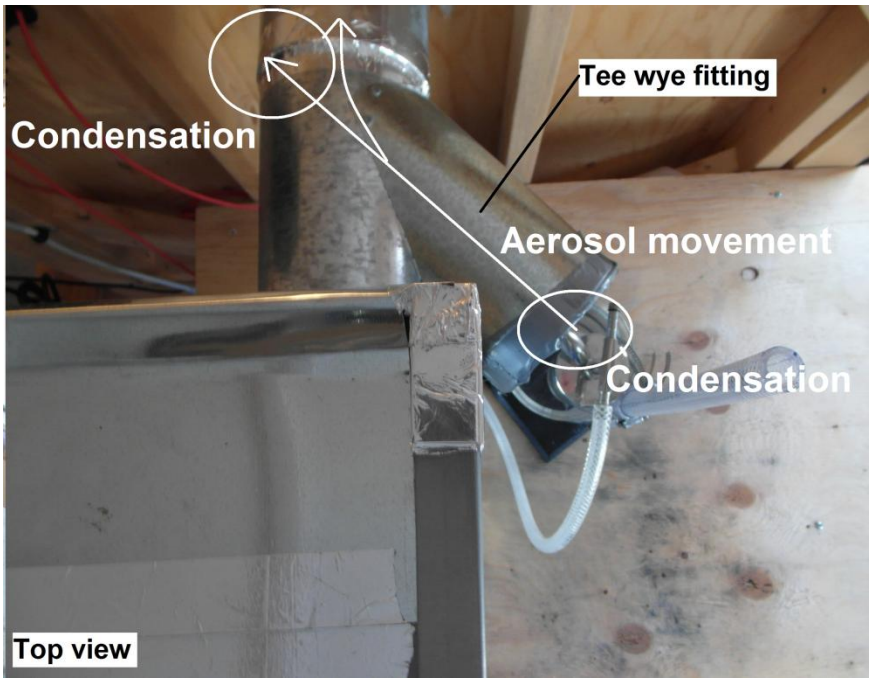

Figure 18. Condensation location prior to source chamber.

The above two scenarios were substantiated by the observation of condensation at the section where the air from the nebulizer entered the tee wye duct: a small pool of liquid was

sometimes found at this location during the cleaning phase of each test. If the pool of liquid was visible, it likely had a volume of at least 1 ml and therefore contained a significant amount of virus (at least 2.50×10^5 PFU), based on the initial concentration of the stock solution (2.50×10^5 PFU ml^{-1}). If this liquid had been tested, the results would have likely showed that it contained a significant amount of virus.

A third potential reason for the difference was aerosols losses via evaporation within the dry, warm air of the experimental chambers during experiments. As discussed in Section 5.3, the relative humidity in the test chambers was very low (17%), and it is possible that some aerosols evaporated. However, evaporation does not explain the difference in measured and calculated virus concentrations as the virus particles were solid and would have remained in the air despite the evaporation of the liquid.

It should be noted that the difference between the calculated and measured values should not affect the objective of this study, which was to measure the changes in aerosol properties and PRRSV before and after air ionization, given that the aerosols and PRRSV were measurable by the instrument. In fact, the measured aerosol concentrations in the chambers were within the typical ranges as reviewed in Section 3.1.2. For example, the exposure limits of 2.4 mg m^{-3} for total dust and 0.23 mg m^{-3} for respirable dust were reported by Donham (1991), and OSHA's TWAEV is 10 mg m^{-3} and 3 mg m^{-3} for inhalable and respirable particulates, respectively.

5.3. Temperature and Relative Humidity

The average ambient (room) temperature during the tests was 24.7˚C with a standard deviation of 2.6˚C, and the average relative humidity was 17.0% with a standard deviation of

1.8%. Relative humidity was low and not comparable to the levels in typical swine barns. The humidifier was unable to raise indoor humidity substantially from low relative humidity (<10%) that was caused by the cold outdoor air. The low relative humidity may have also led to the desiccation and loss of viability of aerosolized PRRSV as enveloped viruses tend to desiccate at low relative humidity values.

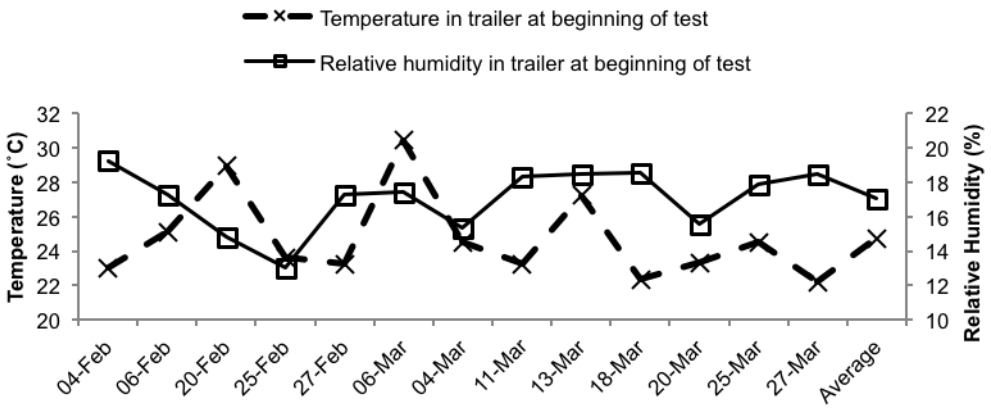

Figure 19. Temperature and relative humidity in trailer during tests

5.4. Ion concentrations

The ion concentration was indirectly measured as voltage by a charge plate monitor and directly by an ion counter. The airflow (ventilation) rate had a significant effect ($P<0.05$) on voltage (Figure 20), but the airflow rate did not significantly ($P>0.05$) affect the ion concentration measured by the ion counter. It should be noted that the ion counter had a low accuracy of ±25% and it was not able to detect changes in ion concentration below 10000 ions cm^{-3}. Comparatively, the charge plate monitor was a more accurate method of measuring presence of ions in the air (but not directly number of ions). Therefore, it was reasonable to conclude that the airflow rate of 135.9 $m^3 h^{-1}$ resulted in less ions in the chambers than 34.0 $m^3 h^{-1}$.

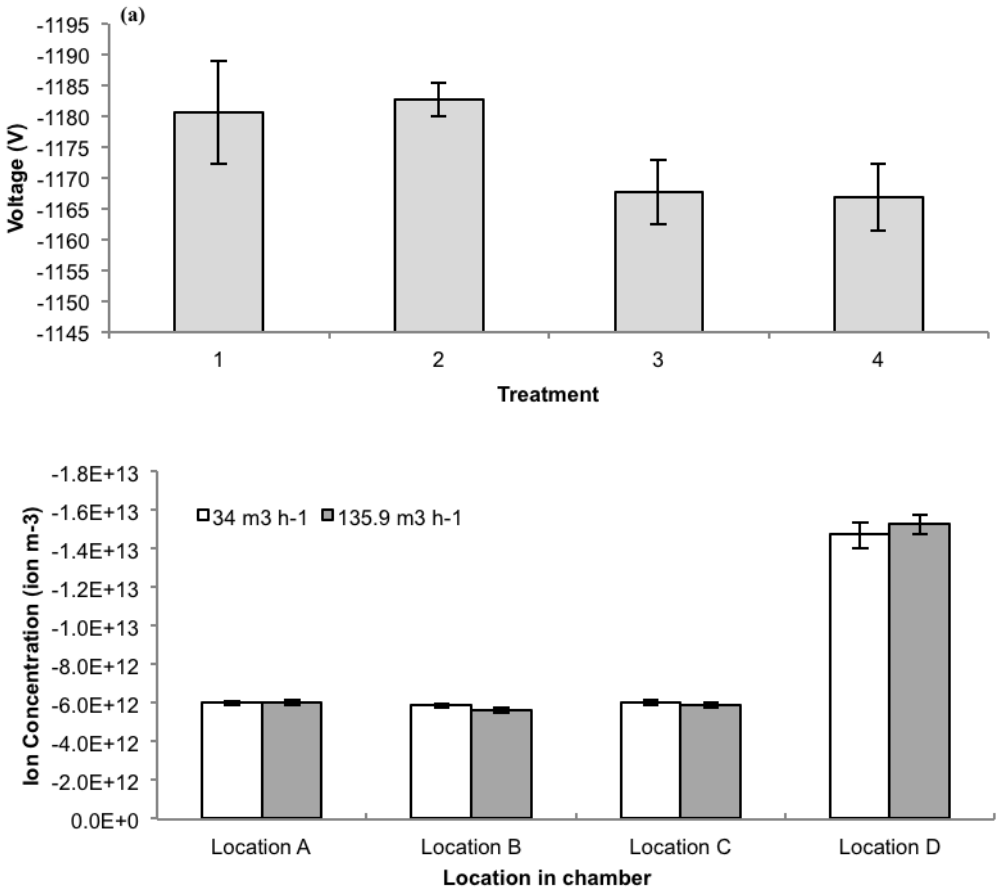

Figure 20. (a) Average voltage measured after activating negative air ionization and (b) average ion concentration measured during preliminary tests. (Treatment 1: 34.0 m^3 h^{-1},14.8 ml h^{-1}; Treatment 2: 34.0 m^3 h^{-1}, 33.0 ml h^{-1}; Treatment 3: 135.9 m^3 h^{-1}, 14.8 ml h^{-1}; Treatment 4: 135.9 m^3 h^{-1}, 33.0 ml h^{-1}).

While the charge plate monitor was more accurate, but it could be placed only at a fixed location, i.e., the location effects was not measured. In contrast, the ion counter was capable of measuring ion concentrations at various locations. It was observed that the location had significant ($P < 0.05$) effect on ion concentrations, which was higher at location D as this was closer to the ion discharge point (the ion counter was placed 30 cm above the chamber floor). The average ion concentrations in this study ranged from $5.62\times10^{12} – 1.52\times10^{13}$ ions m^{-3}. Cambra-López et al. (2009) measured air ion concentration of $2.2 \times10^{8} – 6.4 \times 10^{9}$ ions m^{-3} in poultry facility utilizing the EPI system. Grabarczyk (2001) measured ion concentrations of 5 ×

$10^9 – 1.2 \times 10^{10}$ ions m^{-3} in an unventilated room with an "ion shower" type air ionizer. The ion concentrations measured were 100 times greater than those measured previously in literature. The experimental chambers are small compared to the rooms in the two studies so the ions were more densely concentrated. Additionally, the ion concentration measurements occurred quite close to the corona lines and this likely affected the magnitude of the ion concentrations.

In the current study, ion concentrations were not measured using an ion counter during experimental tests due to the enclosed nature of the experimental chambers. Instead, a charge plate monitor was used to monitor voltage in response to changes in the "air ion imbalances" (MEI 2008). Previous studies have not used this method to measure the performance of the ionization system as electrostatic voltage meters (Tanaka and Zhang 1996) or air ion counter (Cambra-López et al. 2009) were typically used. Cambra-Lopez et al. (2009) did not detect changes in ion concentrations despite changes in ventilation rate but perceived that ventilation rate may have affected the performance of the ionization system.

5.5. Effect of ionization on Particle Size Distribution

5.5.1. Number count vs. mass distribution

A particle size distribution based on number count describes the aerosols in terms of the number of aerosols at given size ranges. This distribution does not differentiate between a small aerosol and a large aerosol so when counted, each would be considered a single aerosol. A particle size distribution based on mass describes aerosols in terms of their mass. A mass PSD takes into account the size of the aerosol. In this study, the aerosols generated had the same density (1000 kg m^{-3}) and larger aerosols had a greater volume and subsequently a greater mass.

An example illustrating the difference between a number count distribution and a mass distribution is shown in Figure 21. In terms of number count, the majority of aerosols were less than one micron in size, which did not significantly contribute to the mass of the aerosols at that size. There were very low counts of aerosols at sizes greater than one micron, but the mass of these aerosols at these sizes was much greater. The mass at a particular aerosol size was dependent on the number of aerosols at the size and also the volume of the aerosol at that size. Liquid aerosols likely had a spherical shape; the volume of a sphere is $\pi/6 \bullet d^3$. Therefore, the mass aerosol concentrations were related to the aerodynamic diameter of aerosols to the third power.

Because of these differences, the spread and the shape of number count particle size distribution was different from that of the mass particle size distribution. Subsequently, both the geometric mean diameter and the geometric standard deviation used to describe the particle size distributions would be different.

A key reason for investigating both types of distributions was to fully understand how EPI affected aerosols at different sizes. A high reduction in the geometric mean diameter by number count (#GMD) but a low reduction in the geometric mean diameter by mass (MGMD) implies that EPI was more efficient at removing small aerosols because small aerosols would contribute more to the geometric mean diameter by number count than by mass. Vice versa, a low reduction in #GMD but a high reduction in MGMD implies that more large aerosols were moved by air ionization.

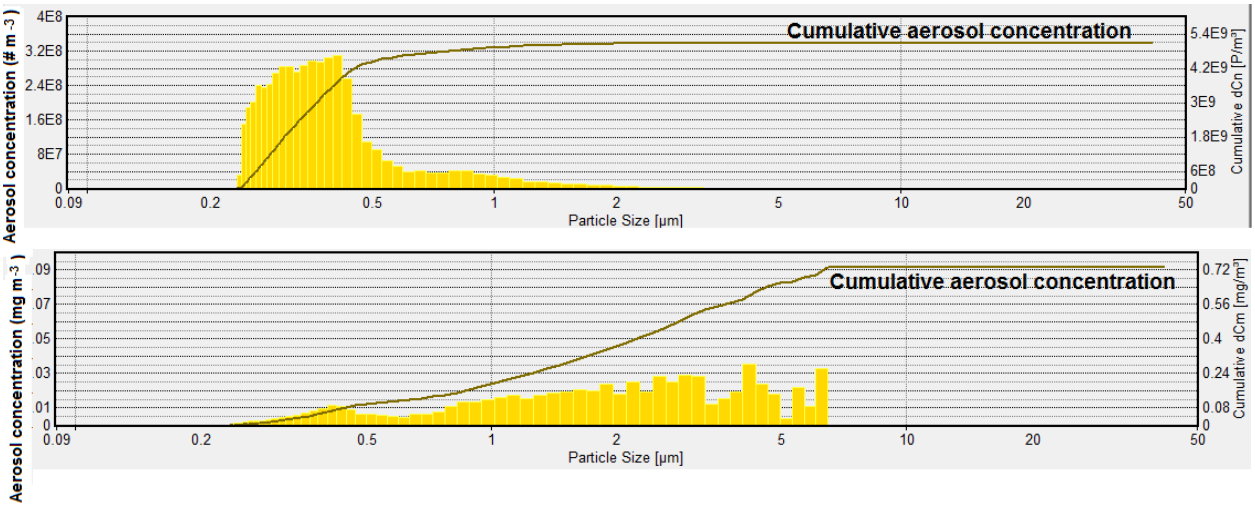

Figure 21. Particle size distributions (top: number count; bottom: mass) of the first replicate of an experiment before ionization with an airflow rate of 34.0 m^3 h^{-1} and an aerosol generation rate of 14.8 ml h^{-1}.

5.5.2. Bioaerosols before ionization

The average geometric mean diameters by number count were 0.365, 0.385, 0.356, and 0.342 µm for treatments 1-4, respectively (Figure 22). Comparatively, the average geometric mean diameters by mass were 1.526, 1.416, 1.508, and 1.147 µm for treatments 1-4, respectively. The average geometric standard deviations by number count (#GSD) were 1.445, 1.492, 1.469, and 1.405 µm for treatments 1-4, respectively (Figure 23), whereas the average geometric standard deviations by mass (MGSD) were 2.414, 2.231, 2.260, and 2.265 µm for treatments 1-4, respectively. The particle size distributions (PSD) for the aerosols by number count and mass were different in terms of shape and spread. There were a large number of small aerosols (approximately 0.3 µm in size) that did not have much mass, which resulted in large peaks in the number count PSD that did not exist for the mass PSD. The number PSD also did not have as large of a spread (GSD) as the mass PSD because large aerosols were more significant in terms of their mass but not in terms of their number count.

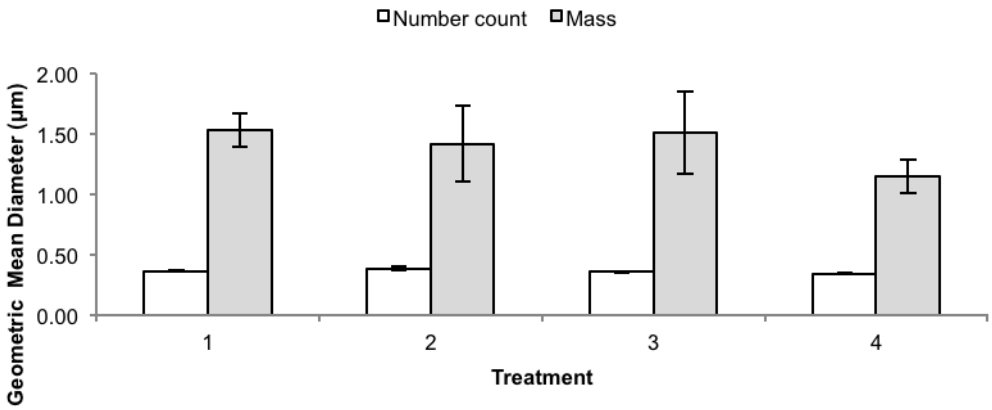

Figure 22. Summary of the #GMD and MGMD before ionization (Treatment 1: 34.0 m^3 h^{-1},14.8 ml h^{-1}; Treatment 2: 34.0 m^3 h^{-1}, 33.0 ml h^{-1}; Treatment 3: 135.9 m^3 h^{-1}, 14.8 ml h^{-1}; Treatment 4: 135.9 m^3 h^{-1}, 33.0 ml h^{-1}).

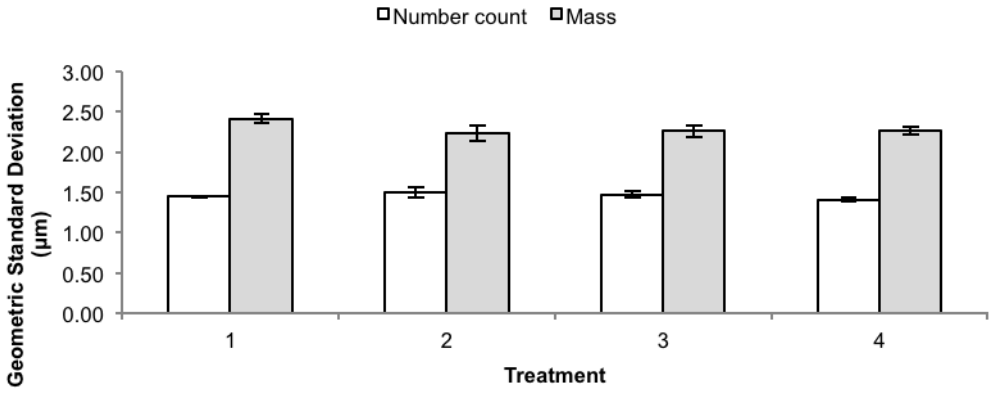

Figure 23. Summary of the #GSD and MGSD before ionization (Treatment 1: 34.0 m^3 h^{-1},14.8 ml h^{-1}; Treatment 2: 34.0 m^3 h^{-1}, 33.0 ml h^{-1}; Treatment 3: 135.9 m^3 h^{-1}, 14.8 ml h^{-1}; Treatment 4: 135.9 m^3 h^{-1}, 33.0 ml h^{-1}).

The measured MGMD ranged from 1.15 – 1.53 µm, which were smaller than what were reported in the literature for swine facilities. Agranovski et al. (2004) used an optical particle sizer to measure dust in a swine building and found an average median diameter of 2.23 µm by number count. Using a cascade impactor, Predicala et al. (2001) found average GMD of 17.9 and 18.1 µm with GSD of 2.2 and 2.1, respectively, for naturally and mechanically ventilated swine

grower-finisher barns. Jerez et al. (2011) found an average MMD of 31.55 μm with a GSD of 1.86 in a mechanically-ventilated swine building. These studies all indicated that aerosols in swine production facilities were composed of greater amounts of larger aerosols than those generated in this current study. However, larger aerosols are less of a concern because they do not penetrate as deeply into the respiratory system and they are more likely to gravimetrically settle. Furthermore, an aerodynamic diameter of 5 μm is commonly used as the upper limit in defining airborne transmission of pathogens. It is generally true that aerosol removal systems are more efficient in removing larger particles. For example, Mitchell et al. (2000) reported that a negative air ionization removed 36.6% of dust between 0.3 – 0.5 μm, but 65.6% for 10 to 25 μm. One of the major contributions this study brings to the research community is the effect of negative air ionization on small aerosols.

5.5.3. Bioaerosols after ionization

The average values of #GMD after ionization were 0.343, 0.326, 0.343, and 0.335 μm for treatments 1-4, respectively, while the average MGMD were 1.070, 0.657, 1.347, and 0.923 μm for treatments 1-4, respectively (Figure 24). The average #GSD values were 1.382, 1.303, 1.423, and 1.356 μm for treatments 1-4, respectively and MGSD 2.284, 2.038, 2.300, and 2.243 μm for treatments 1-4, respectively (Figure 25).

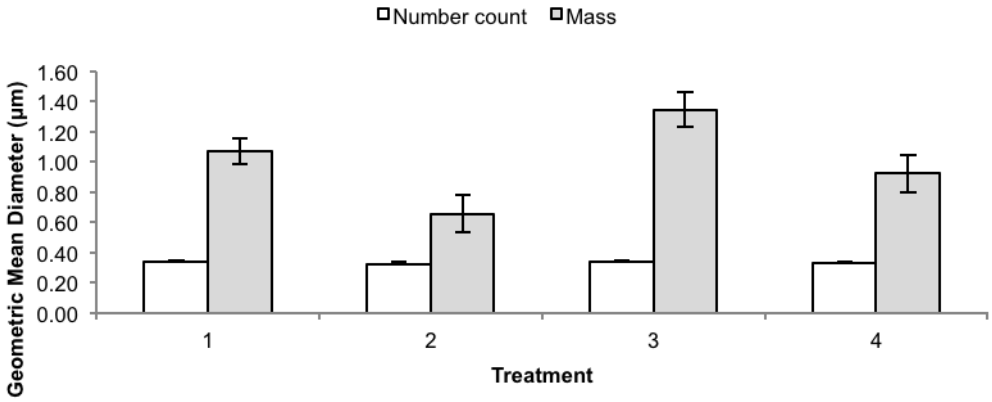

Figure 24. Summary of the #GMD and MGMD after ionization (Treatment 1: 34.0 m^3 h^{-1},14.8 ml h^{-1}; Treatment 2: 34.0 m^3 h^{-1}, 33.0 ml h^{-1}; Treatment 3: 135.9 m^3 h^{-1}, 14.8 ml h^{-1}; Treatment 4: 135.9 m^3 h^{-1}, 33.0 ml h^{-1}).

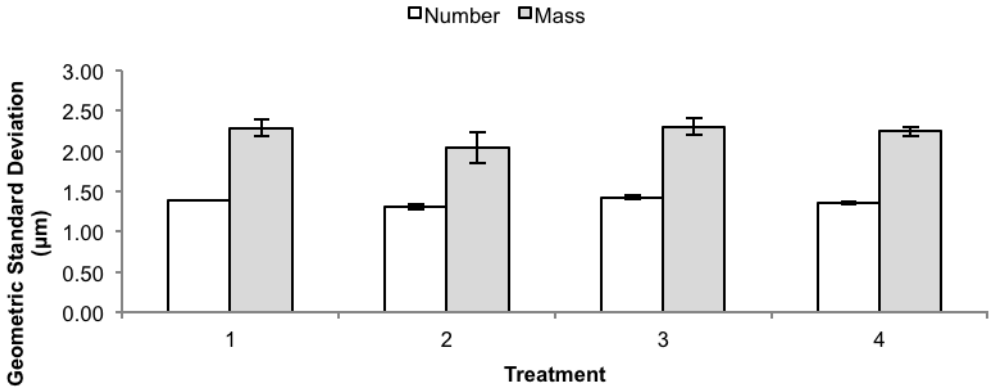

Figure 25. Summary of the #GSD and MGSD after ionization (Treatment 1: 34.0 m^3 h^{-1},14.8 ml h^{-1}; Treatment 2: 34.0 m^3 h^{-1}, 33.0 ml h^{-1}; Treatment 3: 135.9 m^3 h^{-1}, 14.8 ml h^{-1}; Treatment 4: 135.9 m^3 h^{-1}, 33.0 ml h^{-1}).

The changes in the geometric mean diameter after ionization indicated that the EPI was more efficient at removing large aerosols than small aerosols. Firstly, the EPI removed more large aerosols than small aerosols, which resulted in the geometric mean diameter becoming smaller after EPI was applied for all treatments. Secondly, the average reduction in #GMD due

to ionization was 6, 15, 4, and 2% for treatments 1-4, respectively, whereas the average reduction in MGMD was 29, 53, 8, and 19% for treatments 1-4, respectively (Figure 26). Greater reduction in MGMD meant that the more large size aerosols were removed by ionization as they had greater mass than numbers. The order of treatments based on the largest #GMD to smallest #GMD before ionization was treatments 2, 1, 3, and 4. A larger #GMD was caused by the presence of a greater amount of large aerosols in the particle size distribution. The order of treatments based on the largest reduction of #GMD to the smallest reduction of #GMD was also 2, 1, 3, and 4. Treatments that had more large aerosols before ionization (larger #GMD) had greater reductions in #GMD because ionization was more effective at removing large aerosols.

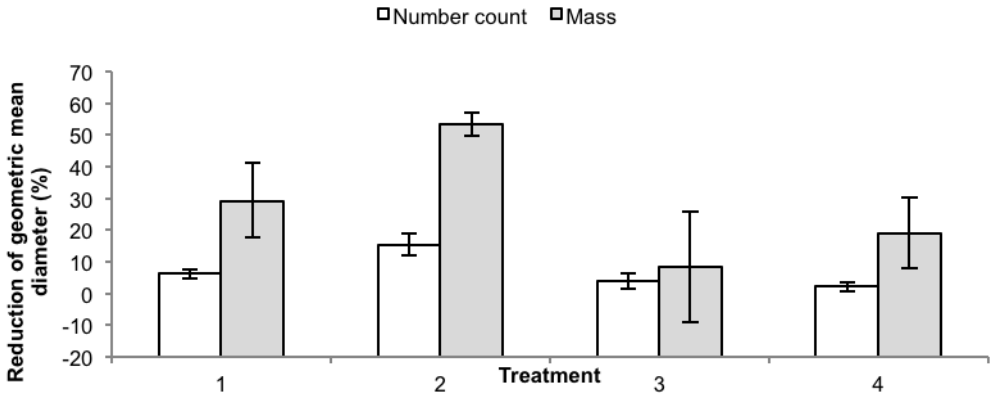

Figure 26. Reduction of #GMD and MGMD (Treatment 1: 34.0 m^3 h^{-1},14.8 ml h^{-1}; Treatment 2: 34.0 m^3 h^{-1}, 33.0 ml h^{-1}; Treatment 3: 135.9 m^3 h^{-1}, 14.8 ml h^{-1}; Treatment 4: 135.9 m^3 h^{-1}, 33.0 ml h^{-1}).

Aerosol generation rate significantly affected the #GMD and MGMD after ionization ($P<0.05$). The average #GMD when an aerosol generation rate of14.8 ml h^{-1} was used (0.343 μm for both treatments 1 and 3) were greater than the average #GMD when an aerosol generation rate of 33 ml h^{-1} was used (0.326 and 0.335 μm for treatments 2 and 4, respectively). Similarly, the average MGMD when an aerosol generation rate of 14.8 ml h^{-1} was used (1.070 and 1.347

μm for treatments 1 and 3, respectively) were greater than the average MGMD when an aerosol generation rate of 33 ml h^{-1} was used (0.657 and 0.923 μm for treatments 2 and 4, respectively). Use of the higher aerosol generation rate (33 ml h^{-1}) coincided with lower #GMD and MGMD after ionization was applied. Aerosol generation rate also significantly affected the magnitude of the reduction of the MGMD due to ionization ($P<0.05$). The reduction in MGMD was greater when an aerosol generation rate of 33 ml h^{-1} was used (53 and 19% for treatments 2 and 4, respectively) than when an aerosol generation rate of 14.8 ml h^{-1} was used at the same airflow rates (29% and 8% for treatments 1 and 3, respectively).

The "aerosol generation rate effects" were likely not directly due to the aerosol generation rate itself but due to the use of different compressed air pressures that were required to operate the nebulizers at these aerosol generation rates. A compressed air pressure of 137.9 kPa was required to operate the nebulizer at an aerosol generation rate of 14.9 ml h^{-1}, while a compressed air pressure of 413.7 kPA was required to operate the nebulizer at an aerosol generation rate of 33 ml h^{-1}. The manufacturer of the Collison Nebulizer indicated that a compressed air pressure of 137.9 kPA generated aerosols with a mass median diameter of 2 μm, while the compressed air pressure of 413.7 kPA generated aerosols with a mass median diameter of 1.8 μm (BGI Inc. 2014). This shows that the nebulizer produces a different particle size distribution that consists of smaller aerosols when an aerosol generation rate of 33 ml h^{-1} was used than when an aerosol generation rate of 14.8 ml h^{-1} was used. Proof that this was indeed the case is found by comparing the mass fractions of small aerosols between treatments. There was a greater mass fraction of aerosols less than or equal to 0.5 μm at 33 ml h^{-1} (49.3 and 32.18% for treatments 2 and 4, respectively) than 14.8 ml h^{-1} (27.7% and 17.9% for treatments 1 and 3, respectively). There was also a significant aerosol effect on the mass fraction less than or equal

to 0.5 μm (P= 0.0015). The removal of large aerosols by ionization in conjunction with the production of more small aerosols at 33 ml h^{-1} resulted in the smaller #GMD and MGMD and larger reductions in MGMD when aerosols were generated at 33 ml h^{-1}. Because the "aerosol generation rate effect" was due to using compressed air at different pressures, it cannot be extrapolated to in-barn conditions (i.e., it is unknown if aerosol generation rate would affect the EPI's performance in a barn setting) as aerosols are generated through natural means in a barn and not by compressed air.

The airflow rate also had a significant effect on the MGMD after ionization ($P<0.05$). Treatments with an airflow rate of 34.0 m^3 h^{-1} resulted in smaller MGMD after ionization (1.070 μm and 0.657 μm for treatments 1 and 2, respectively) than treatments with an airflow rate of 135.9 m^3 h^{-1} when the same aerosol generation rates were used (1.347 μm and 0.923 μm for treatments 3 and 4, respectively). Airflow rate also had a significant effect on the mass fraction that was less than or equal to 0.5 μm ($P<0.05$; Figure 27). Greater mass fraction were ≤0.5 μm in treatments with an airflow rate of 34.0 m^3 h^{-1} after ionization (27.74% and 49.34%) than treatments with an airflow rate of 135.9 m^3 h^{-1} (17.91% and 32.18%). Statistical analysis indicated that the airflow rate effect on the mass fraction of aerosols more than 0.5 μm was significant ($P<0.05$). This indicates that the MGMD were smaller after ionization when an airflow rate of 34.0 m^3 h^{-1} was used because the particle size distribution was composed of a greater mass of small aerosols. The presence of more small aerosols in proportion to large aerosols indicated that more large aerosols were removed when an airflow rate of 34.0 m^3 h^{-1} was used.

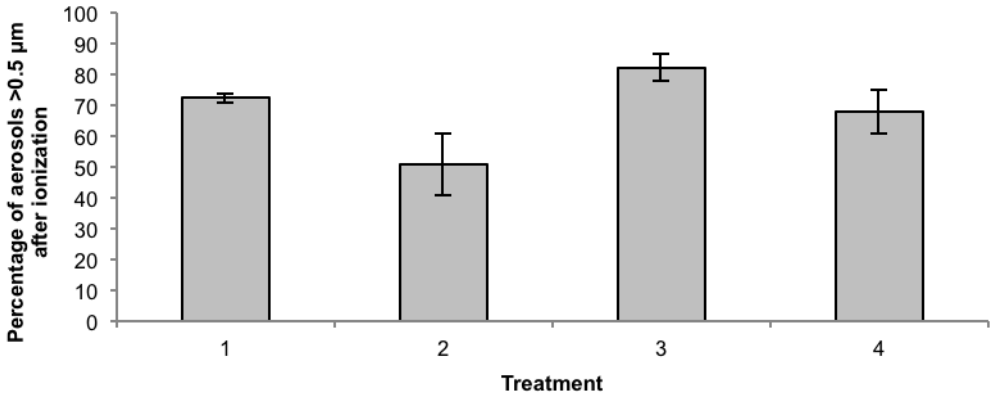

Figure 27. Percentage of aerosols greater than 0.5 µm after ionization during each treatment (Treatment 1: 34.0 m^3 h^{-1},14.8 ml h^{-1}; Treatment 2: 34.0 m^3 h^{-1}, 33.0 ml h^{-1}; Treatment 3: 135.9 m^3 h^{-1}, 14.8 ml h^{-1}; Treatment 4: 135.9 m^3 h^{-1}, 33.0 ml h^{-1}).

A comparison of the mass PSD before and after ionizations (Figure 28) indicated that large aerosols >6 µm are present after ionization only for treatments 3 and 4, which consisted of an airflow rate of 135.9 m^3 h^{-1}. The maximum aerosol sizes measured for both treatments 1 and 2 after ionization were 5.67 µm, while the maximum sizes measured after ionization for treatments 3 and 4 were 8.28 um and 6.45 um, respectively. This further confirms the theory that larger aerosols are more easily removed during an airflow rate of 34.0 m^3 h^{-1} as aerosols >6 µm were not present during these treatments after ionization.

The airflow rate also affected the magnitude of the ionization's reduction of MGMD ($P<0.05$). The average reduction in MGMD due to ionization was greater when an airflow rate of 34.0 m^3 h^{-1} was used (29 and 53%) than when an airflow rate of 135.9 m^3 h^{-1} was used (8% and 19%). To understand why the reduction in MGMD were higher when an airflow rate of 34.0 m^3 h^{-1} was used than when an airflow rate of 135.9 m^3 h^{-1} was used, the mass particle size distributions before and after ionization were compared (Figure 28). Comparison of the mass PSD between treatments indicated that many large aerosols were present before ionization during

treatments 1 and 2 (34.0 m^3 h^{-1}) that were removed during ionization, which subsequently reduced the MGMD more substantially than during treatments with an airflow rate of 135.9 m^3 h^{-1}. Additionally, as stated above, the ionization reduced the size range of the aerosols during treatments with an airflow rate of 34.0 m^3 h^{-1}more than during treatments with an airflow rate of 135.9 m^3 h^{-1}. This likely also affected the magnitude of the reduction of MGMD.

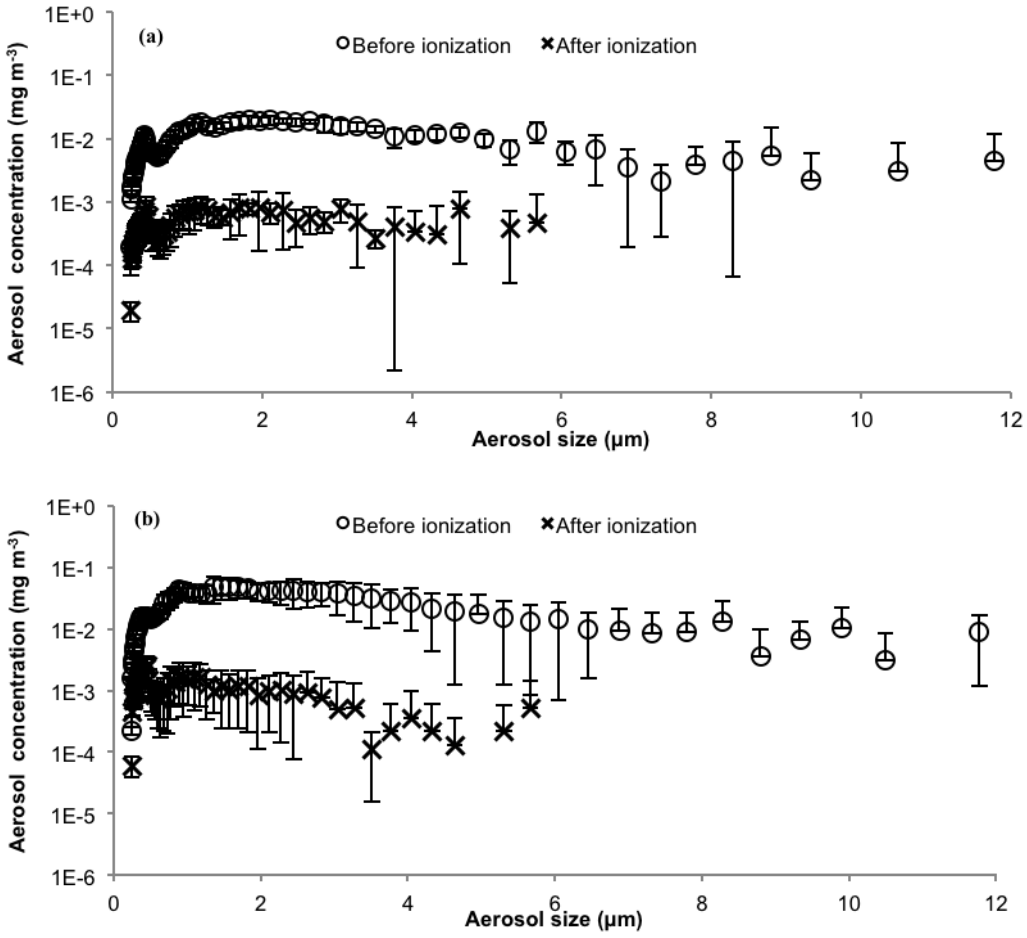

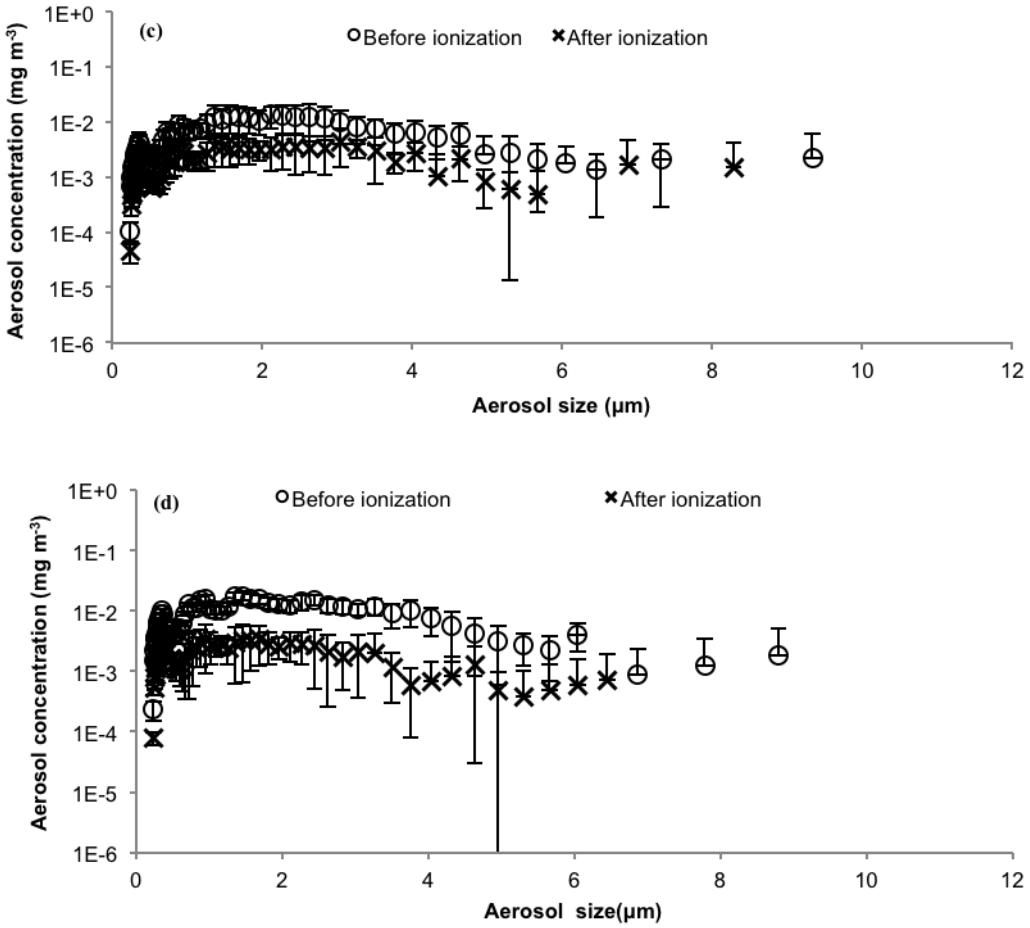

Figure 28. Aerosol concentration at different aerosol sizes before and after ionization for (a) treatment 1: 34.0 m^3 h^{-1},14.8 ml h^{-1}; (b) treatment 2: 34.0 m^3 h^{-1}, 33.0 ml h^{-1}; (c) treatment 3: 135.9 m^3 h^{-1}, 14.8 ml h^{-1}; (d) treatment 4: 135.9 m^3 h^{-1}, 33.0 ml h^{-1}.

5.6. Aerosol concentration

5.6.1. Change in aerosol concentrations

The change in aerosol concentrations with time behaved similarly regardless of the treatment for both the number count and mass. The aerosol concentration increased drastically from baseline measurements when aerosolization was commenced and then reached a plateau at the steady-state concentration (Figure 20). During this phase, there were "spikes" in the aerosol

concentration in which the concentration greatly increased during one measurement but decrease during the next measurement. It was possible that some aerosols became temporarily attached to the wall of the tygon tubing during aerosol sampling. Clumps would form around the initial attached aerosols. Eventually the clumps of aerosols would dislodge and enter the particle sizer for measurement, resulting in the spikes in aerosol concentration. The spikes occurred for both the number count and mass aerosol concentrations, indicating that if this theory was true that the aerosols would separate once they were dislodged from the wall of the tubing. This theory has not been proven and required further testing to confirm.

Once the EPI system was activated, the aerosol concentration decreased drastically and quickly reached the steady-state low concentration. The magnitude of the steady state concentrations differed for different airflow rates and aerosol generation rates (Figure 29).

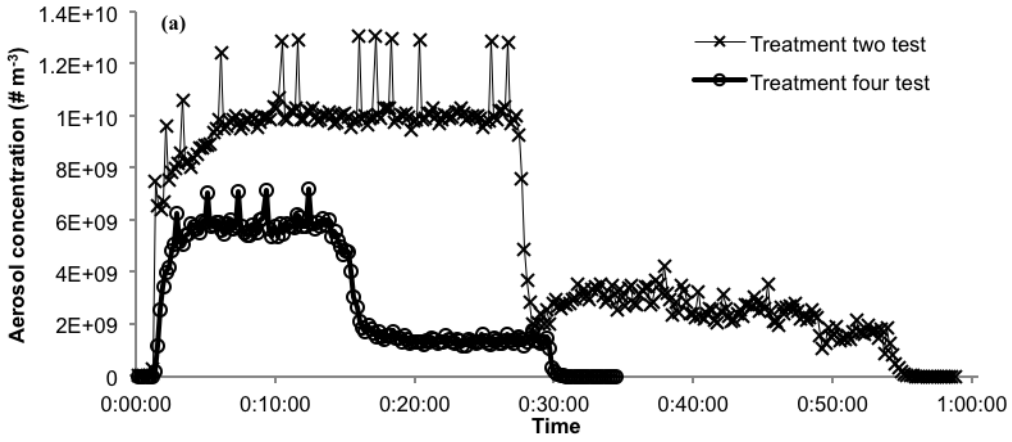

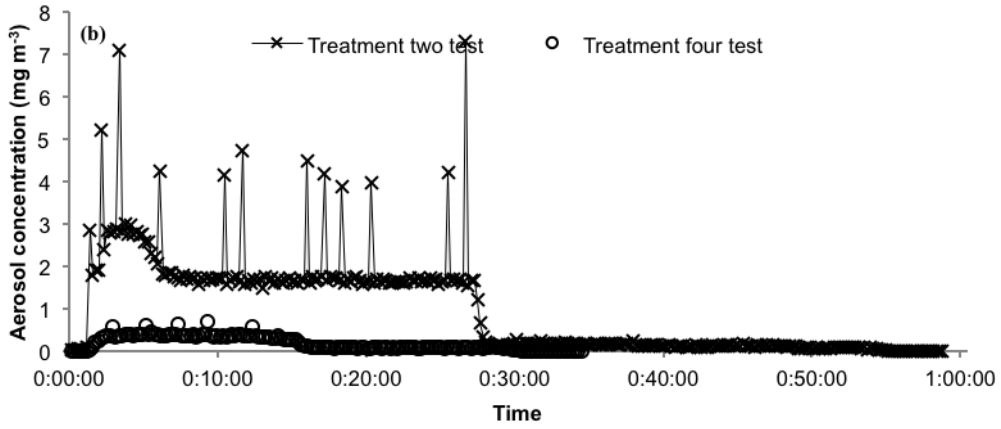

Figure 29. Examples of aerosol concentration of bioaerosols during PRRSV experiments during treatments 2 and 4 by (a) number count and (b) mass.

5.6.2. Aerosol concentration before air ionization

The average bioaerosol concentrations by number count were 5.20×10^{9}, 1.06×10^{10}, 2.72×10^{9}, and 6.00×10^{9} # m^{-3} for treatments 1-4, respectively before ionization (Figure 30). The bioaerosol concentrations by mass were 0.62, 1.47, 0.34, and 0.47 mg m^{-3} for treatments 1-4, respectively. The order of treatments based on the largest mass aerosol concentration to the smallest mass aerosol concentration before ionization was 2, 1, 4, and 3. The order of treatments based on the largest calculated steady-state concentration to the smallest calculated steady-state concentration was also 2, 1, 4, and 3.

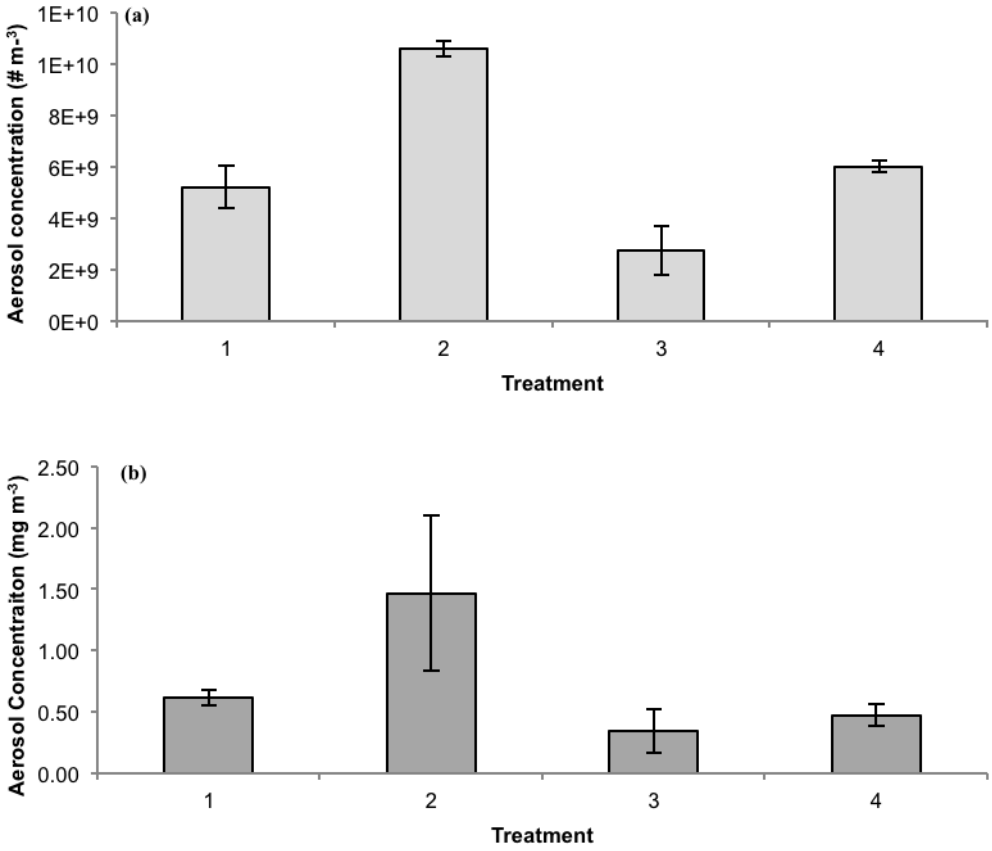

Figure 30. Aerosol concentration of bioaerosols before ionization by (a) number count and (b) mass (Treatment 1: 34.0 m^3 h^{-1},14.8 ml h^{-1}; Treatment 2: 34.0 m^3 h^{-1}, 33.0 ml h^{-1}; Treatment 3: 135.9 m^3 h^{-1}, 14.8 ml h^{-1}; Treatment 4: 135.9 m^3 h^{-1}, 33.0 ml h^{-1}).

The airflow and the aerosol generation rate were both factors that contributed to the steady-state concentration of aerosols before ionization was activated. Both airflow rate and aerosol generation rate significantly ($P<0.05$) affected the aerosol concentration expressed by number count or by mass. An airflow rate of 34 m^3 h^{-1} removed less aerosols from the chambers than did airflow rate of 135.9 m^3 h^{-1}, leading to higher aerosol concentrations. The higher the aerosol generation rate, the higher the aerosol concentration in the chamber.

5.6.3. Aerosol concentration after ionization

The average bioaerosol concentrations by number count after EPI was applied were 3.81×10^{8}, 1.46×10^{9}, 1.09×10^{9}, and 1.80×10^{9} # m^{-3} for treatments 1-4, respectively (Figure 31). The average bioaerosol concentrations in terms of the mass were 0.03, 0.06, 0.10, and 0.10 mg m^{-3} for treatments 1-4, respectively.

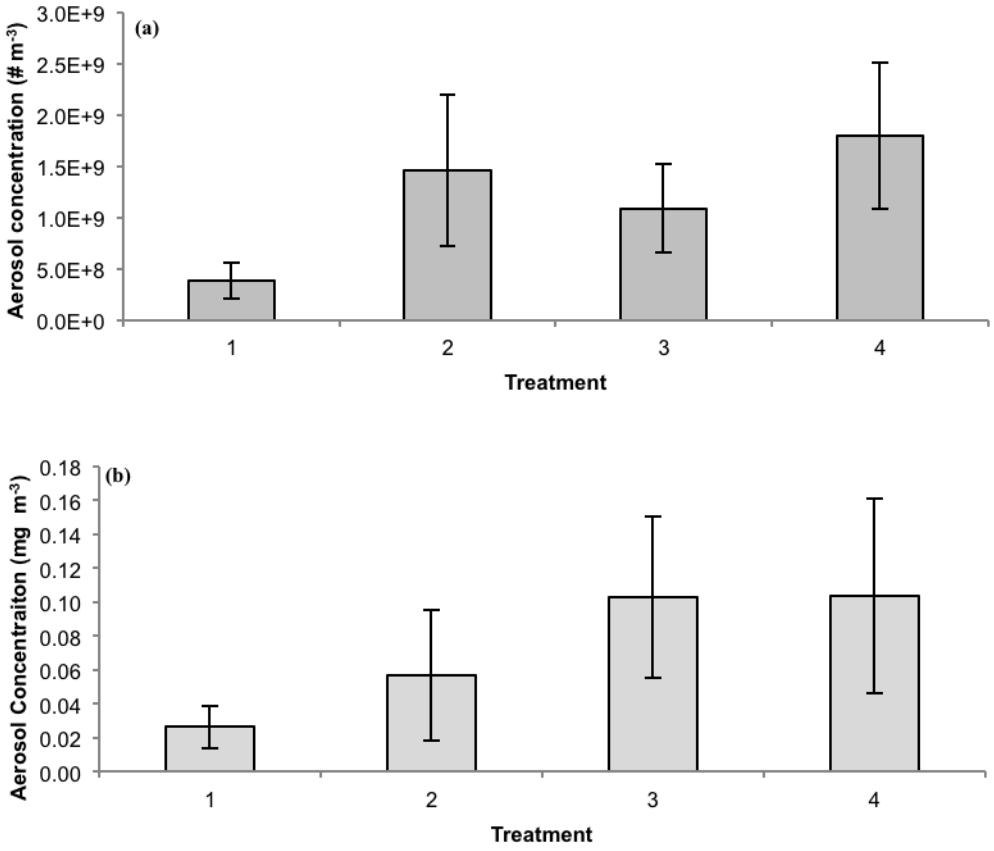

Figure 31. Aerosol concentration of bioaerosols after ionization by (a) number count and (b) mass (Treatment 1: 34.0 m^3 h^{-1},14.8 ml h^{-1}; Treatment 2: 34.0 m^3 h^{-1}, 33.0 ml h^{-1}; Treatment 3: 135.9 m^3 h^{-1}, 14.8 ml h^{-1}; Treatment 4: 135.9 m^3 h^{-1}, 33.0 ml h^{-1}).

The average reductions in aerosol concentration by number count were 93%, 86%, 61%, and 70% for treatments 1-4, respectively. The average reductions in aerosol concentration by mass) were 96%, 96%, 68%, and 78% for treatments 1-4, respectively. The average reduction was higher for mass than number count likely because more large size particles were removed from the air, as discussed previously in the particle size distribution section.

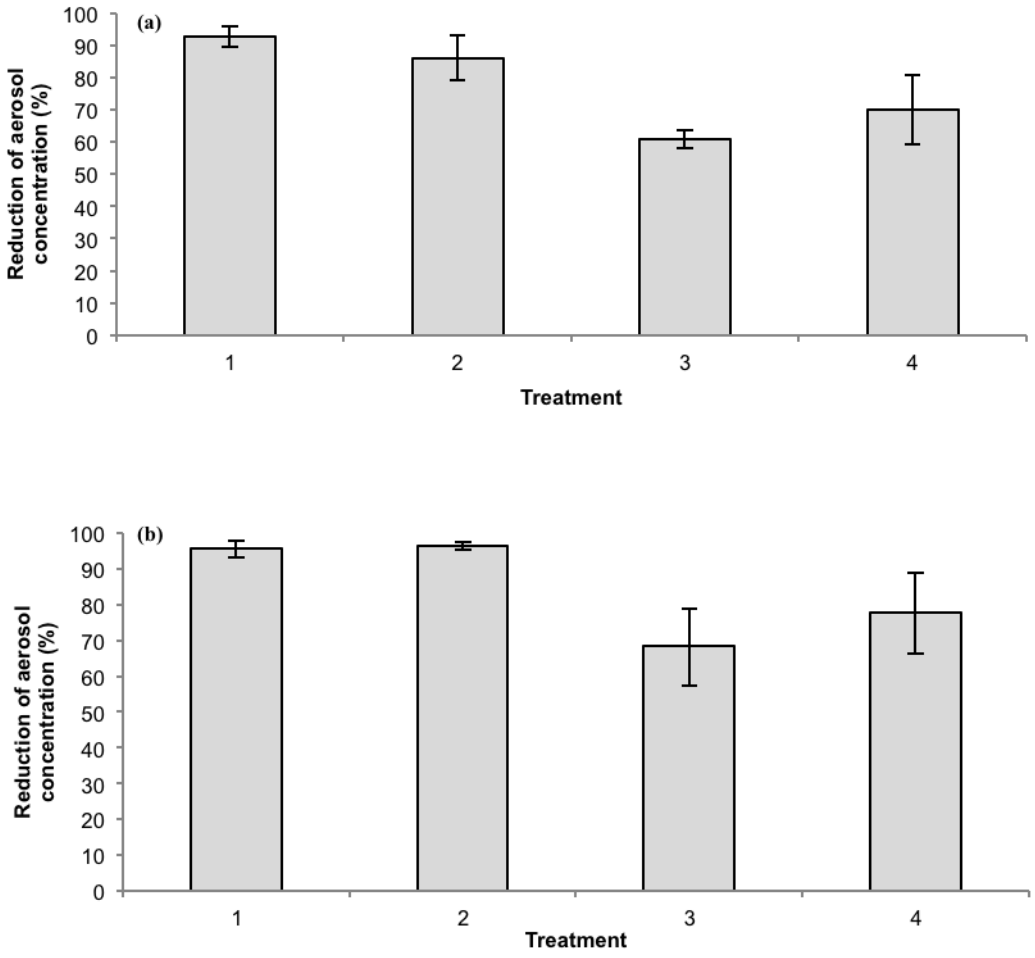

Figure 32. Reduction in aerosol concentration of bioaerosols due to ionization in terms of (a) number count and (b) mass (Treatment 1: 34.0 m^3 h^{-1},14.8 ml h^{-1}; Treatment 2: 34.0 m^3 h^{-1}, 33.0 ml h^{-1}; Treatment 3: 135.9 m^3 h^{-1}, 14.8 ml h^{-1}; Treatment 4: 135.9 m^3 h^{-1}, 33.0 ml h^{-1}).

It is evident that the performance of the EPI at reducing aerosol concentrations was affected by the airflow rate. Higher reductions of aerosol concentration occurred at airflow rate of 34 m^3 h^{-1} (86-96%), than at an airflow rate of 135.9 m^3 h^{-1} (61-78%). Statistical analysis showed that the airflow effect on the reduction of aerosol concentration by both number count and mass was significant ($P<0.05$).

It is interesting to see how the EPI affected the aerosol concentration during different treatments. The aerosol concentration by number count after ionization was greater at 33 ml h^{-1} (1.46×10^9 and 1.80×10^9 # m^{-3}) than at 14.8 ml h^{-1} (3.81×10^8 and 1.09×10^9 # m^{-3}). This was likely because there was a greater amount of smaller aerosols (which EPI is less efficient of removing) being generated at 33 ml h^{-1}. Statistical analysis agreed with this as there was a significant aerosol generation effect ($P<0.05$) on aerosol concentration by number count. Aerosol concentration by mass was greater after ionization at an airflow rate of 135.9 m^3 h^{-1} (0.10 mg m^{-3}) than at airflow rate of 34.0 m^3 h^{-1} (0.03 and 0.06 mg m^{-3}). It was likely that this was related to the presence of aerosols >6 μm after ionization in treatments with 135.9 m^3 h^{-1}, as discussed in the particle size distribution discussion. Statistical analysis agreed that there was an airflow rate effect on the aerosol concentration by mass ($P<0.05$). Overall, both airflow rate and aerosol generation rate had significant effects on the aerosol concentration after ionization was applied; however, the differences between aerosol concentrations due to different treatments were small compared to those prior to ionization. For example, the difference between the average aerosol concentrations for treatments 2 and 3 before ionization was 7.88×10^9 # m^{-3} and 1.13 mg m^{-3}, while the difference in aerosol concentrations for the same treatments after ionization was 3.7×10^8 # m^{-3} and 0.04 mg m^{-3}.

Airflow rate effect on the performance of ionization was previously documented in literature. A computer model that simulated the removal of aerosols under steady-state conditions using ionization found that the concentration reduction factor (CRF; ratio between the initial and final concentration) of an ionizer was higher when there were higher initial concentrations of aerosols (Mayya et al. 2004). The study also found that increasing the ventilation rate from 0 to 0.5 air changes per hour caused a great decrease in the CRF values in cases where there was the same initial concentration of aerosols, indicating that there was also a ventilation rate effect on the performance of negative air ionization. Tanaka and Zhang (1996) previously found that the efficiency of negative air ionization at removing respirable and inhalable dust in a swine barn was reduced when the ventilation rate was increased; a reduction of 46% occurred at airflow rates close to 0.5 $m^3 s^{-1}$ but decreased to 3% at airflow rates close to 2.1 $m^3 s^{-1}$. The authors speculated that the increased ventilation led to a reduction in the number of ions in the air as well as their "time standing in the room". Cambra-Lopez et al. (2009) also described three possible causes for the decrease in aerosol reduction in Tanaka and Zhang (1996) as due to: (1) higher ventilation rates leading to increased air velocity, (2) the ion concentration decreasing because there was a higher PM concentration and also because of increased ventilation rate, and (3) increased dust accumulation on surfaces.

5.7. Aerosol-removal efficiencies for Different size distributions

The efficiency of any aerosol removal (filtration) systems increases non-linearly with the aerosol diameter. Although several studies (e.g., Dee et al. 2012) investigated filtration systems such as HEPA filters for removing airborne PRRSV), few have investigated the removal efficiency for different aerosol sizes. The removal efficiency of the EPI ionization generally

increased with an increase in aerodynamic diameter of aerosols until it reached a maximum value close to 100% (Figure 33). For example, at an aerosol size of 0.24 μm, the reduction of aerosol concentration by mass was 90%, 72%, 55%, and 64% for treatments 1-4, respectively. At a larger aerosol size of 1.019 μm, the reduction of aerosol concentration was 95%, 96%, 68%, and 74% for treatments 1-4, respectively.

Aerosol removal at larger aerosol sizes was more consistent (i.e., less variation between replicates) and also greater in magnitude low airflow of 34 m^3 h^{-1}compared to high airflow rate of 135.9 m^3 h^{-1} (Figure 37). Large variation between replicates of 135.9 m^3 h^{-1} experiments occurred at specific aerosol sizes, and the aerosol concentration after ionization at certain particles sizes was greater than the aerosol concentration before ionization. For example, during a treatment 3 test, the aerosol concentration before ionization was 3.40×10^{-3} mg m^{-3} at 4.63 μm while the corresponding aerosol concentration after ionization was 3.59×10^{-3} mg m^{-3}.

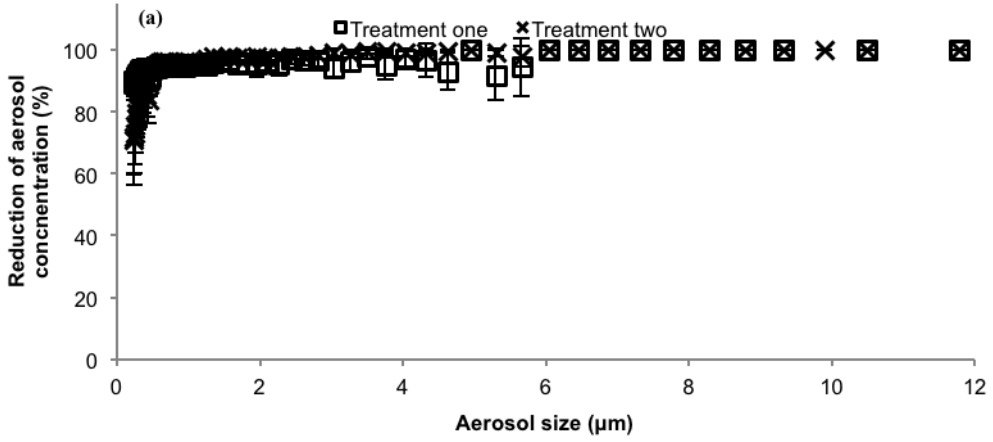

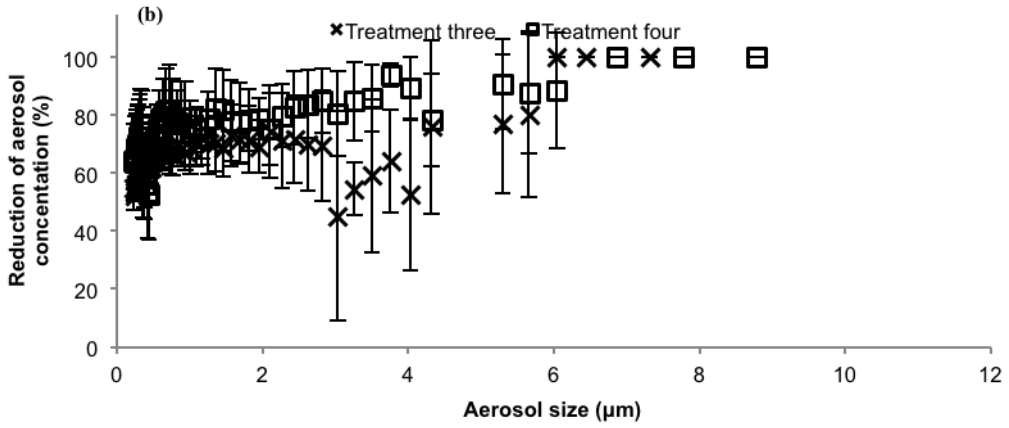

Figure 33. Removal efficiency of the EPI system for aerosols by mass for treatments with (a) an airflow rate of 34 m^3 h^{-1} and (b) an airflow rate of 135.9 m^3 h^{-1}.

5.8. Water aerosols and Bioaerosols Comparison

Many studies reported in the literature used water to generate aerosols. Water aerosols were tested in the current study to compare with the PBS aerosols containing PRRSV (bioaerosols). In comparison with water aerosols, PBS (bioaerosols) contained water, salt compounds, and virus. Different compositions may react differently to air ionization.

5.8.1. EPI effect on particle size distribution

While airflow rate and aerosol generation rate affected the geometric mean diameter and the geometric standard deviation both by number count and by mass for bioaerosols (PBS), the particle size distribution of water aerosols did not vary with treatment ($P>0.05$). The reduction of #GMD by ionization for the bioaerosols ranged from 2% - 15% on average. Comparatively, #GMD of water aerosols was reduced by 0.6%-1.4%. The difference in changes of MGMD

between PBS and water aerosols followed the same trend as #GMD: 8%-53% reduction for PBS and 0%-41% for water.

5.8.2. Aerosol concentration difference

The aerosol concentration of PBS bioaerosols fluctuated during the span of each test, while the water aerosols did not show the same degree of fluctuation. For example, in Figure 34a, the number count of bioaerosols fluctuated between approximately 1×10^{10} # m^{-3} and 1.3×10^{10} # m^{-3} prior to ionization, while the water aerosols fluctuated between approximately 4×10^{8} m^{-3} and 6×10^{8} # m^{-3}. Another difference between the water aerosols and the bioaerosols was that the steady state concentrations in terms of both mass and number count were magnitudes higher during the bioaerosol tests. The lowest average steady state aerosol concentration prior to ionization amongst the treatments was 5.2×10^{9} # m^{-3} for bioaerosol experiments, while the greatest average steady state aerosol concentration during water aerosol experiments was 4.4×10^{8} m^{-3} .

A possible explanation for these differences was the existence of salts within the PBS that did not exist in the water aerosols. While water aerosols can readily evaporate, especially in the dry conditions that the experiments occurred in, solid salt aerosols will not evaporate and will stay in the chamber air, increasing aerosol concentration. Nicas et al. (2005) presented a method of calculating the equilibrium diameter of aerosols after desiccation, which could occur if the relative humidity was less than the crystallization relative humidity of 40%. The calculation for water and bioaerosols was detailed in Appendix C. Overall, the RH within the chambers never reached 40% during the experiments, allowing for the potential for complete desiccation of

aerosols to occur (i.e., it was possible for the liquid to evaporate in aerosols, leaving behind solid particles). Calculations showed that water aerosols that had an initial diameter that was less than 3.04 μm may not have been counted by the APSS after desiccation, while bioaerosols that had an initial diameter of 1.10 μm may not have been counted by the APSS after desiccation. Because the nebulizer generated aerosols with a MMD of 1.8 and 2 μm, it was likely that many of the smaller water aerosols became desiccated to a size that was not measurable by the APSS, while many of the PBS aerosols were still measureable. This could explain the difference in aerosol concentration between water aerosols and PBS aerosols at steady-state.

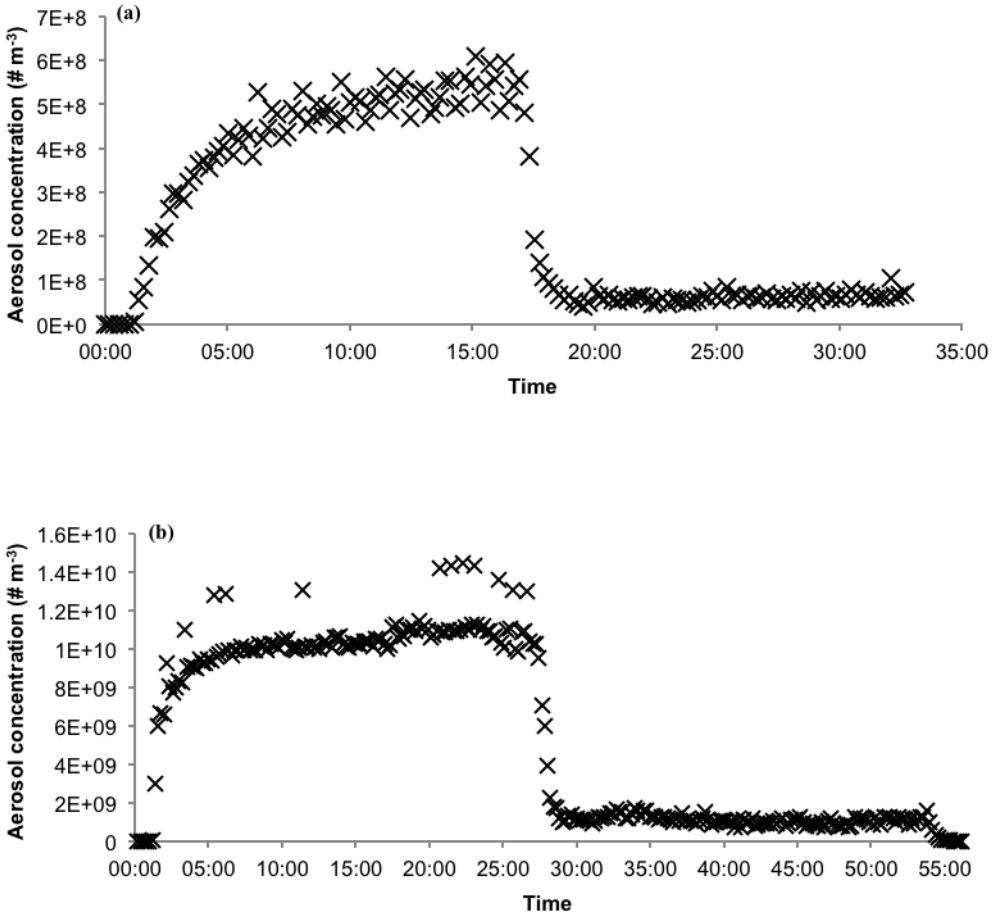

Figure 34. Aerosol concentration during treatment 2 tests for (a) water aerosols and (b) bioaerosols.

There were similarities and differences between water aerosols and bioaerosols in terms of how aerosol concentration was affected by airflow rate and aerosol generation rate. Overall, as discussed previously, the aerosol concentrations of water aerosols at all stages of experiments (i.e. before ionization and after ionization) were less than the aerosol concentrations of bioaerosols. Prior to ionization, the airflow rate and aerosol generation rate affected the aerosol concentration of both water aerosols and bioaerosols in similar ways and further details can be found in the section on aerosol concentration of bioaerosols. Similarly, the reduction percentages were statistically ($P>0.05$) the same for water and bioaerosols in terms of number count and mass (Table 6). This indicates that, despite the type of liquid aerosol, that the ionization has a constant level of performance in terms of reducing the aerosol concentration.

Table 5. Aerosol concentration (standard deviation) of water aerosols in terms of number count and mass

	Aerosol concentration							
	Number count (# m^{-3})				Mass (mg m^{-3})			
Treatment	1	2	3	4	1	2	3	4
Before Ionization	2.55×10^{8} (2.24×10^{7})	4.44×10^{8} (8.97×10^{7})	7.70×10^{7} (8.72×10^{6})	1.09×10^{8} (1.95×10^{7})	7.08×10^{-3} (2.03×10^{-3})	1.05×10^{-2} (2.00×10^{-3})	2.65×10^{-3} (6.92×10^{-4})	2.53×10^{-3} (4.24×10^{-4})
After Ionization	2.20×10^{7} (1.73×10^{6})	5.10×10^{7} (1.80×10^{7})	2.97×10^{7} (4.04×10^{6})	3.30×10^{7} (1.56×10^{7})	4.44×10^{-4} (5.46×10^{-5})	1.04×10^{-3} (3.46×10^{-4})	6.18×10^{-4} (1.04×10^{-4})	7.58×10^{-4} (3.6×10^{-4})
Reduction (%)	91.4 (0.1)	88.7 (1.7)	61.5 (2.6)	70.6 (8.4)	93.5 (1.6)	90.2 (1.7)	74.6 (12.0)	70.8 (9.1)

Table 6. Comparison of the reduction of aerosol concentration for PBS (bioaerosols) and water aerosols

	Reduction of aerosol concentration (number)		Reduction of aerosol concentration (mass)	
Treatment	PBS (bioaerosols)	Water aerosols	PBS (bioaerosols)	Water aerosols
1	92.8 (3.2)	91.4 (0.1)	95.7 (2.2)	93.5 (1.6)
2	86.2 (7.2)	88.7 (1.7)	96.3 (1.2)	90.2 (1.7)
3	60.7 (2.8)	61.5 (2.6)	68.3 (10.9)	74.6 (12)
4	70.2 (10.8)	70.6 (8.4)	77.8 (11.3)	70.8 (9.1)

5.9. PRRSV RNA concentration in air

One replicate from treatment 1 was excluded from statistical analysis due to a mix-up with the order of biosamplers during experimental test. Because qRT-PCR was performed nine times per collected sample, each sample had an average concentration of viral RNA collected in the solution as well as a standard error associated with that average. It must be noted that the standard error for the samples ranged from 0 – 10 VGCN ml^{-1} and was associated with the precision and accuracy of the qRT-PCR analysis. For the purposes of analyzing how negative air ionization rate affected the concentration of PRRSV, the average values obtained from the qRT-PCR analysis were used for each sample in further analyses.

A previous study can be referred to, in which different PRRSV isolates were stored in minimum essential medium to measure the maximum half-life of PRRSV at different temperatures (Jacobs et al. 2010). The study showed that time and temperature did not affect the concentration of PRRSV measured using qRT-PCR (i.e. the concentration of PRRSV measured using this method did not change significantly regardless of temperature and time). Therefore, there is no concern that the qRT-PCR analysis used in the current study was erroneous due to exposure of PRRSV to different temperatures.

The current study estimated the airborne concentration of PRRSV using: (1) the PRRSV concentration within the collection liquid, which was quantified with qRT-PCR (VGCN ml^{-1}); (2) the volume of each air sample collected (ml); (3) the volume of air collected (m^3), which was calculated from the air sampling rate (L min^{-1}) and the collection time (min). This method of quantifying PRRSV is novel to studies that have collected air samples of PRRSV. While previous studies have performed some air sampling measurements from the exhaust of infected

swine facilities, these measurements were usually quantified in terms of $TCID_{50}$ per ml of collection liquid (Otake et al. 2010; Dee et al. 2009a; and Pitkin et al. 2009). Other studies have quantified the PRRSV collected in air samples in terms of the estimated amount of virus collected in units of $TCID_{50}$ (Hermann et al. 2006, 2008). Comparing the PRRSV found in the liquid sample or the total PRRSV collected in an air sample between different studies is difficult when different equipment is utilized to collect air samples. For example, the SKC biosampler has an approximate collection rate of 12.5 L min^{-1}, while the Midwest Microtek sampler has a collection rate of 400 L min^{-1} (Hermann et al. 2008). It is likely that the Midwest Microtek will collect more virus than the SKC biosampler if there is not a finite amount of virus to sample. In other words, if a room contained infectious PRRSV aerosols and a Midwest Microtek and a SKC biosampler were to perform air sample collection for the same period of time, the Midwest Microtek would likely collect more PRRSV due to its collection rate. Additionally, it is also difficult to compare the results between different studies if the same equipment was utilized but different sampling times and volume of collection fluid were used. Determining the estimated PRRSV per unit volume of air takes into account the sampling time, the sampling rate, and the volume of collection fluid unique to each study to allow for an easier comparison between studies.

5.9.1. PRRSV concentration before ionization

The amount of PRRSV RNA sampled from the air prior to ionization for the four treatments is shown in Figure 35. The airflow rate of 34 m^3 h^{-1} (3647-27045 VGCN m^{-3}) resulted in higher PRRSV RNA concentration than the airflow rate of 135.9 m^3 h^{-1} (1479-12212 VGCN m^{-3}) The higher aerosol generation rate (7319-27045 VGCN m^{-3}) also resulted in higher

PRRSV RNA concentration than the lower aerosol generation rate (1479-6143 VGCN m^{-3}), as expected. Statistical analysis indicated that the effects of airflow rate and aerosol generation rate on the concentration of PRRSV RNA were significant ($P<0.05$). The Scheffé's comparison test indicated that treatments 1 and 3 belonged to the first family, treatments 1 and 4 belonged to a second family, and treatments 2 and 4 belonged to a third family. An aerosol generation rate of 14.8 ml h^{-1} generated statistically equal amount of PRRSV RNA in the air at both airflow rates, as did the aerosol generation rate of 33 ml h^{-1}.

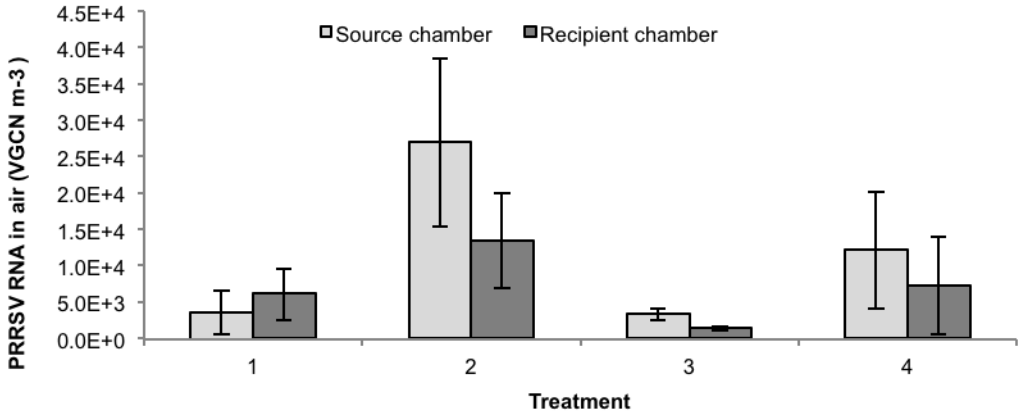

Figure 35. PRRSV RNA concentration in the air in the source and recipient chambers before ionization (Treatment 1: 34.0 m^3 h^{-1},14.8 ml h^{-1}; Treatment 2: 34.0 m^3 h^{-1}, 33.0 ml h^{-1}; Treatment 3: 135.9 m^3 h^{-1}, 14.8 ml h^{-1}; Treatment 4: 135.9 m^3 h^{-1}, 33.0 ml h^{-1}).

The average PRRSV airborne concentration quantified with qRT-PCR prior to ionization ranged from $1.5 \times 10^3 – 2.7 \times 10^4$ VGCN m^{-3}. This range was similar to that reported by Otake et al. (2010) where air samples were collected over a period of 21 days from the exhaust of a swine barn infected with various isolates of PRRSV. Based on the information given in their study, the level of PRRSV concentration in the exhaust was estimated to be from 6.25 $TCID_{50}$ m^{-}

^{3} to 2.6×10^{5} $TCID_{50}$ m^{-3} with an average value of 3.6×10^{4} $TCID_{50}$ m^{-3}. Under the assumption that the PRRSV prior to ionization in the current study was infectious, the range of values found within this study was similar to that reported by Otake et al. (2010).

5.9.2. EPI effect on PRRSV RNA concentration in air

The EPI was effective at removing PRRSV in both the source and recipient chambers. The average PRRSV RNA concentrations in the air after ionization were 154 VGCN m^{-3}, 2295 VGCN m^{-3}, 800 VGCN m^{-3}, and 4593 VGCN m^{-3} in the source chamber for treatments 1-4, respectively. Comparatively, the average PRRSV RNA concentrations in the air after ionization were 305 VGCN m^{-3}, 498 VGCN m^{-3}, 488 VGCN m^{-3}, and 498 VGCN m^{-3} in the recipient chamber for treatments 1-4, respectively (Figure 36). The reductions in PRRSV RNA concentration by air ionization were 90%, 90%, 73%, and 68% in the source chamber for treatments 1-4, respectively (Figure 37). Alternatively, the percentage of the PRRSV RNA concentration remaining in the air after ionization was 10%, 10%, 27%, and 32% in the source chamber for treatments 1-4, respectively (Figure 37b).

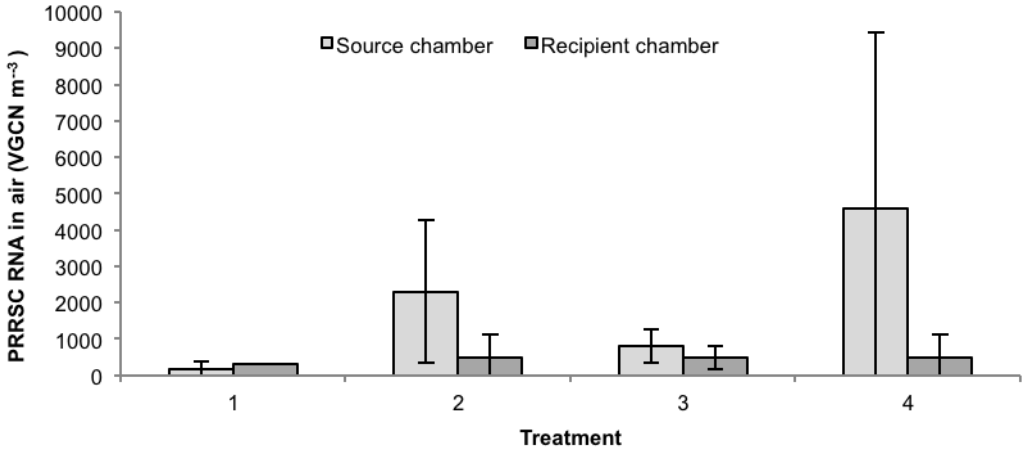

Figure 36. PRRSV concentration in air within source and recipient experimental chambers after ionization (Treatment 1: 34.0 m^3 h^{-1},14.8 ml h^{-1}; Treatment 2: 34.0 m^3 h^{-1}, 33.0 ml h^{-1}; Treatment 3: 135.9 m^3 h^{-1}, 14.8 ml h^{-1}; Treatment 4: 135.9 m^3 h^{-1}, 33.0 ml h^{-1}).

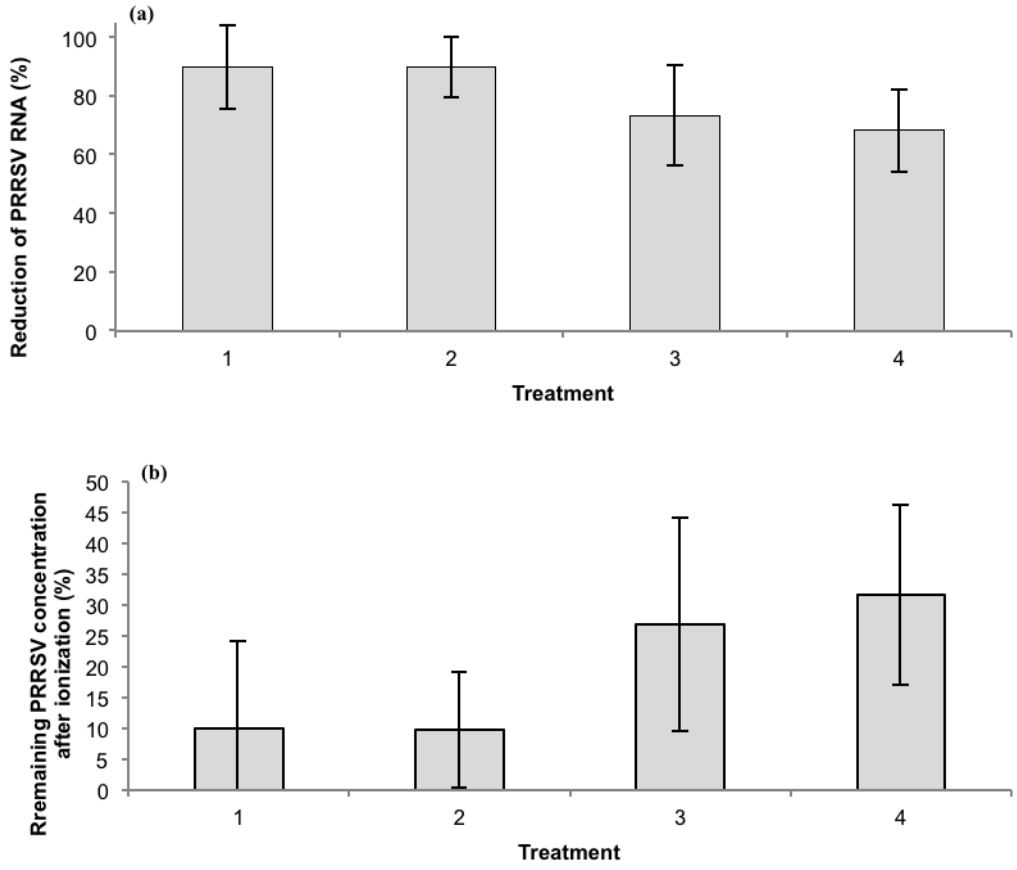

Figure 37. (a) Reduction of PRRSV concentration within source chamber air due to ionization and (b) Percentage of PRRSV RNA concentration remaining in source chamber after ionization (Treatment 1: 34.0 m^3 h^{-1},14.8 ml h^{-1}; Treatment 2: 34.0 m^3 h^{-1}, 33.0 ml h^{-1}; Treatment 3: 135.9 m^3 h^{-1}, 14.8 ml h^{-1}; Treatment 4: 135.9 m^3 h^{-1}, 33.0 ml h^{-1}).

The EPI successfully reduced the PRRSV RNA concentration in the source chamber (68 – 90%) where the EPI was activated. The magnitude of the reductions in PRRSV RNA was not affected by airflow rate or aerosol generation rate ($P>0.05$). Reducing the aerosol concentration in the source chamber meant that the outgoing air (i.e., air that was entering the recipient chamber) was already treated. Therefore, the air entering the recipient chamber already contained lower concentrations of PRRSV than the concentrations measured before ionization, causing the reduction in the recipient chamber that ranged on average from 69 – 96%. It is arguable that further reduction may have occurred in the recipient chamber if the ions that entered the recipient chamber from the source chamber had continued to interact with aerosols and remove them from the air. However, if this were true, wall swabs in the recipient chamber would have measured some level of PRRSV RNA. There was no PRRSV RNA detected in wall swabs in the recipient chamber. Comparatively, the amount of viral RNA on the swabbed surfaces of the source chamber walls was 83 VGCN, 414 VGCN, 21 VGCN, and 116 VGCN for treatments 1-4, respectively. Therefore, no action of ions occurred in the recipient chamber and no further reduction occurred in the recipient chamber.

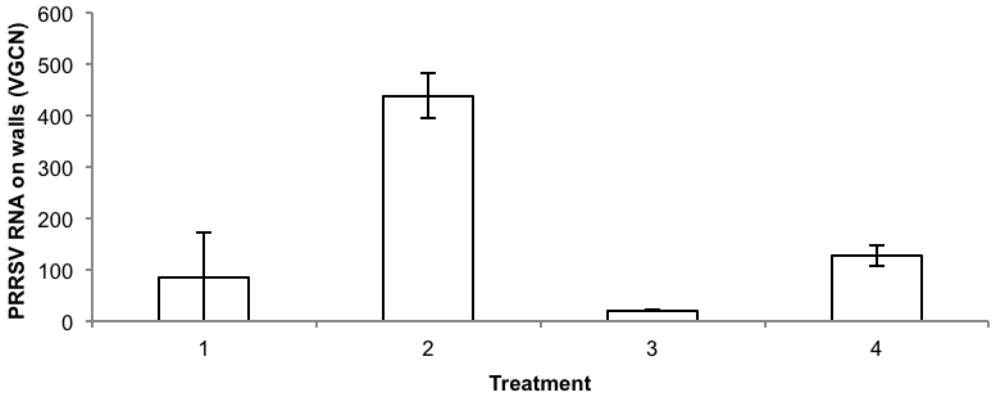

Figure 38. PRRSV collected from wall swabs in source chamber (Treatment 1: 34.0 m^3 h^{-1},14.8 ml h^{-1}; Treatment 2: 34.0 m^3 h^{-1}, 33.0 ml h^{-1}; Treatment 3: 135.9 m^3 h^{-1}, 14.8 ml h^{-1}; Treatment 4: 135.9 m^3 h^{-1}, 33.0 ml h^{-1}).

It is important to note that PRRSV RNA concentrations were not the same as the concentration of infectious PRRSV because RNA concentrations do not measure the amount of active virus and some of the measured virus may be dead. Previously, Cutler et al. (2011) predicted the median infectious dose (i.e., the dose required to infect 50% of a population) of PRRSV isolate MN-184 using a combination of experimental testing and two different generalized linear regression models. The predicted median infectious dose values for PRRSV isolate MN-184 ranged from $10^{-0.14}$ to $10^{0.26}$ $TCID_{50}$ (0.72 – 1.82 $TCID_{50}$). Hermann et al. (2009) performed a similar experiment and analysis for PRRSV isolate VR-2332 but did not specify the median infectious dose, although Cutler et al. (2011) later stated that the median infectious dose was $10^{3.1}$ $TCID_{50}$ (equal to 1.3×10^3 $TCID_{50}$). The measured PRRSV RNA concentration after ionization ranged from 3.1×10^2 to 4.6×10^3 VGCN m^{-3}. If ionization reduced airborne concentration due to removal of aerosols from the air, but not the infectivity of PRRSV, the infectious PRRSV concentration after ionization would be approximately equal to 3.1×10^2 to

4.6×10^3 $TCID_{50}$ in 1 m^3 of air. It was possible that post-ionization concentration would still cause infections, based on the median infectious dose for both the MN-184 and VR-2332 isolates and assuming a pig was to inhale 1 m^3 of air.

Lastly, another observation was the different effects of aerosol generation rate and airflow rate on aerosol and PRRSV concentrations in the source chamber air after ionization. Aerosol generation rate affected the PRRSV RNA concentration in the source chamber air after ionization and also the aerosol concentration by number count after ionization ($P<0.05$). Aerosol generation rate did not affect the aerosol generation by mass ($P>0.05$) after ionization but the airflow rate did ($P<0.05$). From this, it is possible that there was a relationship between the aerosol concentration in terms of number count and the PRRSV; however, further investigation is required to verify this and to determine the circumstances of the relationship.

CHAPTER 6. CONCLUSIONS

The current study experimentally assessed the performance of negative air ionization (specifically EPI) at reducing the airborne PRRSV concentration in the air and also at improving air quality via removal of aerosols. This study also sought to investigate the effect of airflow (ventilation) rate, which changes in magnitude at different seasons in swine facilities, and aerosol generation rate on the performance of EPI on removal of PRRSV and aerosols. The following conclusions were drawn from this study:

1. The chamber system, instruments and laboratory analysis designed for the laboratory study of air ionization was capable of collecting, measuring, and quantifying both PRRSV and aerosol properties.
2. Assessment of the standard curve and the limit of detection of the laboratory analysis showed that the methodology and materials used for RNA extraction and qRT-PCR during laboratory analysis was highly efficient and had a good performance for quantifying PRRSV in the air collected by biosamplers.
3. The size distribution of aerosols before ionization partially dictates the success of EPI as the EPI air was more efficient at removing larger aerosols than small aerosols.
4. The EPI's ability to remove aerosols at particular sizes was influenced by the airflow rate. Larger aerosols (>6 um) were present after ionization only at an airflow rate of 135.9 m^3 h^{-1}. Lastly, there was a greater difference between aerosol concentrations before and after ionization at all size ranges at an airflow rate of 34 m^3 h^{-1} than an airflow rate of 135.9 m^3 h^{-1}.

5. The EPI air caused higher reductions in aerosol concentration at an airflow rate of 34 m^3 h^{-1}. The aerosol concentrations (mass) were also greater after ionization when an airflow rate of 135.9 m^3 h^{-1} was used.
6. The type of aerosols (water vs. PBS) may affect how the EPI air reduces aerosols at particular size ranges but does not affect the proportion of reduction. While the geometric mean diameters of water aerosols were reduced differently than bioaerosols, the percentage of reduction between water aerosols and mass were not statistically different.
7. In the two-chamber system, the removal of PRRSV occurred in the first chamber where the EPI was installed. There was no additional aerosol reduction in the second chamber as wall swabs did not find PRRSV RNA in the second chamber.
8. EPI reduced the concentration of PRRSV RNA in the air by 68-90% (on average) and the reduction was not influenced by airflow rate or aerosol generation rate.
9. The amount of PRRSV in the air was likely related more to the aerosols in terms of number count than by mass due to the aerosol generation rate effect on both PRRSV RNA and aerosol concentration (number count) after ionization.
10. The method of quantifying air samples in terms of the amount of PRRSV found in a volume of air used in this study has not been used previously and would be a way to easily compare the results of different studies that use different sampling methods and equipment.

CHAPTER 7. RECOMMENDATIONS

There are many recommendations for future study into this area of research:

1. Because of the difference in EPI effect on the particle size distribution of water and bioaerosols, it is pertinent to perform a similar study that uses swine dust from a swine barn. The dust should also be contaminated with PRRSV to see if the effects differ from those of this study.
2. It was difficult to control the relative humidity and temperature in the current study due to the effect of the outdoor temperature on the environment within the facility. It is recommended that in future tests the facility is modified to reduce the effect of outdoor fluctuations in temperature and relative humidity. The effect of EPI at different temperatures and relative humidity (especially at those usually measured in swine facilities at different seasons) should be investigated on the aerosols and specifically the infectiveness of PRRSV.
3. Further research into the relationship between voltage (measured with the charge plate monitor) and the ion concentration would allow for a greater understanding of how the ion concentration emitted by the EPI is affected by airflow rate or other in-barn parameters.
4. The aerosol injection point (the tee wye fitting) should be modified to reduce the possible condensation of liquid at the bend. Additionally, the entrance of the chamber system could be modified so that the nebulizer tip was not placed inside of a small hole. The nebulizer could be placed inside of a small box at the entrance to reduce the chance of condensation at the entry.

5. Further investigation comparing the difference between aerosol concentration of water aerosols and PBS-based bioaerosols should be performed to assess why this phenomenon occurred in this study.
6. A potential theory on the fluctuation in aerosol concentration in both mass and number count for bioaerosols was the potential for aerosols to become lodged in the tygon tubing and dislodged during the sampling process. It is unknown if this is indeed the case and further investigation is required in future studies.
7. Only two airflow rates were investigated in this study. Due to the effect of airflow rate on PRRSV, further investigations are warranted. In-barn studies should also occur as the size and dimensions of the experimental chamber do not replicate the environment of a barn and the required ventilation rates in a barn.
8. It is pertinent to gain information on how EPI affects the infectivity of PRRSV. If future studies on this were performed in the current chamber system, care should be used to prevent the loss of infectivity due to exposure to high temperatures. The biosampler methodology could be modified such that tubing is attached to the collection port of biosamplers that are placed outside of the chambers so that the collected samples could be stored on ice or dry ice. This would help reduce the loss of infectivity.
9. The relationship between aerosol concentration by number count and PRRSV RNA should be further investigated to define the relationship.

APPENDIX A. LIMIT OF DETECTION CALCULATION FOR QRT-PCR

Tube	1	2	3	4	5	6	7
Concentration (PFU/ml)	10^7	10^6	10^5	10^4	10^3	10^2	10^1
Initial volume (ul)	1000	1000	1000	1000	1000	1000	1000
Initial PRRSV (PFU)	10^7	10^6	10^5	10^4	10^3	10^2	10^1
Volume removed for dilution (ul)	100	100	100	100	100	100	0
Final volume after dilution (ul)	900	900	900	900	900	900	1000
Final PRRSV after dilution (PFU)	9×10^6	9×10^5	9×10^4	9×10^3	9×10^2	9×10^1	10^1
Volume used for RNA extraction (ul)	140	140	140	140	140	140	140
PRRSV in sample that will be extracted (PFU)	1.4×10^6	1.4×10^5	1.4×10^4	1.4×10^3	1.4×10^2	1.4×10^1	1.4×10^0
Volume of eluted sample (ul)	80	80	80	80	80	80	80
Max PRRSV concentration of extracted sample (PFU/ul)	1.75×10^4	1.75×10^3	1.75×10^2	1.75×10^1	1.75×10^0	1.75×10^{-1}	1.75×10^{-2}
Volume used in qRT-PCR reaction (ul)	7	7	7	7	7	7	7
PRRSV quantity being "analyzed" during qRT-PCR (PFU)	1.23×10^5	1.23×10^4	1.23×10^3	1.23×10^2	1.23×10^1	1.23×10^0	1.23×10^{-1}
PRRSV concentration during qRT-PCR (PFU/ml)	4.92×10^6	4.92×10^5	4.92×10^4	4.92×10^3	4.92×10^2	4.92×10^1	4.92

A 1000-ul volume of 10^7 PFU/ml PRRSV was used as the initial sample for developing the dilutions of PRRSV for the standard curve development. 100 ul was pipetted from the tube containing 1000-ul volume of 10^7 PFU/ml PRRSV into a tube with 900 ul of PBS. One tenth of the original volume and PRRSV quantity was taken from the 10^7 tube. The remaining quantity left in that first tube was:

$$10^7 PFU - \frac{10^7 PFU}{10} = 9 \times 10^6 PFU$$

The quantity of virus moved into the second tube was:

$$\frac{10^7 PFU}{10} = 10^6 PFU$$

The concentration of virus in the second tube was:

$$\frac{10^6 PFU}{(100 + 900\ \mu l)} = \frac{10^6 PFU}{(1000\ \mu l)} = \frac{10^6 PFU}{1\ ml}$$

The same methods were used to calculate the remaining quantity left in the remaining tubes as well as the concentrations of PRRSV in the tubes.

For RNA extraction, 140 μl of virus were utilized from each tube for each replicate. The quantity of virus that would be used for RNA extraction from the first tube was calculated as follows:

$$\frac{140\ \mu l}{900\ \mu l} = \frac{x\ amount\ of\ virus}{9 \times 10^6 PFU}$$

$$(x\ amount\ of\ virus) = \frac{(140\ \mu l) \times (9 \times 10^6 PFU)}{900\ \mu l}$$

$$x\ amount\ of\ virus = 1.4 \times 10^6\ PFU$$

The volume of virus used in RNA extraction for the remaining tubes were similarly calculated.

At the end of the RNA extraction, 80 µl was used to elute the extracted RNA from the spin column. Therefore, the maximum concentration of extracted PRRSV within the first tube (assuming 100% efficiency of RNA extraction) is calculated as follows:

$$\frac{1.4 \times 10^6\ PFU}{80\ \mu l} = 1.75 \times 10^4\ \frac{PFU}{\mu l}$$

Lastly, for qRT-PCR, 7 µl of the extracted RNA sample is used. The maximum quantity of PRRSV used during qRT-PCR from the extracted RNA from the first tube was:

$$1.75 \times 10^4\ \frac{PFU}{\mu l} \times 7 \mu l = 1.23 \times 10^5\ PFU$$

The maximum quantity of PRRSV used during qRT-PCR from the extracted RNA from the last tube was 1.23×10^{-1} PFU, which is equivalent to 0.123 PFU. The concentration of PRRSV in the PCR tube was 4.92 PFU/ml.

APPENDIX B. STATISTICAL ANALYSIS DETAILS

Factorial Analysis: Water aerosols

					Probability					
Variable	Stage	Procedure	Satterthwaite Method	Transformation	Airflow	Aerosol generation rate	Interaction	Normal Data	Normal Residuals	Predicted x Studentized Residuals good
Geometric Diameter (Number count)	Before Ionization	Proc Mixed – REML Method	No	No	0.1004	0.564	0.1757	No	Yes	No
	After Ionization	Proc Mixed – REML Method	No	No	0.9191	0.2101	0.4840	No	Yes	No
	Reduction	Proc Mixed – REML Method	No	No	0.1029	0.8512	0.7787	Yes	Yes	No
Geometric Diameter (Mass)	Before Ionization	Proc Mixed – REML Method	Yes (P=0.0047)	No	0.5309	0.0862	0.4045	No	Yes	No
	After Ionization	Proc Mixed – REML Method	No	No	0.1629	0.3905	0.3495	Yes	Yes	Yes
	Reduction	Proc Mixed – REML Method	No	No	0.7742	0.0479	0.3090	Yes	Yes	No

					Probability					
Variable	Stage	Procedure	Satterthwaite Method	Transformation	Airflow	Aerosol generation rate	Interaction	Normal Data	Normal Residuals	Predicted x Studentized Residuals good
Geometric Standard Deviation (Number count)	Before Ionization	Proc Mixed – REML Method	No	No	0.8688	0.0974	0.4552	Yes	Yes	No
	After Ionization	Proc Mixed – REML Method	No	No	0.0406	0.121	0.7814	Yes	Yes	No
	Change	Proc Mixed – REML Method	No	No	0.1021	0.2800	0.9979	Yes	Yes	No
Geometric Standard Deviation (Mass)	Before Ionization	Proc Mixed – REML Method	No	No	0.562	0.0573	0.7898	Yes	Yes	No
	After Ionization	Proc Mixed – REML Method	Yes (P=0.0479)	No	0.3000	0.8759	0.8632	Yes	Yes	Yes
	Change	Proc Mixed – REML Method	No	No	0.3392	0.5774	0.4091	Yes	Yes	No

					Probability					
Variable	Stage	Procedure	Satterthwaite Method	Transformation	Airflow	Aerosol generation rate	Interaction	Normal Data	Normal Residuals	Predicted x Studentized Residuals good
Aerosol Concentration (Number count)	Before Ionization	Proc Mixed – REML Method	No	Yes conct=log(conc)	<0.0001	0.0010	0.2751	Yes	Yes	Yes
	After Ionization	Proc Mixed – REML Method	No	Yes Conct=log(conc)	0.6282	0.0347	0.0528	Yes	Yes	No
	Reduction	Proc Mixed – REML Method	Yes P=0.0003	No	0.0049	0.3129	0.1218	No	Yes	Yes
Aerosol Concentration (Mass)	Before Ionization	Proc Mixed – REML Method	No	Yes conct=log(conc)	<0.0001	0.2049	0.1496	Yes	Yes	Yes
	After Ionization	Proc Mixed – REML Method	No	Yes conct=log(conc)	0.9452	0.0226	0.0838	Yes	Yes	No
	Reduction	Proc Mixed – REML Method	No	Yes conct= arsin(sqrt(conc/100))	0.0009	0.3240	0.8893	Yes	Yes	No

Factorial Analysis: Bioaerosols

					Probability					
Variable	Stage	Procedure	Satterthwaite Method	Transformation	Airflow	Aerosol generation rate	Interaction	Normal Data	Normal Residuals	Predicted x Studentized Residuals good
Geometric Diameter (Number count)	Before Ionization	Proc Mixed – REML Method	No	No	0.0014	0.6155	0.0146	Yes	Yes	No
	After Ionization	Proc Mixed – REML Method	Yes (P=0.0093)	No	0.2838	0.0306	0.2838	Yes	Yes	Yes
	Reduction	Proc Mixed – REML Method	No	Yes dgeot= arsin(sqrt(dgeo/100))	0.0008	0.1254	0.0119	Yes	No	Yes
Geometric Diameter (Mass)	Before Ionization	Proc Mixed – REML Method	No	No	0.3510	0.1431	0.4139	Yes	No	No
	After Ionization	Proc Mixed – REML Method	No	No	0.0033	0.0002	0.9314	Yes	Yes	Yes
	Reduction	Proc Mixed – REML Method	No	No	0.0042	0.0367	0.3670	Yes	yes	No

					Probability					
Variable	Stage	Procedure	Satterthwaite Method	Transformation	Airflow	Aerosol generation rate	Interaction	Normal Data	Normal Residuals	Predicted x Studentized Residuals good
Geometric Standard Deviation (Number count)	Before Ionization	Proc Mixed – REML Method	No	Yes sgeot = sqrt(log(sgeo)	0.1964	0.6367	0.0408	Yes but one test for normality P<0.1	Yes	No
	After Ionization	Proc Mixed – REML Method	No	No	0.0044	0.0003	0.6494	Yes	Yes	No
	Change	Proc Mixed – REML Method	No	Yes sgeot = sqrt(abs(sgeo));	0.0207	0.0603	0.1496	Yes	Yes	No
Geometric Standard Deviation (Mass)	Before Ionization	Proc Mixed – REML Method	No	No	0.1854	0.0638	0.0516	Yes	Yes	No
	After Ionization	Proc Mixed – REML Method	No	No	0.1704	0.0728	0.2365	Yes but two tests for normality P<0.1	Yes	No
	Change	Proc Mixed – REML Method	No	Yes sgeot=sqrt(abs(sgeo))	0.1632	0.5303	0.4230	Yes	Yes	No

					Probability					
Variable	Stage	Procedure	Satterthwaite Method	Transformation	Airflow	Aerosol generation rate	Interaction	Normal Data	Normal Residuals	Predicted x Studentized Residuals good
Aerosol Concentration (Number count)	Before Ionization	Proc Mixed – REML Method	Yes	Yes conct= log(conc);	0.0198	0.0115	0.6686	Yes	Yes	Yes
	After Ionization	Proc Mixed – REML Method	No	No	0.1463	0.0253	0.5945	Yes	Yes	No
	Reduction	Proc Mixed – REML Method	No	Yes conct=arsin(sqrt(conc/**100**));	0.0002	0.9898	0.0640	Yes	Yes	Yes
Aerosol Concentration (Mass)	Before Ionization	Proc Mixed – REML Method	No	Yes conct=log(sqrt(conc));	0.0029	0.0199	0.3723	Yes	Yes	No
	After Ionization	Proc Mixed – REML Method	No	Yes conct=sqrt(CONC);	0.0226	0.4250	0.4308	Yes	Yes	No
	Reduction	Proc Mixed – REML Method	No	Yes conct=arsin(sqrt(conc/**100**));	0.0003	0.2855	0.3978	Yes		

Factorial Analysis: PRRSV Concentration

			Probability						
Stage	Procedure	Transformation	Airflow	Aerosol generation	Interaction	Chamber	Normal	Normal residuals	Predicted x Studentized Residuals good
Before Ionization	Proc Mixed Type 3 RCB	VGCNt=log(VGCN);	0.0139	<0.0001	0.7086	0.0885	Yes	Yes but one test of normality P<0.1	Yes
After Ionization	Proc Mixed Type 3 RCB	No	0.3905	0.102	0.6837	0.0739	No		
After Ionization (Source)	Proc Mixed Type 3	Yes VGCNt= sqrt(sqrt(VGCN));	0.1081	0.0162	0.3888	N/A	Yes	Yes	Yes
After Ionization (Recipient)	Proc Mixed Type 3	Yes VGCNt=sqrt(VGCN);	0.8179	0.8034	0.8249	N/A	No	Yes	No
Reduction	Proc Mixed Type 3 RCB	Yes VGCNt= arsin(sqrt(VGCN/**100**));	0.0122	0.3521	0.3441	0.1481	Yes	No	Yes
Reduction (Source)	Proc Mixed Type 3	No	0.0639	0.7666	0.7949	N/A	Yes	Yes but one test of normality P<0.1	No
Reduction (Recipient)	Proc Mixed Type 3	Yes VGCNt= arsin(sqrt(VGCN/100)	0.0840	0.0387	0.1165	N/A	Yes	Yes	No
Wall (Source; total)	Proc Mixed Type 3	Yes VGCNt= sqrt(sqrt(VGCN));	0.0039	0.0003	0.2717	N/A	Yes but one test of normality P<0.1	No	No

Simplified Anova for Scheffe

Parameter		Procedure	Transformation	Treatment Probability
Water aerosol concentration (Number)	Before Ionization	Proc Mixed REML	conct=log(conc);	<0.0001
	After Ionization	Proc Mixed REML	conct=log(conc);	0.0533
	Reduction	Proc Mixed REML[A]	None	<.0001
Water aerosol concentration (Mass)	Before Ionization	Proc Mixed REML	conct=log((conc));	0.0002
	After Ionization	Proc Mixed REML	conct=log(conc);	0.0535
	Reduction	Proc Mixed REML	conct=arsin(sqrt(conc/100));	0.0057
Bioaerosol concentration (Number)	Before Ionization	Proc Mixed REML[A]	conct=log(conc)	0.0004
	After Ionization	Proc Mixed REML	None	0.0706
	Reduction	Proc Mixed REML	conct=arsin(sqrt(conc/**100**));	0.0013
Bioaerosol concentration (Mass)	Before Ionization	Proc Mixed REML	conct=log(sqrt(conc));	0.0059
	After Ionization	Proc Mixed REML	conct=sqrt(CONC);	0.0887
	Reduction	Proc Mixed REML	conct=arsin(sqrt(conc/**100**));	0.0017
PRRSV Concentration	Before Ionization	Proc Mixed Type 3	VGCNt=log(VGCN);	0.0002
	After Ionization (Source)	Proc Mixed Type 3	VGCNt=sqrt(sqrt(VGCN));	0.0563
	After Ionization (Recipient)	Proc Mixed Type 3	VGCNt=sqrt(VGCN);	0.9768
	Reduction (Source)	Proc Mixed Type 3	None	0.2522
	Reduction (Recipient)	Proc Mixed Type 3	VGCNt= arsin(sqrt(VGCN/100)	0.0353
	Wall (amount)	Proc Mixed Type 3	VGCNt=sqrt(sqrt(VGCN));	0.0005

A Performed Satterthwaite in factorial model but in the simplified ANOVA, the Satterthwaite was taken out of coding because results did not make sense

APPENDIX C. EQUILIBRIUM CALCULATION FOR WATER AND PBS AEROSOLS

The relative humidity in the chamber air after aerosolization was determined using a psychometric chart at sea level. The humidity ratio after ionization was determined based on the added humidity in the air due to airflow rate and aerosol generation rate. The humidity ratio was calculated using the following formulas:

$$\text{Humidity ratio}\,(\text{g H}_2\text{O / kg air}) = \frac{\text{Moisture flow rate (g/s)}}{\text{Airflow rate (kg/s)}}$$

$$\text{Moisture flow rate (g/s)} = \text{Aerosol generation rate (ml/h)} \times \frac{3600\,\text{s}}{1\,\text{h}} \times \frac{1\,\text{g}}{\text{ml}}$$

$$\text{Airflow rate (kg/s)} = \text{Airflow rate}\,(\text{m}^3\ \text{h}^{-1}) \times \frac{1\,\text{h}}{3600\,\text{s}} \times \text{density of air},$$

$$\text{where density of air at } 25^\circ\text{C} = 1.1839\,\frac{\text{kg air}}{\text{m}^3}$$

Humidity ratio after aerosolization =

Humidity ratio before aerosolization + Humidity ratio added to air during aerosolization

Temperature	Range of humidity ratios after aerosolization	Humidity ratio at 30% relative humidity	Humidity ratio at 40% relative humidity
˚C	g H_2O / kg air	g H_2O / kg air	g H_2O / kg air
20	1.34 – 3.57	4.00	5.625
25	1.97 – 4.57	5.625	8
30	2.59 – 6.07	8	10.5

Since the humidity ratios after ionization were always less than the humidity ratios at a relative humidity of 30%, the relative humidity never surpassed the crystallization relative humidity of 40% (Nicas et al. 2005) and therefore it was possible that aerosols were completely desiccated (i.e., all liquid was removed from aerosols and only solutes remained).

Nicas et al. (2005) stated an equation that related the diameter of a desiccated aerosol to its initial diameter, the concentration of non-volatile species, and the density of the non volatile species. The density of non-volatile species was given as the density of water, 1000 g L^{-1} (Nicas et al. 2005), while the concentration of non-volatile components was dependent on the liquid type. The water quality information from the distribution systems (Water and Waste Department 2014), was used to estimate the concentration of non-volatile species (0.464 g L^{-1}) in the water aerosols. The information given from the manufacturer (Life Technologies 2014) was used to calculate the concentration of non-volatile components in PBS (9.615 g L^{-1}). Based on this information, the equilibrium diameters for water aerosols and the bioaerosols were:

$$\text{Equilibrium diameter for water} = 0.077 \times \text{Initial diameter}$$
$$\text{Equilibrium diameter for PBS} = 0.213 \times \text{Initial diameter}$$

Since the APSS was set to detect a range of 0.234 to 40 μm, water aerosols with initial diameters less than 3.04 μm and bioaerosols with initial diameters less than 1.10 μm would not have been measured with the APSS after desiccation.

REFERENCES

Aarnink, A. J. A., R. F. M. M. Roelofs, H. Ellen, and H. Gunnink. 1999. Dust sources in animal houses. In *Proceedings on Dust Control in Animal Production Facilities*, 34-40. Horsens, Denmark.

Agranovski, V., Z. Ristovski, P. J. Blackall, and L. Morawska. 2004. Size-selective assessment of airborne particles in swine confinement building with the UVAPS. *Atmospheric Environment* 38: 3893-3901.

Alonso, C., S. Otake, P. Davies, and S. Dee. 2012. An evaluation of interventions for reducing the risk of PRRSV introduction to filtered farms via retrograde air movement through idle air. *Veterinary Microbiology* 157: 304-310.

Andersen, C.I., S.G. Von Essen, L.M. Smith, J. Spencer, R. Jolie, and K.J. Donham. 2004. Respiratory symmptons and airway obstruction in swine veterinatians: a persistent problem. *American Journal of Industrial Medicine* 46: 386-392.

Andres, A. and T. Banhazi. 2013. *Livestock housing : Modern management to ensure optimal health and welfare of farm animals.* Wageningen, NLD: Wageningen Academic Publishers.

BGI Inc. 2014. Collison Nebulizers. http://www.bgiusa.com/agc/collison.htm/ (2014/02/05).

Brockmeier, S.L. and K.M. Lager. 2002. Experimental airborne transmission of porcine reproductive and respiratory syndrome virus and *Bordetella bronchiseptica*. Veterinary Microbiology 89: 267-275.

Bundy, D.S. 1984. Rate of dust decay as affected by relative humidity, ionization, and air movement. *Transactions of ASAE* 27(3): 865-870.

Bundy, D.S. and T.E. Hazen. 1975. Dust levels in swine confinement systems associated with different feeding methods. *Transaction of the ASAE* 18(1): 137-144.

Cambra-López, M., A. Winkel, J. van Harn, N.W.M. Ogink, and A.J.A. Aarnink. 2009. Ionization for reducing particulate matter emissions from poultry houses. *ASABE* 52(5): 1757-1771.

Cambra-Lopez, M., A.J.A. Aarnink, Y. Zhao, S. Calvet, and A. G. Torres. 2010. Airborne particulate matter from livestock production systems: a review of an air pollution problem. *Environmental Pollution* 158: 1-17.

Cambra-Lopez, M., T. Hermosilla, H.T.L. Lai, A.J.A. Aarnink, and N.W.M. Ogink. 2011. Particulate matter emitted from poultry and pig houses: source identification and quantification. *Transactions of American Society of Agricultural and Biological Engineers* 54(2): 629-642.

Cho, J.G. and S.A. Dee. 2006. Porcine reproductive and respiratory syndrome virus. *Theriogenology* 66: 655-662.

Cho, J.G., J. Deen, and S.A. Dee. 2007. Influence of isolate pathogenicity on the aerosol transmission of Porcine reproductive and respiratory syndrome virus. Canadian Journal of Veterinary Research (71): 23-27.

Cho, J.G., S.A. Dee, J. Deen, C. Trincado, E. Fano, Y. Jiang, K. Faaberg, M.P. Murtaugh, A. Guedes, J.E. Collins, and H.S. Joo. 2006. The impact of animal age, bacterial coinfection,

and isolate pathogenicity on the shedding of Porcine reproductive and respiratory syndrome virus in aerosols from experimentally infected pigs. *The Canadian Journal of Veterinary Research* 70: 297-301.

Christopher-Hennings, J., E.A. Nelson, J.K. Nelson, R.J. Hines, S.L. Swenson, H.T. Hill, J.J. Zimmerman, J.B. Katz, M.J. Yaeger, C.C.L. Chase, and D.A. Benfield. 1995. Detection of porcine reproductive and respiratory syndrome virus in boar semen by PCR. *Journal of Clinical Microbiology* 33(7): 1730-1734.

Continental Fans. 2013. IRIS dampers http://www.continentalfan.com/ecatalog.php?fantype=industrial&fid=19&s=Dampers (2014/02/05).

Cormier, Y., L. Boulet, G. Bedard, and G. Tremblay. 1991. Respiratory health of workers exposed to swine confinement buildings only or to swine confinement buildings and dairy barns. *Scandinavian Journal of Work, Environment & Health* 17(4): 269-275.

Cutler, T.D., C. Wong, S.J. Hoff, A. Kittawornrat, and J.J. Zimmerman. 2011. Median infectious dose (ID50) of porcine reproductive and respiratory syndrome virus isolate MN-184 via aerosol exposure. *Veterinary Microbiology* 151: 229-237.

Daniel, S.L. 2002. "On the Ionization of Air for Removal of Noxious Effluvia" (Air Ionization of Indoor Environments for Control of Volatile and Particulate Contaminants With Nonthermal Plasmas Generated by Dielectric-Barrier Discharge). *IEEE Transactions on Plasma Science* 30(4): 1471-1481.

Dee, S., A. Pitkin, and J. Deen. 2009b. Evaluation of alternative strategies to MERV 16-based air filtration systems for reduction of the risk of airborne spread of porcine reproductive and respiratory syndrome virus. Veterinary Microbiology 138: 106-133.

Dee, S., A. Pitkin, S. Otake, and J. Deen. 2011. A four-year summary of air filtration system efficacy for preventing airborne spread of porcine reproductive and respiratory syndrome virus and Mycoplasma hyopneumoniae. Journal of swine health and production 19(5): 292-294.

Dee, S., J. P. Cano, G. Spronk, D. Reicks, P. Ruen, A. Pitkin, and D. Polson. 2012. Evaluation of the long-term effect of air filtration on the occurrence of new PRRSV infections in large breeding herds in swine-dense regions. Viruses 4: 654-662.

Dee, S., L. Batista, J. Deen, and C. Pijoan. 2005a. Evaluation of an air-filtration system for preventing aerosol transmission of Porcine reproductive and respiratory syndrome virus. The Canadian Journal of Veterinary Research 69: 293-298.

Dee, S., S. Otake, and J. Deen. 2010. Use of a production region model to assess the efficacy of various air filtration systems for preventing airborne transmission of porcine reproductive and respiratory syndrome virus and Mycoplasma hyopneumoniae: Results from a two year study. Virus research 154: 177-184.

Dee, S., S. Otake, S. Oliveira, and J. Deen. 2009a. Evidence of long distance airborne transport of porcine reproductive and respiratory syndrome virus and *Mycoplasma hyopneumoniae*. Veterinary Research 40(4):39.

Dee, S.A., J. Deen, L. Jacobson, K.D. Rossow, C. Mahlum, and C. Pijoan. 2005b. Laboratory model to evaluate the role of aerosols in the transport of porcine reproductive and respiratory syndrome virus. *Veterinary Record* 156: 501-504.

Dee, S.A., L. Batista, J. Deen, and C. Pijoan. 2006a. Evaluation of systems for reducing the transmission of Porcine reproductive and respiratory syndrome virus by aerosol. The Canadian Journal of Veterinary Research 70: 28-33.

Dee,S.A., J. Deen, J.P Cano, L. Batista, and C. Pijoan. 2006b. Further evaluation of alternate air-filtration systems for reducing the transmission of porcine reproductive and respiratory syndrome virus by aerosol. The Canadian Journal of Veterinary Research 70:168-175.

Desrosiers, R. 2011. Transmission of swine pathogens: different means, different needs. *Animal Health Research Reviews* 12(10: 1-13.

Donham, K., L.J. Scallon, W. Popendorf, M.W. Treuhaft, and R. C. Roberts. 1986. Characterization of dust collected from swine confinement buildings. *American Industrial Hygiene Association* 47(7): 404-410.

Dosman, J.A., A. Senthilselvan, S.P. Kirychuk, S. Lemay, E.M. Barber, P. Willson, Y. Cormier, and T.S. Hurst. 2000. Positive human health effects of wearing a respiratory in a swine barn. *Occupational and environmental lung disease* 118: 852-860.

Egli, C., B. Thür, L. Liu, and M.A.Hofmann. 2001. Quantitative TaqMan® RT-PCR for the detection and differentiation of European and North American strains of porcine reproductive and respiratory syndrome virus. Journal of Virological Methods 98: 63-75.

EPI Air. 2013. How EPI works. http://epiair.com/why-epi/how-epi-works/ (2013/6/20).

Fano, E., C. Pijoan, and S. Dee. 2005. Evaluation of the aerosol transmission of a mixed infection of *Mycoplasma hyopneumoniae* and porcine reproductive and respiratory syndrome virus. Veterinary Record 157: 105-108.

Fletcher, L.A., L.F. Gaunt, C.B. Beggs, S.J. Shepherd, P.A. Sleigh, C.J. Noakes, and K.G. Kerr. 2007. Bacterial action of positive and negative ions in air. *BMC Microbiology* 7:32.

Fletcher, L.A., L.F. Gaunt, C.B. Beggs, S.J. Shepherd, P.A. Sleigh, C.J. Noakes, and K.G. Kerr. 2007. Bacterial action of positive and negative ions in air. *BMC Microbiology* 7:32.

Gerber, P.F., K. O'Neill, O. Owolodun, C. Wang, K. Harmon, J. Zhang, P.G. Halbur, L. Zhou, X.-J. Meng, and T. Opriessnig. 2013. Comparison of commercial real-time reverse transcription-PCR assays for reliable, early, and rapid detection of heterologous strains of porcine reproductive and respiratory syndrome virus in experimentally infected or noninfected boars by use of different sample types. *Journal of Clinical Microbiology* 51(2): 547.

Gilbert, S.A., R. Larochelle, R. Magar, H.J. Cho, and D. Deregt. 1997. Typing of porcine reproductive and respiratory syndrome viruses by multiplex PCR assay. *Journal of Clinical Microbiology* 35(1): 264-267.

Grabarczyk, Z. 2001. Effectiveness of indoor air cleaning with corona ionizers. *Journal of Electrostatics* 51-52: 278-283.

Grinshpun, S.A., G. Mainelis, M. Trunov, A. Adhikari, T. Reponen, and K. Willeke. 2005. Evaluation of ionic air purifiers for reducing aerosol exposure in confined indoor spaces. *Indoor Air* 15: 235-245.

Guarino, H., S.M. Goyal, and M.P. Murtaugh. 1997. Comparison of four RNA extraction methods for the detection of porcine reproductive and respiratory syndrome virus by rt-pcr. *Microbiologica* 20: 319-324.

Guarino, M., L.D. Jacobson, and K.A. Janni. 2007. Dust reduction from oil-based feed additives. *ASAE* 23(3): 329-332.

Gunston, Bill (2009). Cambridge Aerospace Dictionary (2nd Edition). Cambridge University Press. Online version available at: http://app.knovel.com/hotlink/toc/id:kpCADE0003/cambridge-aerospace-dictionary

Gustafson, G. 1999. Factors affecting the release and concentration of dust in pig house. *Journal of Agricultural Engineering Research* 74: 379-390.

Hafer, A.L., R.L. Langley, M. Morrow, and J.J. Tulis. 1996. Occupational hazards reported by swine veterinarians in the United States. *Swine Health and Production* 4(3): 128-141.

Harmon, K.M., S.A. Abate, A.J. Chriswell, W.A. Chittick, and E.L. Strait. 2012. Comparison of two commercial real-time reverse transcriptase polymerase chain reaction assays for porcine reproductive and respiratory syndrome virus. *Journal of Swine Health and Production* 20(4): 184-188.

Hartung, J. and V.R. Phillips. 1994. Control of gaseous emissions from livestock buildings and manure stores. *Journal of Agricultural Engineering Research* 57: 173-189.

Heber, A.J. M. Stroik, J.L. Nelssen, and D.A. Nichols. 1988b. Influence of environmental factors on concentrations and inorganic content of aerial dust in swine finishing buildings. *Transactions of ASAE* 31(3): 875-881.

Heber, A.J., M. Stroik, J.M. Faubion, and L.H. Willard. 1988a. Size distribution and identification of aerial dust particles in swine finishing buildings. *Transactions of ASAE* 31(3): 882-887.

Hermann, J., S. Hoff, C. Muñoz-Zanzi, K.Yoon, M. Roof, A. Burkhardt, and J. Zimmerman. 2007. Effect of temperature and relative humidity on the stability of infectious porcine reproductive and respiratory syndrome virus in aerosols. Veterinary Research 38: 81-93.

Hermann, J., S. Hoff, C. Muñoz-Zanzi, K.Yoon, M. Roof, A. Burkhardt, and J. Zimmerman. 2007. Effect of temperature and relative humidity on the stability of infectious porcine reproductive and respiratory syndrome virus in aerosols. Veterinary Research 38: 81-93.

Hermann, J. R., S.J. Hoff, K.J. Yoon, A.C. Burkhardt, R.B. Evans, and J.J. Zimmermann. 2006. Optimization of a Sampling System for Recovery and Detection of Airborne Porcine Reproductive and Respiratory Syndrome Virus and Swine Influenza Virus. *Applied and Environmental Microbiology* 72(7): 4811-4818.

Hermann, J., C.A. Munoz-Zanzi, and J.J. Zimmerman. 2009. A method to provide improved dose-response estimates for airborne pathogens in animals: An example using porcine reproductive and respiratory syndrome virus. *Veterinary Microbiology* 133: 297-302.

Hermann, J.R., S.L. Brockmeier, K.-J. Yoon, and J.J. Zimmerman. 2008. Detection of respiratory pathogens in air samples from acutely infected pigs. *The Canadian Journal of Veterinary Research* 72: 367-370.

Hermann. J. and J.J. Zimmerman. 2008. Analytical sensitivity of air samplers based on uniform point-source exposure to airborne Porcine reproductive and respiratory syndrome virus and swine influenza virus. *The Canadian Journal of Veterinary Research* 72: 440-443.

Hofer, B.J. and D.E. Nicolai. 2007. Electrostatic space charge system for reducing dust in a swine finishing barn. *In 2007 ASABE/CSBE North Central Intersectional Conference.* St. Joseph, MI: ASABE.

Holthamp, D.J., J.B. Kliebenstein, E. J. Neumann, J.J. Zimmerman, H.F. Rotto, T. K. Yoder, C. Wang, P.E. Yeske, C. L. Mowrer, and C. A. Haley. 2014. Assessment of the economic impact of porcine reproductive and respiratory syndrome virus on United States pork producers. *Journal of Swine Health and Production* 21(2): 72-84.

Hu, J. and C. Zhang. 2014. Porcine reproductive and respiratory syndrome virus vaccines: current status and strategies to a universal vaccine. *Transboundary and Emerging Disease* 61: 109-120.

Jacobs, A.C., J.R. Hermann, C. Munoz-Zanzi, J.R. Prickett, M.B. Roof, K. Yoon, J.J. Zimmerman. 2010. Stability of Porcine Reproductive and Respiratory Syndrome virus at Ambient Temperatures. *Journal of Veterinary Diagnostic Investigation* 22: 257-260.

Jerez, S.B., Y. Zhang, and X. Wang. 2011. Measurement of particle size distribution in a swine building. *ASABE* 54(3): 1103-1117.

K.J. Donham. 1991. Association of environmental air contaminants with disease and productivity in swine. *American Journal Veterinary Research* 10: 1723-1730.

Kaufford, J., A. Wehrend, B.A. Schwarz, D. Knauf, R. Willig, G. Schagemann, and F. Schmoll. 2010. Exhaust expulsion of the porcine reproductive and respiratory syndrome virus (PRRSV) through ultrasound machines, *Tierärztliche Praxis Großtiere* 5: 285-292

Kerr, K.G., C.B. Beggs, J. Thornton, J.K. Donnelly, N.J. Todd, P.A. Sleigh, A. Qureshl, and C.C. Taylor. 2006. Air ionisation and colonisation/infection with methicillin-resistant Staphylococcus aureus and Acinetobacter species in an intensive care unit. *Intensive Care Med.* 32:315-317.

Kristensen, C.S., A. Bøtner, H. Takai, J.P. Nielsen, and S.E. Jorsal. 2004. Experimental airborne transmission of PRRSV. Veterinary Microbiology 99: 197-202.

Lee, B.U. M. Yermakov, and S.A Grinshpun.2004. Removal of fine and ultrafine particles from indoor environments by unipolar ion emission. *Atmospheric Environment* 38: 4815-4823

Lemay, S. P. and L. Chénard. 2001. What should I know about air quality in pig buildings. In *Proceedings from Manitoba Swine Seminar*, 143-157.

Life Technologies. 2012. Real-time PCR handbook. Carlsbad, California, USA: Life Technologies Corporation.

Life Technologies. 2014. PBS - phosphate-buffered saline (10x) pH 7.4. https://www.lifetechnologies.com/order/catalog/product/AM9624?CID=search-am9624 (2014/12/15).

Mayya, Y.S., B.K. Sapra, A. Khan, and F. Sunny. Aerosol removal by unipolar ionization in indoor environments. *Aerosol Science* 35: 923-941.

MEI. 2008. Operator's manual. Lyndonville, N.Y.: Monroe Electronics Inc.

Midwest Plan Service. 1983. Swine housing and equipment handbook. MWPS-8. Ames, Iowa: Midwest Plan Service.

Mikkelsen, T., S. Alexandersen, P. Astrup, H.J. Champion, A. I. Donaldson, F.N. Dunkerley, J. Gloster, J.H. Sørensen, and S. Thykier-Nielsen. 2003. Investigation of airborne foot-and-mouth disease transmission during low-wind conditions in the early phase of the UK 2001 epidemic. *Atmospheric Chemistry and Physics* 3:2101-2110.

Mitchell, B.W. and Baumgartner, J.W. 2007. Electrostatic space charge system for reducing dust in poultry production houses and the hatchery. In *ASAE Annual Meeting*, 074176, St. Joseph, MI: ASABE.

Mitchell, B.W. and Waltman. 2003. Reducing airborne pathogens and dust in commercial hatching cabinets with an electrostatic space charge system. *Avian Diseases* 47(2):247-253.

Mitchell, B.W., L.J. Richardson, J.L. Wilson, and C.L. Hofacre. 2004. Application of an electrostatics space charge system for dust, ammonia, and pathogen reduction in a broiler breeder house. *Applied Engineering in Agriculture* 20(1): 87-93.

Mitchell, B.W., P.S. Holt, K.-H. Seo. 2000. Reducing dust in a caged layer room: an electrostatic space charge system. *Journal of Applied Poultry Research* 9:292-296.

Murtaugh, M.P., S. Yuan, E.A. Nelson, and K.S. Faaberg. 2002. Genetic interaction between porcine reproductive and respiratory syndrome virus (PRRSV) strains in cell culture and in animals. *Journal of Swine Health and Production* 10(1): 15-21.

Nicas, M., W. W. Nazaroff, and A. Hubbard. 2005. Toward understanding the risk of secondary airborne infection: emission of respirable pathogens. *Journal of Occupational and Environmental Hygiene* 2: 143-154.

Opriessnig, T., P.G. Halbur, K.-J. Yoon, R.M. Pogranichniy, K.M. Harmon, R. Evans, K.F. Key, F.J. Pallares, P. Thomas, and X.J. Meng. 2002. Comparison of molecular and biological charactersistics of a modified live porcine reproductive and respiratory syndrome virus (PRRSV) vaccine (Ingelvac PRRS MLV), the parent strain of the vaccines (ATCC VR 2332), ATCC VR 2385, and two recent field isolates of PRRSV. *Journal of Virology* 76(23): 11837-11844.

OSHA. Occupational Health and Safety Act. 2004. http://www.e-laws.gov.on.ca/html/source/regs/english/2004/elaws_src_regs_r04100_e.htm (2014/07/10)

Otake, S., S. Dee, C. Corzo, S. Oliveira, and J. Deen. 2010. Long distance airborne transport of infectious PRRSV and Mycoplasma hyopneumonaie from a swine population infected with multiple viral variants. Veterinary Microbiology 145: 198-208.

Otake, S., S.A. Dee, L. Jacobson, M. Torremorrell, and C. Pijoan. 2002. Evaluation of aerosol transmission of porcine reproductive and respiratory syndrome virus under controlled field conditions. Veterinary Record 150:804-808.

Phillips, P.A. and B.K. Thompson. 1989. Respirable dust in fan and naturally ventilated hog barns. *ASAE* 32(5): 1807-1810.

Pitkin, A., J. Deen, and S. Dee. 2009. Use of a production region model to assess the airborne spread of porcine reproductive and respiratory syndrome virus. Veterinary Microbiology 136: 1-7.

Predicala, B.Z., R.G. Maghirang, S. B. Jerez, J. E. Urban, and R.D. Goodband. 2001.Dust and bioaerosol in two swine-finishing buildings in Kansas. *Transactions of ASAE* 44(5): 1291-1298.

Prickett, J., R. Simer, J. Christopher-Hennings, K. Yoon, R.B. Evans, and J.J. Zimmerman. 2008. Detection of Porcine reproductive and respiratory syndrome virus in porcine oral fluid samples: a longitudinal study under experimental conditions. *Journal of Veterinary Diagnostics Investigation* 20: 156-163.

Qiagen. 2012. QIAamp Viral RNA Mini Handbook – June 2012. Venlo, Germany: Qiagen.

Rademacher, C., G. Bradley, S. Pollmann, B. Coffelt, M. Baumgartner, and J. Baumgartner. 2012. Electrostatic particle ionization (EPI) improves nursery pig performance and air quality. *In 2012 American Association of Swine Veterinarians Annual Meeting, 257-258,* Perry Iowa: AASV.

Richardson, L.J., B.W. Mitchell, J.L. Wilson, and C.L. Hofacre. 2003b. Effect of an electrostatic space charge system on airborne dust and subsequent potential transmission of microorganisms to broiler breeder pullets by airborne dust. *Avian Diseases* 47(1): 128-133.

Richardson, L.J., C.L. Hofacre, B.W. Mitchell, and J.L. Wilson. 2003a. Effect of electrostatic space charge on reduction of airborne transmission of salmonella and other bacteria in broiler breeders in production and their progeny. *Avian Diseases* 47(4): 1352-1361.

Rosentrater. K.A. 2004. Laboratory analysis of an electrostatic dust collection system. *CIGR Journal of Scientific Research and Development* 6.

Rule, A.M., A.R. Chapin, S.A. McCarthy, K.E. Gibson, K.J. Schwab, and T.J. Buckley. 2005. Assessment of an aerosol treatment to improve air quality in a swine concentrated animal feeding operation (CAFO). *Environmental Science Technology* 39: 9649-9655.

Sawant, V.S., G.S. Meena, and D.B. Jadhav. 2012. Effect of negative air ions on fog and smoke. *Aerosol and Air Quality Research* 12: 1007-1015.

Siggers, J.L., S.P. Kirychuk, S.P, Lemay, and P. J. Willson. 2011. Size distribution of particulate and associated endotoxin in traditional swine barn rooms and rooms sprinkled with oil. *Journal of Agromedicine* 16: 271-279.

Sowiak, M., K. Bródka, A. Buczyńska, M. Cyprowski, A. Kozajda, W. Sobala, I. Szadkowska-Stańcyzk. 2012. An assessment of potential exposure to bioaerosols among swine farm workers with particular reference to airborne microorganisms in the respirable fraction under various breeding conditions. *Aerobiologia* 28: 121-133.

Spronk, G., S. Otake, and S. Dee. 2010. Prevention of PRRSV infection in large breeding herds using air filtration. Veterinary Record 166: 758-759.

Takai, H. and S. Pedersen. 2000. A comparison study of different dust control methods in pig buildings. *ASAE* 16(3): 269-277.

Tanaka, K. and Y. Zhang. 1996. Dust settling efficiency and electrostatic effect of a negative ionization system. *Journal of Agricultural Safety and Health* 2(1): 39-47.

Taylor, S., Wakem, M., Dijkman, G., Alsarraj, M., & Nguyen, M. (2010). A practical approach to RT-qPCR—Publishing data that conform to the MIQE guidelines. *Methods, 50*(4), S1-S5.

Timoshkin, I.V., M. Maclean, M.P. Wilson, M.J. Given, S.J. MacGregor, T. Wang, and J.G.Anderson. 2012. Bacterial Effect of Corona Discharges in Atmospheric Air. *IEEE Transactions on Plasma Science* 40(10): 2322-2333.

Topas GmbH. 2013. Particle analysis software PASWin 3.2. Dresden, Saxony, Germany: Technologie-orientierte Partikel-, Analysen- und Sensortechnik GmbH.

Torremorrell, M., C. Pijoan, K. Janni, R. Walker, and H.S. Joo. 1997. Airborne transmission of *Actinobacillus pleuropneumoniae* and porcine reproductive and respiratory syndrome virus in nursery pigs. American Journal of Veterinary Research 58(8): 828-832.

Torremorrell, M., C. Pijoan, K. Janni, R. Walker, and H.S. Joo. 1997. Airborne transmission of *Actinobacillus pleuropneumoniae* and porcine reproductive and respiratory syndrome virus in nursery pigs. American Journal of Veterinary Research 58(8): 828-832.

Trincado, C., S. Dee, L. Jackson, S. Otake, K. Rossow, and C. Pijoan. 2004. Attempts to transmit porcine reproductive and respiratory syndrome virus under controlled field conditions field conditions. Veterinary Record 154: 294-297.

VIDO-InterVAC. 2014. Replication-Defective Porcine reproductive and respiratory syndrome (PRRSV) Vaccine. http://www.vido.org/research/viral_vaccines/replication_defective_prrsv_vaccine.php (2014/05/13).

Wasilk, A., J.D. Callahan, J. Christopher-Hennings, T.A. Gay, Y. Fang, M. Dammen, M.E. Reos, M. Torremorell, D. Polson, M. Mellencamp, E. Nelson, and W.M. Nelson. 2004. Detection of U.S., Lelystad, and European-Like Porcine Reproductive and Respiratory Syndrome

Viruses and Relative Quantitation in Boar Semen and Serum Samples by Real-Time PCR. *Journal of Clinical Microbiology* 42(10): 4453-4461.

Water and Waste Department. 2014. 2013 Winnipeg distribution system water quality test results. http://www.winnipeg.ca/waterandwaste/water/testResults/Winnipeg2013.stm (2014/12/15).

Wu. C.C., G.W.M. Lee, P.C.S. Yang, K.P. Yu, Effect of wall surface materials on deposition of particles with the aid of negative air ions. 2006. *Aerosol Science* 37: 616-630.

Yoon, K.-J., J.J. Zimmerman, C.-C. Chang, S. Cancel-Tirado, K M. Harmon, and M. J. McGinley. 1999. Effect of challenge dose and route on porcine reproductive syndrome virus (PRRSV) infection in young swine. *Veterinary Research* 30: 629-638.

Zhao, Y., A.J.A. Aarnink, M. C. M. De Jong, and P. W. G.G. Koerkamp. 2014 Airborne microorganisms from livestock production systems and their relation to dust. *Critical Reviews in Environmental Science* 44:1071-1128.